Radiotext: an application of computer and communication systems in distance teaching

Thesis

RADIOTEXT

An Application of Computer and Communication Systems in Distance Teaching

Thesis submitted by

P. Smith B.A. (Hons)

for the degree of

Doctor of Philosophy

Faculty of Technology
The Open University
Milton Keynes
England

Date of submission: SEPT.'82
Date of award: 11.10.82

August 1982

ProQuest LLC
789 East Eisenhower Parkway
P.O. Box 1346
Ann Arbor, MI 48106 - 1346

ABSTRACT

To enhance the way in which the Open University is able to communicate with its students, learning at a distance, this study has involved the design of a system to allow material in the form of computer-coded text and graphics to be transmitted over an unmodified V.H.F. radio broadcast network. In addition to providing a low-cost rapid method of communication for course management, the system can be used for delivery of material such as audio-visual packages and computer software.

To enable the unmodified broadcast network and conventional radio receivers to be used, it is intended that Radiotext transmissions will take place at the end of the normal broadcast schedule. This implies that the system should be capable of unattended operation within the student's home. It is achieved by the use of a time-switched radio receiver and interface unit, together with an audio cassette recorder for storage of the received data. The received material may then be displayed on a television or printed out on a low-cost printer at a later, more convenient, time.

Each component of the system is described. The major emphasis is placed on the problem areas which are either unique to this system or not adequately solved elsewhere. These include, choice of a modulation method for the transmission of data and the design of suitable encoder and decoder circuits, provision of a fast reliable method of storage of the received data, and the design of a suitable error correction procedure for use throughout the system.

The system design enables data to be transmitted, stored on audio

cassette and finally displayed at a minimum data rate of 2400 baud. The error correction procedure reduces the probability of data error to less than 10^{-8} per transmitted bit, equivalent to an average of one error in every 10,000 low resolution pages, achieved with a code redundancy of 29%.

PREFACE

This thesis describes the design of an electronic method for the transmission of computer-coded text and graphics via Very High Frequency (V.H.F.) radio. The study was prompted by the desire to provide a more cost-effective means of delivery of teaching material to Open University students, than the present print-based method.

Each component of the resulting system design is described. Emphasis is placed on those elements of the design that were found to require original work, because they were either unique to this system, or had not been adequately investigated elsewhere.

These design areas include:-

(1) The choice of transmission method on the V.H.F. radio broadcast path, given the constraints on the system imposed by properties of that path and the need to employ the services and facilities of an external broadcasting authority.

The design of broadcast channel encoder and decoder circuitry.

(2) The design of a fast, reliable method of data storage for use with low-cost audio cassette recorders.

(3) The survey and measurement of data error rates throughout the

system and the resulting design of a suitable error correction procedure.

Material presented in this thesis has been the subject of two publications:-

Smith P. and Zorkoczy P.I., Data Recording on Audio Cassette, Wireless World, Vol. 88, No. 1553, February 1982, 50-52, 63.

Smith P. and Zorkoczy P.I., Radiotext, Paper to be presented to the 6th International Conference on Computer Communication, London, 7-10 September 1982 (I.C.C.C. Northwood Hills, Middlesex, England).

No part of this material has been submitted for a degree or other qualification at the Open University or at any other university or institution.

ACKNOWLEDGEMENTS

The work described in this thesis owes much to the advice and guidance of my supervisor, Dr. P.I. Zorkoczy. I am deeply grateful to him for making my period of study under his supervision such a worthwhile and rewarding experience.

I am indebted to the members of staff of the Electronics Discipline for many helpful discussions throughout the duration of the project. Particular thanks are due to Mr. N. Heap, for his assistance in the preparation of the experimental procedure to investigate multipath propagation, and Mr. N. Angoy, for his valuable help with circuit board construction. I am also grateful to Mr. S. Edwardson and Mr. D. Wright of the Research Laboratories of the British Broadcasting Corporation for their useful advice during early feasibility studies and for the loan of multipath simulation equipment.

Finally, it is important to me that I thank my wife, Ann Marie, for her continued encouragement and support throughout my studies at the Open University.

CONTENTS

LIST OF DIAGRAMS

LIST OF TABLES

LIST OF PHOTOGRAPHS

1. INTRODUCTION

The Open University was established in 1969 to enable adults to pursue courses leading to a first or higher degree. In 1982, it has some 60,000 undergraduate students and a further 20,000 associate students taking courses in the continuing education programme.

Students study at home, mainly through printed material in the form of specially prepared correspondence texts, set books and recommended reading. Facilities for practical work are provided by residential summer schools, and by experimental equipment supplied on loan to the student for the duration of the course. In addition, use is made of open-circuit radio and television broadcasts and recorded audio-visual material. Tuition and counselling is provided by part-time staff at study centres throughout the country. Computer terminals and audio-visual replay facilities are also provided at these centres.

At present, the University communicates with its students primarily by the postal service. This method of delivery is well tried and, in most cases, works satisfactorily. However, the time involved in both the preparation of printed material and its distribution through the postal system is such that rapid communication between University and student is not possible. As the pressure on material resources increases, and postal charges rise, the cost-effectiveness of the present method of communication becomes increasingly in doubt.

In an effort to improve the communication process, this study has involved the design of a system which will allow material in the form of computer-coded text and graphics to be transmitted over an unmodified V.H.F. radio broadcast network. Such computer-aided communication may provide a cost-effective alternative to the current methods of preparation and mailing of printed correspondence texts, particularly in rapidly changing topic areas where information committed to print becomes out of date in a short space of time.

To provide a realistic alternative delivery method, such a system needs to be:-

(1) low cost - to be acceptable for general use by the Open University, it was considered that implementation costs should not exceed £50 per student, and that operational costs should be significantly lower than those of the existing postal-based system.

(2) highly reliable - equipment supplied for student use needs to be robust with an expected life-span of 8 years or more. (In general, the cost of equipment supplied by the University is amortized over 8 years).

(3) multi-functional - e.g. usable for the delivery of computer software and audio-visual teaching material.

(4) simple and convenient to use

Prior to the formulation of an initial system design, existing information systems were examined for their suitability in this application.

Teletext systems have the advantage that, except for the initial purchase of the decoder, they provide simple text and graphic facilities at low cost. However, the limited number of 'pages' available for use imposes a severe constraint on the volume of data transmitted. Videotext systems have no such limitation on the volume of data, together with the considerable advantage of use in the interactive mode. The disadvantage of such systems is in their relatively high implementation and usage costs. Each access to the videotext computer involves separate telephone charges and would result in considerable expense for large volumes of data and high numbers of students.

In some European countries, notably Sweden and West Germany, and to a lesser extent in the United States of America, the V.H.F. radio broadcast network is used for the transmission of supplementary public information [1]. These data transmissions use the available frequency range above 53 kHz, the highest stereophonic channel 'difference' frequency (in the United States of America, this frequency range is called the 'supplementary carrier authorization' or S.C.A. channel).

Experience with these transmissions has shown that harmful interference can be caused to main programme reception [2]. This interference is the result of intermodulation products produced by non-linearities in the radio frequency stages of some receivers, and by multipath propagation. It is unlikely, therefore, that such transmissions will be authorized for use in the United Kingdom unless the transmission data rate is severely restricted.

Initial System Design

The inability of existing techniques to fulfil the requirements of the system led to an examination of suitable alternatives and to the proposal to use an unmodified V.H.F. radio broadcast transmission, outside normal hours. In this way, existing resources can be used to provide reliable data transmission without influencing the conventional service in any significant way. To ensure that the system is as acceptable as possible to the broadcast authority, the data transmissions must be compatible with existing broadcasting standards and be handled for transmission in a similar manner to conventional sound broadcasts.

By using the unmodified broadcasting service and, as a result, radio receivers of conventional design, the implementation costs of this component of the system should be low. The operating costs are dependent on the charges imposed by the broadcasting authority, which on a 'per-student' basis are expected to be small.

Transmission of data outside the normal schedule of the broadcast service implies that the system should be capable of unattended reception in the student's home. In consequence, the received data must be stored before being displayed by the student. Students make use of audio cassette recorders in their conventional study programme and therefore, to keep costs to a minimum, these recorders are used for data storage.

In addition to the radio receiver and audio cassette recorder, an interface unit is required in each student's home. This interface

provides the necessary channel encoding and decoding functions together with display generation facilities to enable the received data to be displayed on a conventional television or printed out on a low-cost printer supplied with the interface unit.

System Operation

A diagram of the Radiotext system is shown in Figure 1.1 . The material to be transmitted is prepared in a suitable format at the data preparation terminal, and given a header code to indicate for which group of students it is intended. It is then recorded onto magnetic tape and passed to the broadcasting authority.

Prior to receiving the transmissions, the student is required to set a time clock and select an identifier code on the interface. The audio cassette recorder is set to record although it will remain remotely switched off by the interface.

At the scheduled time for transmission, the radio receiver and interface are switched on by the time clock. The interface compares the header code of each item in the transmission with the identifier code previously entered by the student. Selected items are then automatically recorded onto audio cassette by switching the recorder on and off as required.

At a convenient time, the student may play back the recording through the interface unit for display on a television or printing out on the printer. Computer software is provided in serial format with a clock signal when required.

The system enables data to be transmitted, stored and displayed at a minimum data rate of 2400 baud. At this rate, it is possible to transmit and store on audio cassette the equivalent of approximately 400 low resolution (1 kilobyte) display 'pages' or 50 high resolution (8 kilobyte) display 'pages' during a single 30 minute transmission.

A suitable error correction procedure is used throughout the system which reduces the probability of data error to less than 10^{-8} per transmitted bit resulting in an average of one page in every 10,000 low resolution 'pages' or 1,200 high resolution 'pages' being in error.

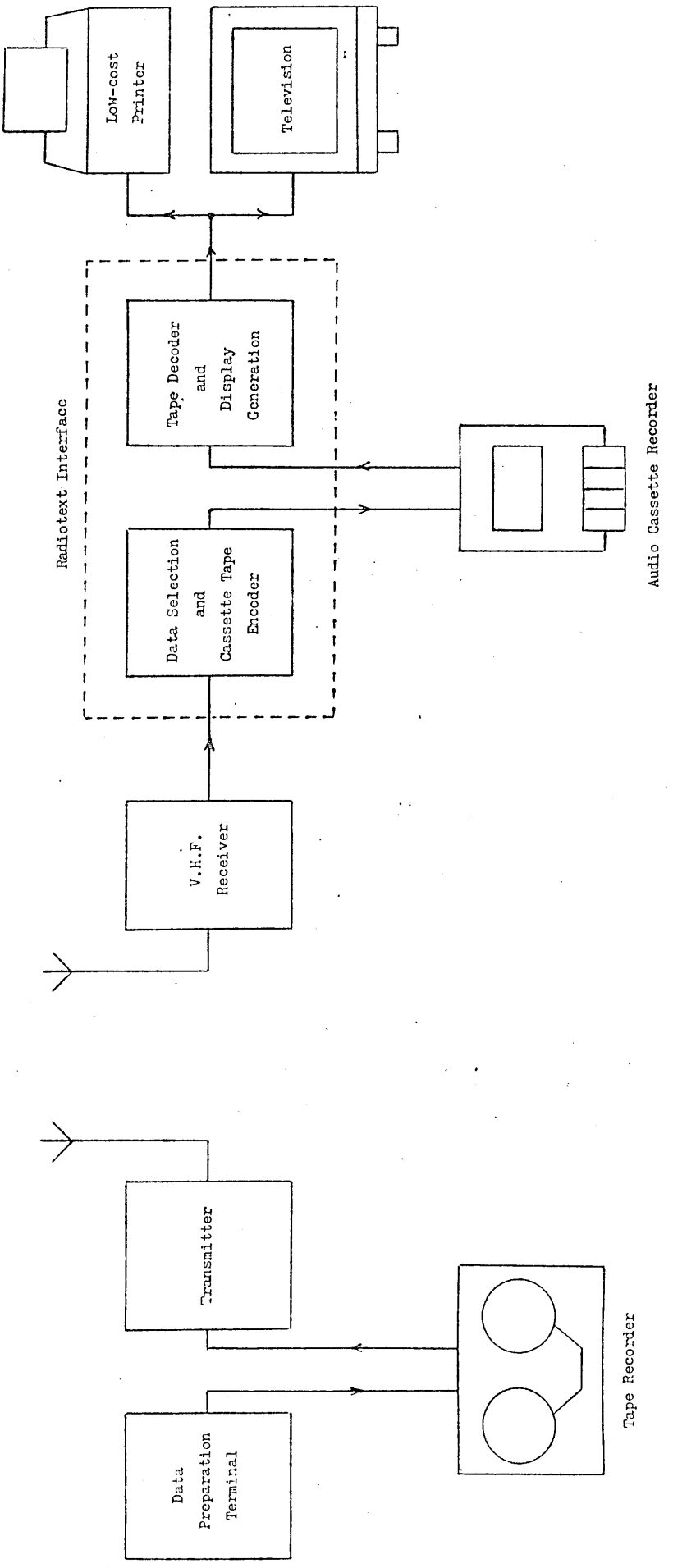

Figure 1.1 The Radiotext System.

2. DATA PREPARATION

The implementation of the data preparation terminal is based on a conventional microcomputer system as shown in Figure 2.1 .

The existing realisation of the system provides two display modes .

(1) Text and Low Resolution Graphics. A screen 'page' is made up of 24 lines of characters at 40 characters per line. The characters may be letters, figures or special symbols including coloured squares. They are formed by a dot matrix 7 dots high and 5 dots wide.

(2) High Resolution Graphics. Here a screen 'page' is made up of a matrix of 192 dots high and 280 dots wide.

Figure 2.1 shows examples of these two display modes.

The pages are created with the use of a generally available text and graphics screen editor. The Radiotext control software may be called from the editor at any time. Once each page is finalised, it may be temporarily stored on floppy disk or moved into a buffer area to be assembled into the correct Radiotext format.

Computer software, created at the terminal or on an external computer, may be loaded directly into this buffer area, via a serial interface

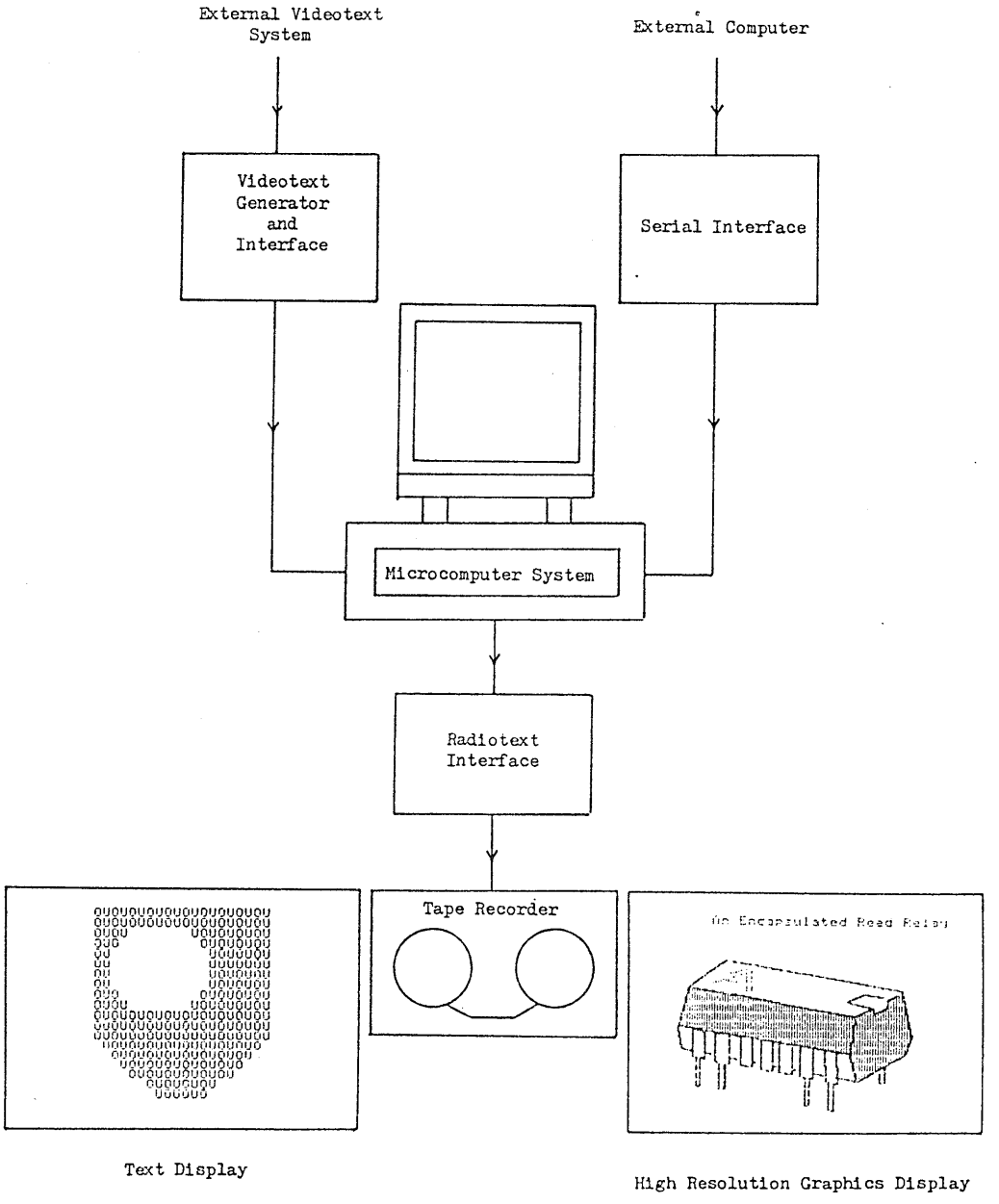

Figure 2.1 The data preparation system.

if necessary. In addition, the terminal is provided with a videotext facility, so that videotext compatible 'pages' may be created at the terminal, or received from external videotext systems such as 'Optel', the University's in-house videotext system.

In the buffer area, every page is divided into fixed length blocks to enable a block code error correction technique to be employed. Additional 'parity' rows are created, one per block, and are added to the end of a 'page'. Every block row (16 bytes of data) is given a row number. This row number identifies the display mode (low resolution, high resolution or software) and provides character level synchronization at the display interface.

In addition to these row numbers, each 'page' is given a header code. This code contains an identifier to indicate the group of students for which the 'page' is intended and a unique 'page' number to allow selection on display.

The formatting is sufficiently flexible to allow software of any length to be transmitted. Once this formatting is complete, the contents of the buffer area are recorded onto magnetic tape via a serial interface and coder circuit. The recording commences with the header code followed by the contents of the buffer. A 16 bit cyclic check character is added to each block row during recording.

3. RADIO BROADCAST

3.1 Introduction

The Open University, like the majority of educational and similar institutions for which a Radiotext service would be useful, does not control or have unlimited access to a radio broadcasting system. These facilities must be provided by an external broadcasting authority and, as a result, it is important that the system should be as acceptable as possible to such an organisation. It is necessary, therefore, to ensure that Radiotext transmissions are compatible with existing broadcasting standards, and that the procedures adopted for broadcasting are similar to those for conventional sound broadcasts.

3.2 System Constraints

Use of an unmodified broadcast service, together with the need for low cost implementation and subsequent operation, places constraints on the system design. These constraints are outlined below.

(1) It is unlikely that transmitter modification will be possible and therefore data transmission by employment of the 'supplementary carrier authorisation' channel, or by modulation of a 38 kHz subcarrier, is ruled out. Consequently, use must be made of the existing monophonic and stereophonic channels.

(2) A physical link for direct data transfer between the University and the broadcasting authority may not be available. As a result it will be necessary to record the data on magnetic tape prior to transmission.

(3) The amplitude response of the broadcast system is fully specified at each point of the transmission and reception process. However, the system phase response is of little consequence in conventional sound broadcasts (with the exception of stereo channel compatibility [3]), and, as a result, it is less well defined. There may not be sufficient consistency in the phase responses of the tape recorders, studio equipment, distribution network and transmitters making up the broadcast system, to enable accurate predictions of the overall system phase response to be made. Therefore, the modulation method used for data transmission needs to be tolerant to the phase distortion which may be created within the broadcast system.

(4) The cost of the radio broadcast channel decoder, part of the Radiotext interface required in every student's home, should be as low as possible. This low cost requirement must inevitably be reflected in the simplicity of the decoder design.

In addition to these constraints, the overall system design is influenced by the performance characteristics of the radio broadcast path.

Frequency-modulated V.H.F. radio broadcasts generally provide a signal of high quality with a bandwidth of 15 kHz per audio channel and a signal to noise ratio in excess of 60 dB. The main cause of signal

quality deterioration, particularly in stereophonic transmissions, is multipath propagation. For the listener, multipath propagation is mainly experienced as distortion of sibilants and breaking up of loud high frequency components of the signal. The influence of this type of distortion on data signals has not previously received attention in the literature. Therefore, it was necessary to examine multipath propagation in some detail in order to produce a system design which provided sufficient immunity from likely multipath effects.

In addition to multipath propagation, data signals are vulnerable to short duration impulse-type noise which is experienced at some receiver locations. This noise is rarely noticed in normal reception, however, its effect on data signals can be severe. The extent and effect of this noise required examination to ensure sufficient data protection was provided within the system.

3.3 Multipath Propagation

3.3.1 Introduction

Large obstructions such as tall buildings, mountains and the like, reflect frequency-modulated V.H.F. radio broadcast waves. Multipath propagation is caused by the simultaneous reception of the direct and reflected signals. The reflected signals are time-delayed and attenuated versions of the direct signal and result in the introduction of harmonic distortion into the detected audio signal.

The first major analysis of this distortion was made by Crosby [4] following attempts to use frequency modulation at transmission frequencies within the high frequency band (3 - 30 MHz). At these

frequencies, propagation is primarily via the ionosphere, so transmissions of similar strength may be received over different path lengths, resulting in severe signal distortion. Corrington [5] showed the existence of similar distortion at V.H.F. In this case, the reflection from physical objects is such that the delayed wave is usually sufficiently attenuated for the consequent distortion to be less severe.

In general, the level of multipath-induced distortion in monophonic V.H.F. broadcast transmissions is acceptably low. As a result, little attention has been given in the literature to investigation of the levels of multipath propagation likely to be experienced in practice. In stereophonic broadcasts, however, the effects of multipath are significant and considered by some to be the major cause of signal degradation [6,7]. In these transmissions, the harmonic distortion produced in the sum channel (L + R) moves into the difference channel (L - R) and affects both upper and lower sidebands. In addition, intermodulation products are produced between the harmonics and the 19 kHz stereo pilot tone. The distortion is thus more severe and coupled with crosstalk between the channels [8].

It is important that the presence of multipath propagation should not reduce the reliability of Radiotext data transmissions. The simple theoretical analysis of section 3.3.2 identified the factors which influence the level and character of the distortion. Conclusions from this analysis were confirmed by laboratory tests using a multipath simulator (3.3.3). It was then possible to select suitable transmission parameters to minimise the influence of the multipath propagation on the data signal (3.3.4).

3.3.2 Theoretical Analysis

To simplify the following discussion, it is useful to restrict the analysis to the transmission of a sinusoidally modulated wave with two path transmission, where one path is longer than the other by a fixed distance. To expression (8), the analysis follows that of Crosby [9] and Corrington [10].

Let e_d and e_r be the direct and reflected wave at the receiver respectively, given by

$$e_d = E_d \sin \left(\omega_c t + \frac{f_d}{f_m} \sin 2\pi f_m t\right) \qquad .....(1)$$

$$e_r = E_r \sin \left[\omega_c (t-t_o) + \frac{f_d}{f_m} \sin 2\pi f_m (t-t_o)\right], \qquad .....(2)$$

where, E_d is the amplitude of the direct wave (V)

E_r is the amplitude of the reflected wave (V)

ω_c is the carrier angular frequency (rad s^{-1})

f_m is the modulating frequency (Hz)

f_d is the frequency deviation (Hz)

t_o is the time delay between the direct and reflected waves (s)

From Figure 3.1 , the amplitude E of the resultant $E_d + E_r$ is given by the cosine rule,

$$E = \sqrt{E_d^2 + E_r^2 + 2 E_d E_r \cos \theta} \qquad .....(3)$$

where θ is the angle between the two phasors, given by the difference between the expressions for the angles of the two waves e_d and e_r.

$$\theta = \left[\omega_c t + \frac{f_d}{f_m} \sin 2\pi f_m t\right] - \left[\omega_c (t-t_o) + \frac{f_d}{f_m} \sin 2\pi f_m (t-t_o)\right]$$

$$\theta = \omega_c t_o + \frac{f_d}{f_m} \sin 2\pi f_m t - \frac{f_d}{f_m} \sin 2\pi f_m (t-t_o)$$

$$\theta = \omega_c t_o + 2 \frac{f_d}{f_m} \sin \pi f_m t_o \cos (2\pi f_m t - \pi f_m t_o). \qquad .....(4)$$

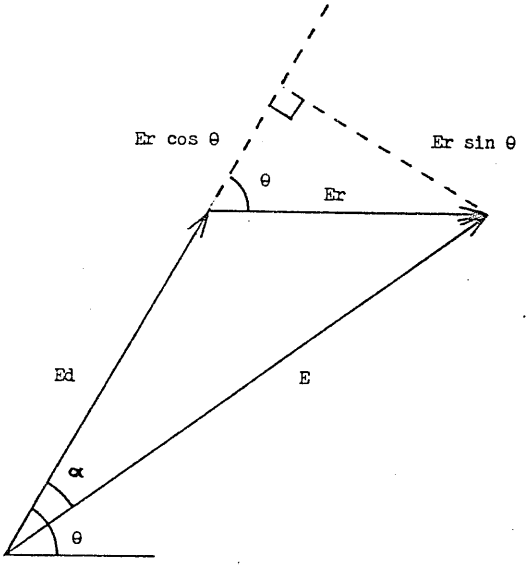

Figure 3.1 The phasor diagram of the direct and reflected waves at an arbitrary point in time.

By substituting (4) into (3), the expression for E becomes

$$E = \sqrt{E_d^2 + E_r^2 + 2 E_d E_r \cos\left[\omega_c t_o + 2 \frac{f_d}{f_m} \sin \pi f_m t_o \cos (2\pi f_m t - \pi f_m t_o)\right]} \qquad .....(5)$$

The angle α between the resultant voltage E and the direct wave E_d is given by

$$\tan \alpha = \frac{E_r \sin \theta}{E_d + E_r \cos \theta}$$

$$= \frac{R \sin \theta}{1 + R \cos \theta} \qquad \ldots\ldots(6)$$

where $R = \frac{E_r}{E_d}$, the ratio of the amplitude of the reflected wave to that of the direct wave.

From (4), (5) and (6) the equation for the resultant voltage, $e = e_d + e_r$, is

$$e = \sqrt{E_d^2 + E_r^2 + 2 E_d E_r \cos \left[2 \frac{f_d}{f_m} \sin \pi f_m t_o \cos (2\pi f_m t - \pi f_m t_o) + \omega_c t_o \right]}$$

$$X \sin \left[\omega_c t + \frac{f_d}{f_m} \sin 2\pi f_m t - \arctan \frac{R \sin \left\{ \omega_c t_o + 2 \frac{f_d}{f_m} \sin \pi f_m t_o \cos(2\pi f_m t - \pi f_m t_o) \right\}}{1 + R \cos \left\{ \omega_c t_o + 2 \frac{f_d}{f_m} \sin \pi f_m t_o \cos(2\pi f_m t - \pi f_m t_o) \right\}} \right] \qquad \ldots\ldots(7)$$

Provided R is less than 1 (which is a reasonable assumption, as the reflected wave is attenuated), the receiver limiter stage should prevent the variation in resultant carrier amplitude E from having any effect on the output of the discriminator. This output is, therefore, proportional to the instantaneous frequency of e.

$$\text{Discriminator Output} = \frac{K}{2\pi} \frac{d(\text{ angle of e })}{dt}$$, where K (V Hz^{-1}) is discriminator constant.

Substituting from (7),

$$\text{Discriminator Output} = \frac{K}{2\pi}\frac{d}{dt}\left[\omega_c t + \frac{f_d}{f_m}\sin 2\pi f_m t - \arctan\frac{R\sin\left\{\omega_c t_o + 2\frac{f_d}{f_m}\sin\pi f_m t_o \cos(2\pi f_m t - \pi f_m t_o)\right\}}{1 + R\cos\left\{\omega_c t_o + 2\frac{f_d}{f_m}\sin\pi f_m t_o \cos(2\pi f_m t - \pi f_m t_o)\right\}}\right]$$

$$= K\left[f_c + f_d\cos 2\pi f_m t + \frac{\dfrac{2 f_d \sin\pi f_m t_o \sin(2\pi f_m t - \pi f_m t_o)}{\frac{1}{R} + \cos\left\{2\frac{f_d}{f_m}\sin\pi f_m t_o \cos(2\pi f_m t - \pi f_m t_o) + \omega_c t_o\right\}}}{R + \cos\left\{2\frac{f_d}{f_m}\sin\pi f_m t_o \cos(2\pi f_m t - \pi f_m t_o) + \omega_c t_o\right\}} + 1\right]$$

The discriminator will remove the carrier frequency component Kf_c. $Kf_d \cos 2\pi f_m t$ is the desired signal component and therefore the third term represents the distortion.

$$\text{Distortion component at output} = K\left[\frac{R^2 + R\cos\left\{2\frac{f_d}{f_m}\sin\pi f_m t_o \cos(2\pi f_m t - \pi f_m t_o) + \omega_c t_o\right\}}{R^2 + 2R\cos\left\{2\frac{f_d}{f_m}\sin\pi f_m t_o \cos(2\pi f_m t - \pi f_m t_o) + \omega_c t_o\right\} + 1}\right.$$
$$\left. X\ 2 f_d \sin\pi f_m t_o \sin(2\pi f_m t - \pi f_m t_o)\right] \qquad \ldots\ldots(8)$$

This expression can be resolved into a Fourier series in order to calculate the level of distortion for various parameter values[11,12].

For the transmission of data, where waveform integrity is more important than sound quality, it is useful to examine the characteristics of the distortion waveform to give a physical picture of the distortion experienced.

Figure 3.2 , in essence a repeat of Figure 3.1 , shows a phasor representation of direct wave e_d , reflected wave e_r and resultant e . In this case, E_d is the reference phasor.

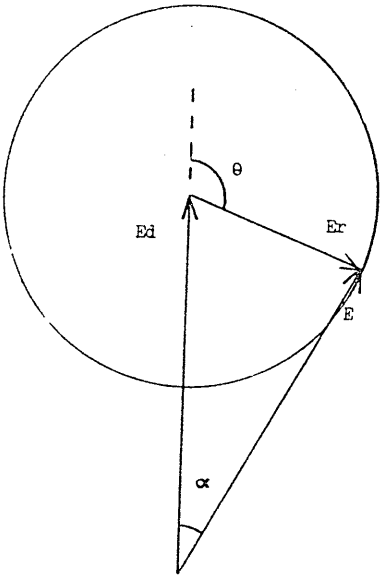

Figure 3.2 Phasor diagram of the direct and reflected waves with E_d taken as reference.

As shown previously in the expression for the discriminator output, the distortion produced at the output of the discriminator is proportional to the rate of change of angle α .

As E_r rotates about E_d , with say a clockwise rotation, the rate of change of α will peak at $\theta = 0^\circ$, with E rotating clockwise with respect to E_d . As θ approaches 90°, the rate of change of α reduces, eventually to zero, before increasing again to peak at $\theta = 180^\circ$. In this case, dependent on the ratio R , the peak is significantly greater than that at $\theta = 0^\circ$, with E now rotating anticlockwise with respect to E_d . At $\theta = 270^\circ$, the rate of change of α is again zero

and rises once more as θ approaches 0^{o}. The distortion is, therefore, periodic with asymmetrical amplitude peaks. The highest peak (at $\theta = 180^{o}$) is positive when the instantaneous frequency of e_r is below that of e_d , and negative when the instantaneous frequency of e_r is above that of e_d .

The frequency of the distortion, f , is the frequency of rotation of E_r about E_d . This is the difference in frequency between e_r and e_d . It is found directly from expressions (1) and (2),

$$f = f_d \sin 2\pi f_m t - f_d \sin 2\pi f_m (t - t_o).$$

$$\text{Therefore , } \quad f = 2 f_d \sin \pi f_m t_o \cos (2\pi f_m t - \pi f_m t_o) \qquad .....(9)$$

This expression shows that the frequency of the distortion varies sinusoidally at a rate determined by the modulating signal frequency, f_m . It is demonstrated diagramatically in Figure 3.3 , which shows the reflected wave e_r delayed in time by t_o seconds from direct wave e_d .

At points c and g, the frequencies of e_d and e_r are equal and hence the distortion frequency is zero. Either side of these points, the distortion frequency rises as the frequency difference between e_d and e_r rises, until, at points a and e, it reaches a maximum. At these points, in the example with $t_o = \frac{1}{6f_m}$, $f = f_d$.

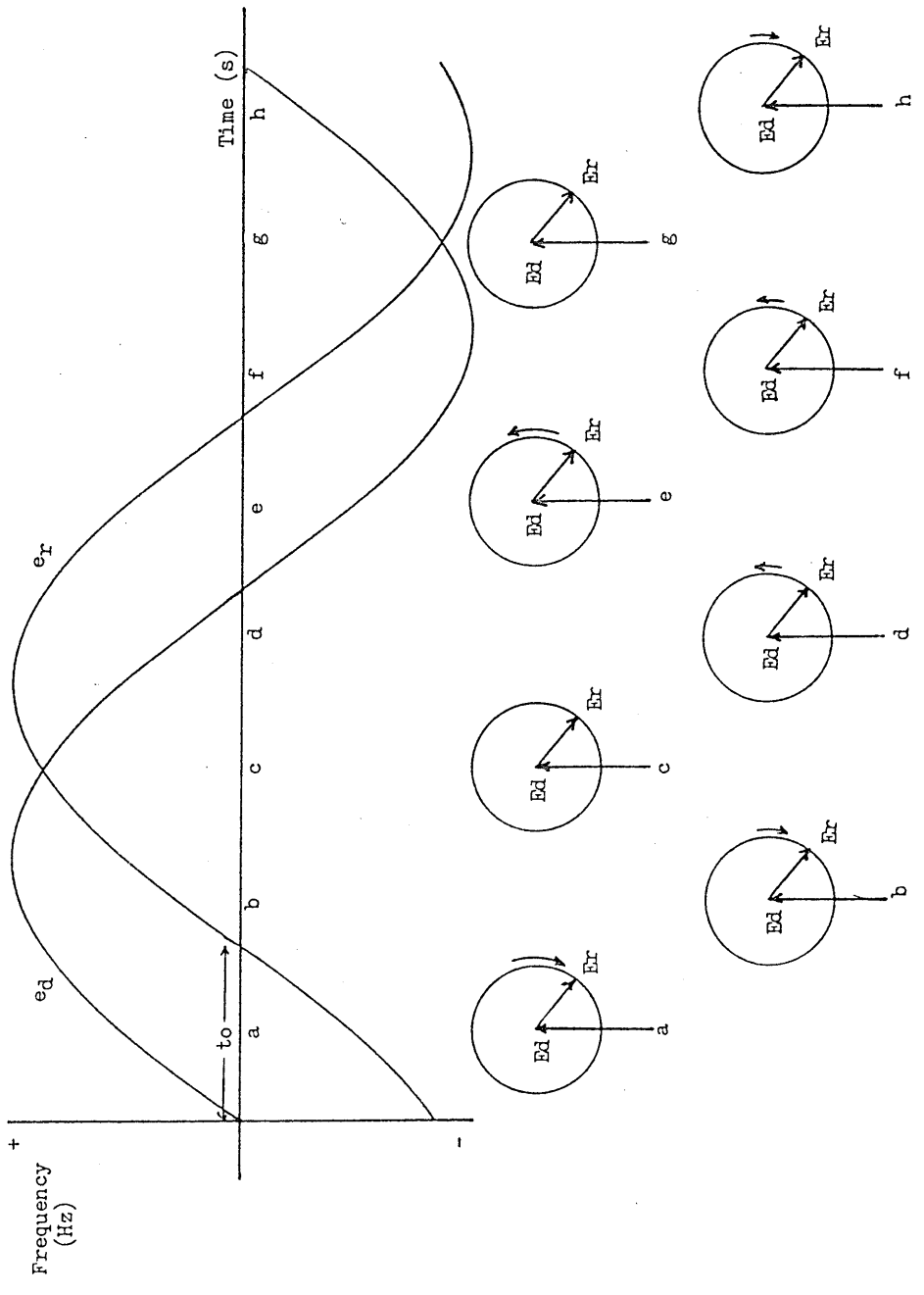

Figure 3.3 Instantaneous frequencies of direct and reflected waves with phasor representation of these waves at selected points in time.

An example of the resulting distortion waveform (superimposed upon the desired output signal) is shown in Figure 3.4 .

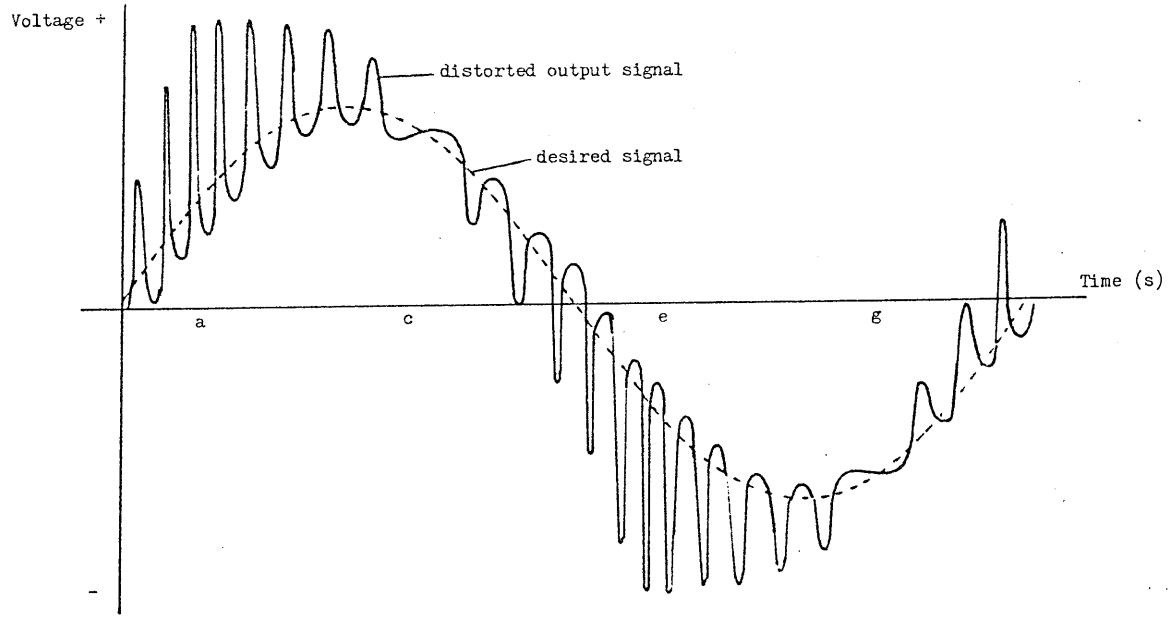

Figure 3.4 Distorted output waveform.

The peakiness of the distortion component increases as R increases, up to a limit imposed by the bandwidth and phase shift characteristics of the receiver. Practical levels of multipath propagation are, however, unlikely to be such that E_r is more than a small fraction of E_d , ($R < 0.2$). In this case, the distortion component will appear to be more symmetrical.

When R is small, a useful simplification of the expression for the distortion component of the output signal can be made [13]. The distortion output in this case can be likened to a sinusoidally phase modulated wave, because the angle α remains small and the amplitude E remains close to E_d .

The peak frequency deviation of a phase modulated wave is given by

$$\text{Deviation} = \phi F_m$$

where, ϕ is the peak phase deviation, and

F_m is the modulating frequency.

Therefore, from Figure 3.2 the peak frequency deviation produced by the rotation of E_r about E_d is given by

$$F_d = \alpha f \qquad \text{.....(10)}$$

For small angles, and α measured in radians,

$$\alpha = \tan \alpha$$

$$\text{Therefore,} \quad \alpha = \frac{E_r}{E_d} = R.$$

From (9) and (10), the distortion component at the output of the discriminator becomes

$$\text{Distortion} = K\left[\left\{2 R f_d \sin\pi f_m t_o \cos\left(2\pi f_m t - \pi f_m t_o\right)\right\} \sin 2\pi\left\{2 f_d \sin\pi f_m t_o \cos\left(2\pi f_m t - \pi f_m t_o\right)\right\} t\right] \qquad \text{.....(11)}$$

For small values of R, equation (11) may be extremely useful for predicting the influence of the various transmission parameters on the distortion waveform. It shows that the distortion has a frequency modulated waveform, sweeping sinusoidally between limits of $\pm 2f_d \sin\pi f_m t_o$, at a rate determined by the frequency of the modulating signal. With the delay expressed in terms of the phase of the modulating signal, the largest frequency sweep will occur with a

delay of $n\pi$ radians ($n = 1,3,5 \ldots$), i.e. when the delay t_o is equal to half the period of the modulating signal.

The amplitude of the distortion is given by KRf and is, therefore, proportional to the distortion frequency, reaching a peak when the frequency peaks and falling to zero when the frequency falls to zero. Thus, the distortion component is both amplitude and frequency modulated and contains frequency components well above the peak sweep frequency given by $2f_d \sin\pi f_m t_o$.

The characteristic relationship between modulating frequency and distortion is shown in Figure 3.5 . In this example, the modulating frequency is plotted against the peak amplitude of the distortion as a percentage of the amplitude of the desired signal.

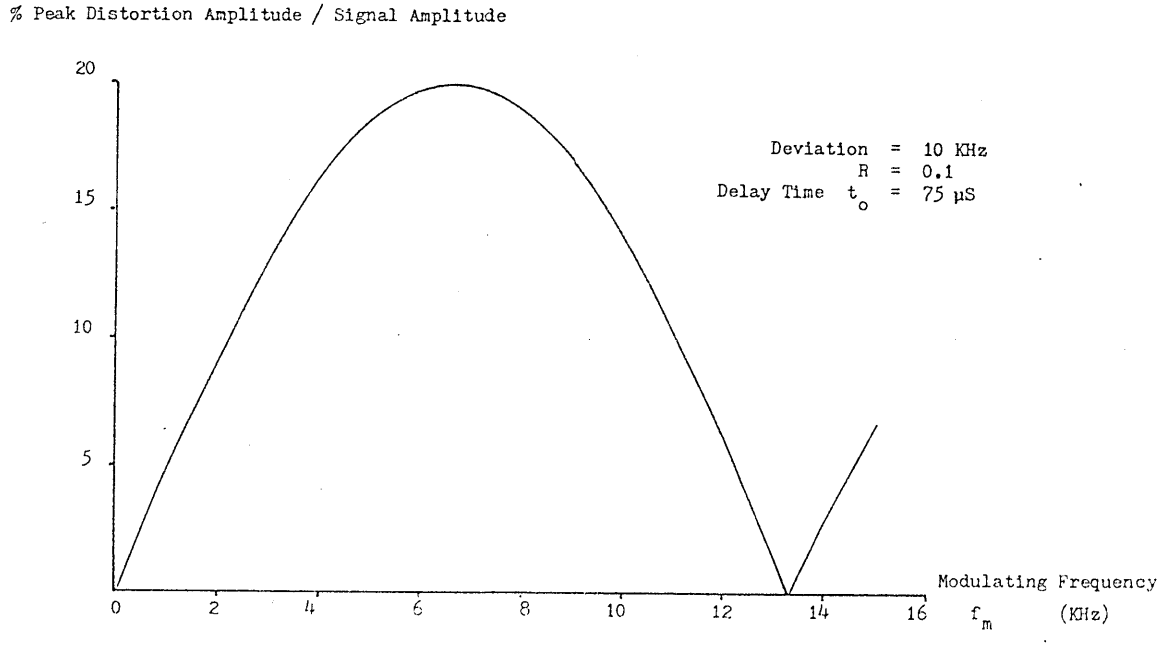

Figure 3.5 The relationship between modulating frequency and peak distortion amplitude.

The peak distortion reaches a maximum at $f_m = \frac{1}{2t_o}$, and zero at $f_m = \frac{1}{t_o}$. Consequently, the shorter the delay time the higher will be the modulating frequency that produces maximum distortion. For example, as shown in Figure 3.5 , a delay of 75 μs produces maximum distortion at 6.67 kHz. If the delay is reduced to 25 μs, the modulating frequency for maximum distortion increases to 20 kHz.

The relationship between the modulating frequency f_m and the delay time t_o, to produce the highest distortion component, is shown in Figure 3.6 .

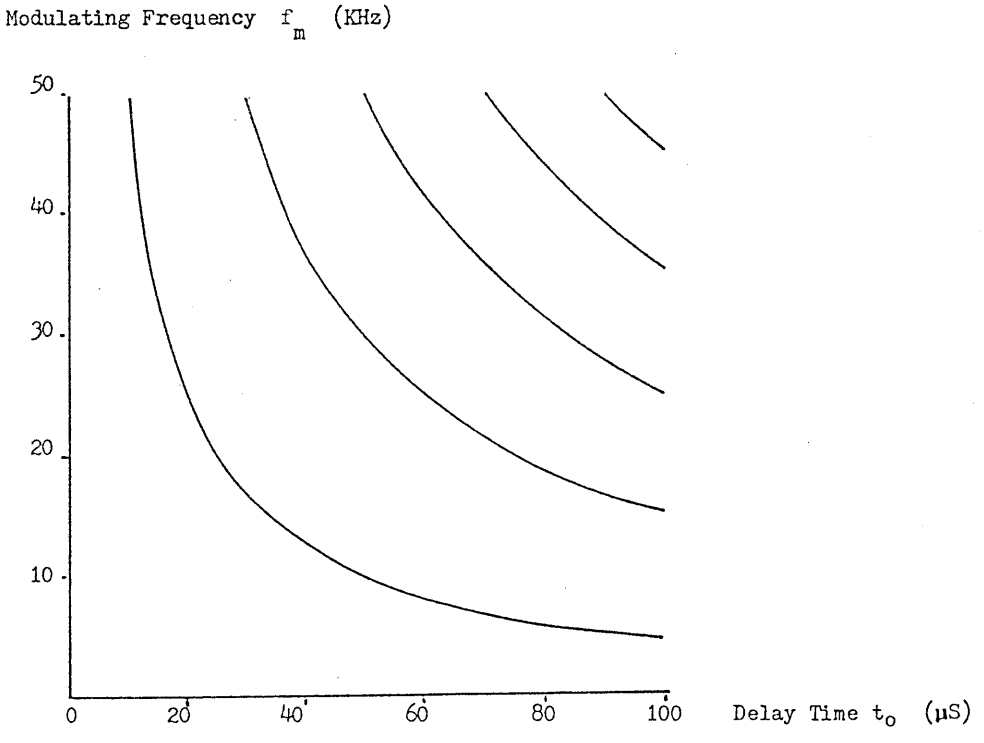

Figure 3.6 Relationship between modulating frequency and delay time at points of maximum distortion.

At points on the curves of Figure 3.6, the distortion frequency reaches its highest value of $2f_d$, and the peak amplitude its highest value of $2KRf_d$.

To confirm the results of this analysis, and examine the consequences of R rising to higher levels, a laboratory experiment was set up to measure the distortion experienced in practice.

3.3.3 Practical Analysis (by Laboratory Simulation)

Introduction

This experimental procedure was set up to confirm the results of the theoretical analysis and to examine the effects of high values of R, the ratio of the amplitude of the reflected wave to that of the direct wave.

With the use of a multipath simulator, it was possible to simulate multiple path reception over the range of delay times likely to be experienced in practice [14].

Experimental Technique

The multipath simulator used for the laboratory simulation operated at 90 MHz and provided a bandwidth of 550 kHz at this frequency. The delay lines within the simulator consisted of a variable delay unit with a range of 0 to 15.9 μs, followed by a series of seven units each giving a fixed delay of 12.5 μs. Thus, it was possible to provide delay times up to approximately 100 μs, representing a difference in path length of approximately 30 Km.

A variable attenuator in the delayed signal path of the simulator enabled the value of R to be varied from 0 to 1. In addition, the phase of the reflected carrier component could be varied through 360° with respect to the carrier of the direct wave.

A schematic diagram of the test circuit is shown in Figure 3.7.

The sinusoidal modulating signal, at frequencies of 1 kHz to 15 kHz in 1 kHz steps, was produced by a high quality signal generator. Before being applied to an F.M. signal generator, it was passed through a spectrum shaper to reduce the relative amplitude of harmonic components to less than -60 dB. Following this filtering, the modulating signal was frequency modulated onto a carrier of 90 MHz.

The frequency modulated signal, with a deviation of 10 Hz, and subsequently 20 kHz, was then applied to the multipath simulator. In the majority of tests, delays from 12.5 μs to 87.5 μs in steps of 12.5 μs were used with values of R from 0.05 to 0.2 in steps of 0.05, and from 0.2 to 1.0 in steps of 0.2. The carrier frequencies of the direct and delayed signals, initially kept in phase, were later varied from 0° to 360° in steps of 45°, to determine the effect of carrier phase on the resultant distortion.

The output of the simulator was taken directly to an F.M. receiver tuned to 90 MHz. A fast Fourier transform analyser was used to examine the output of the receiver discriminator. The analyser was controlled by a minicomputer, and provided a display of the average frequency spectrum from 16 successive samples of the discriminator output, as the minicomputer calculated the percentage total harmonic distortion.

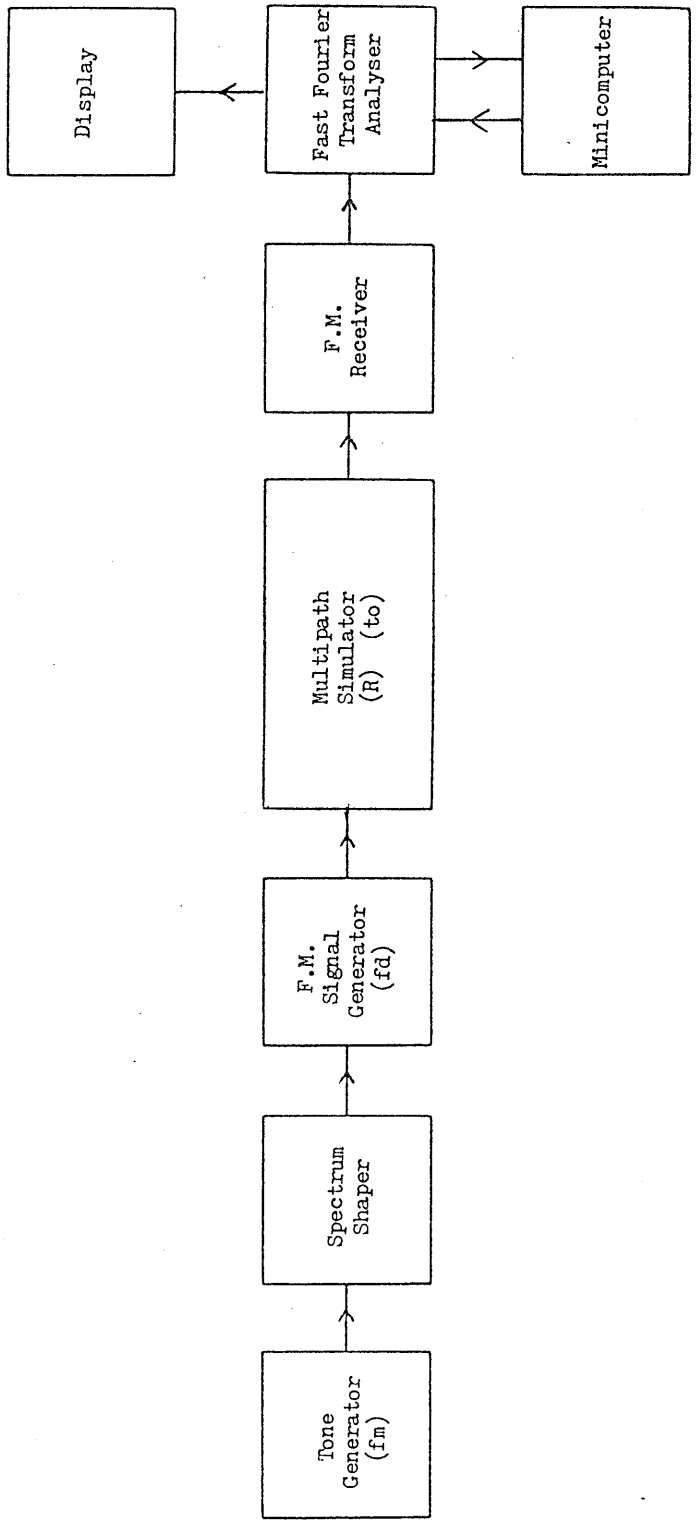

Figure 3.7 Laboratory simulation test circuit.

Results

The relationship between total harmonic distortion and modulating frequency is typified by Figures 3.8 and 3.9 .

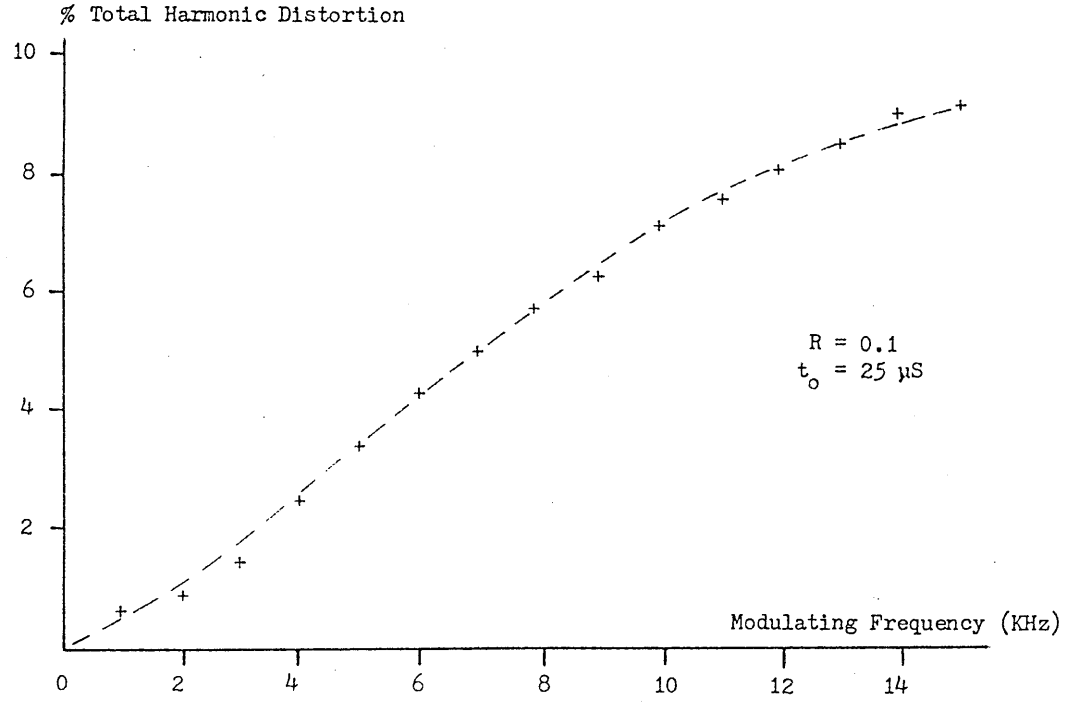

Figure 3.8 Relationship between distortion and modulating frequency

Delay time t_o = 25 µs

In Figure 3.8, with R = 0.1 and delay time t_o = 25 µs, the distortion increases steadily as the modulating frequency increases, in the manner expected from the analysis of section 3.3.2 . Figure 3.6 predicts that the distortion will reach maximum at 20 kHz and this is borne out by the extrapolation of the curve of Figure 3.8 .

Figure 3.9 shows that, with a delay of 75 µs, the distortion rises more sharply with frequency, reaching maximum at approximately 6.5 kHz and

then falling to zero at approximately 13 kHz before rising once again. Comparison of Figures 3.5 and 3.9 demonstrates the close relationship between the predicted distortion levels (Figure 3.5) and those found in practice (Figure 3.9).

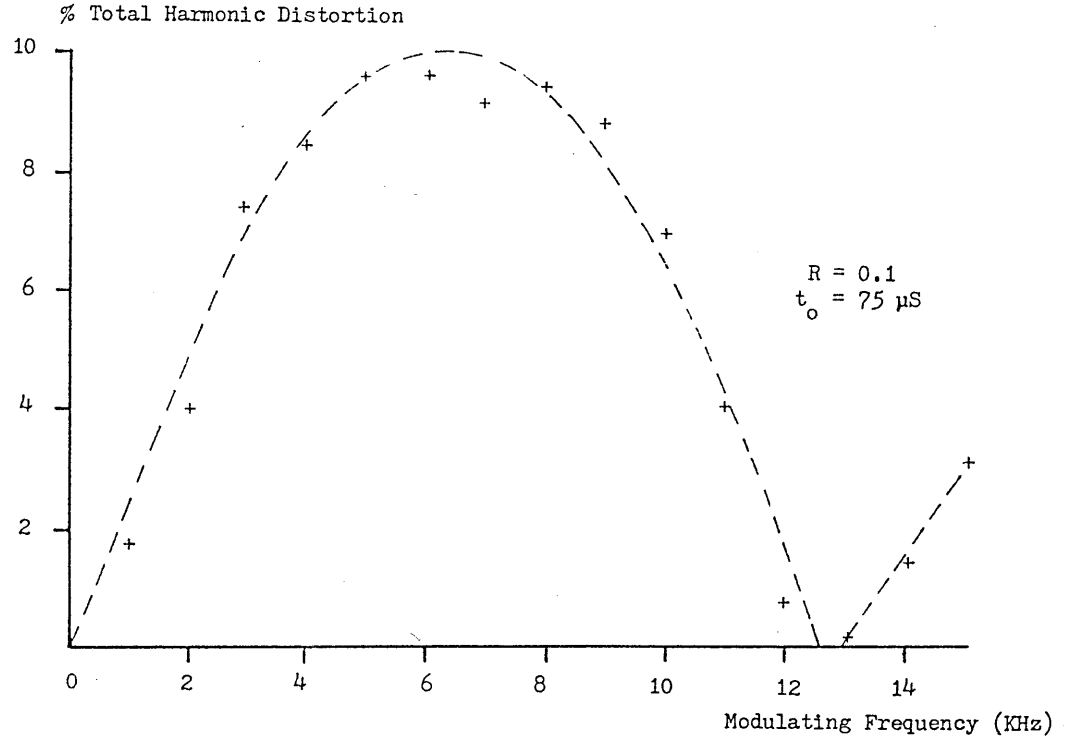

Figure 3.9 Relationship between distortion and modulating frequency
Delay time t_o = 75 μs

Figures 3.10 and 3.11 show the relationship between distortion and delay time for values of modulating frequency of 3 kHz and 12 kHz respectively. Again these curves show that, as predicted, maximum distortion occurs with $f_m = \frac{1}{2t_o}$. Extrapolation of Figure 3.10 shows the delay time to give maximum distortion is in the region of 120-150 μs (theoretically 166 μs) at a modulating frequency of 3 kHz and Figure 3.11 shows this delay time to be approximately 40 μs (theoretically 42 μs) at the higher modulating frequency of 12 kHz.

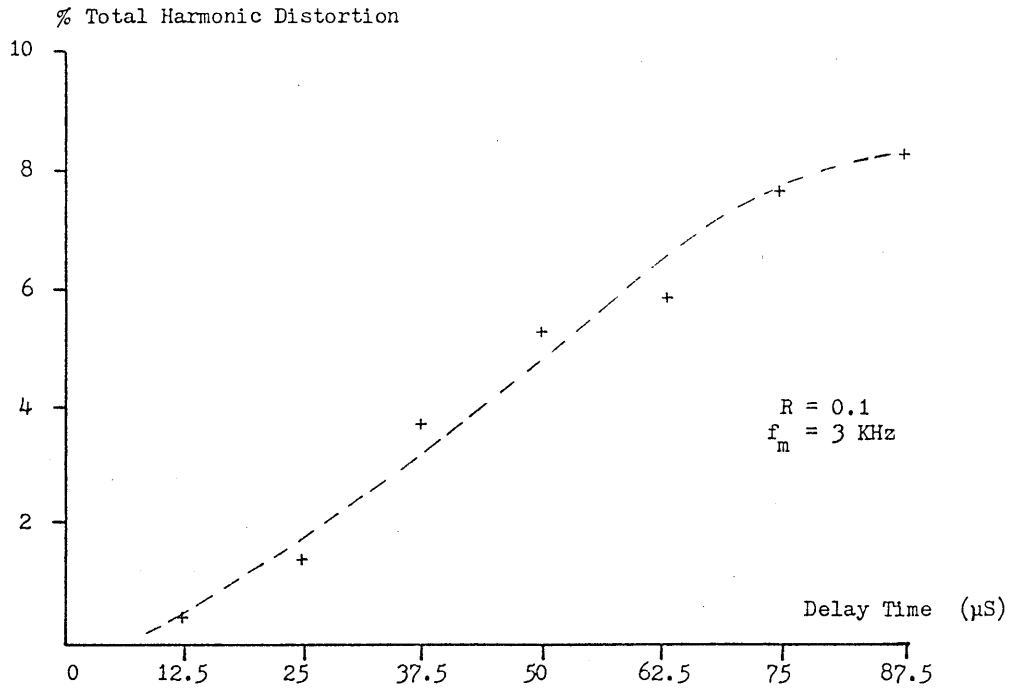

Figure 3.10 Relationship between distortion and delay time

Modulation frequency f_m = 3 kHz

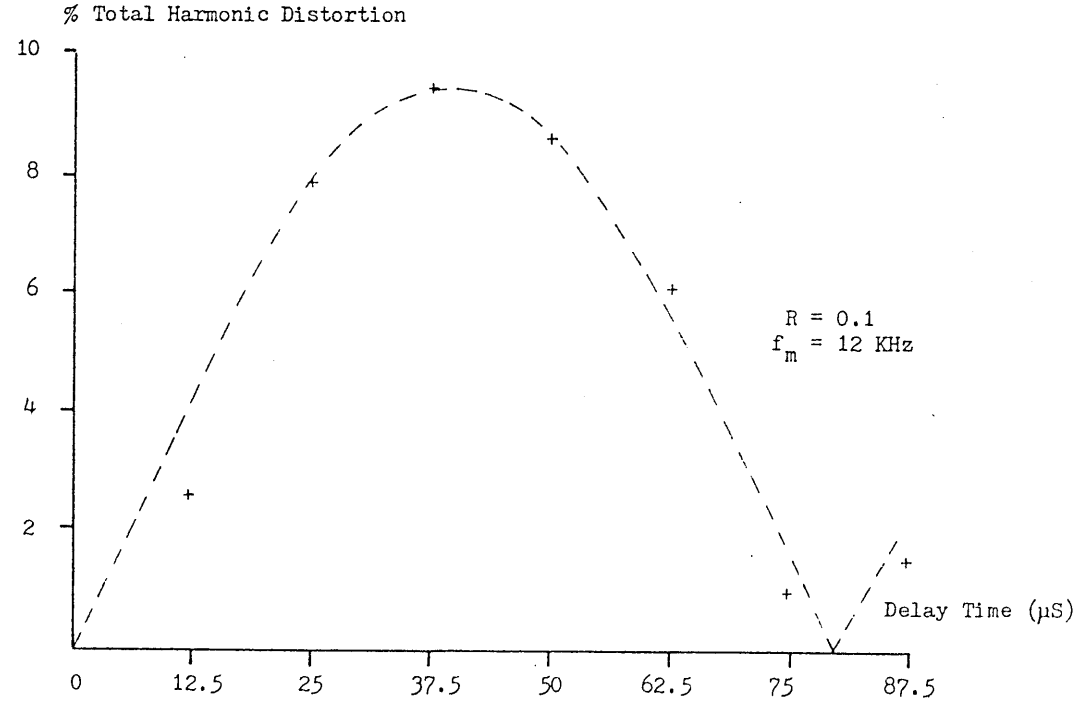

Figure 3.11 Relationship between distortion and delay time

Modulation frequency f_m = 12 kHz

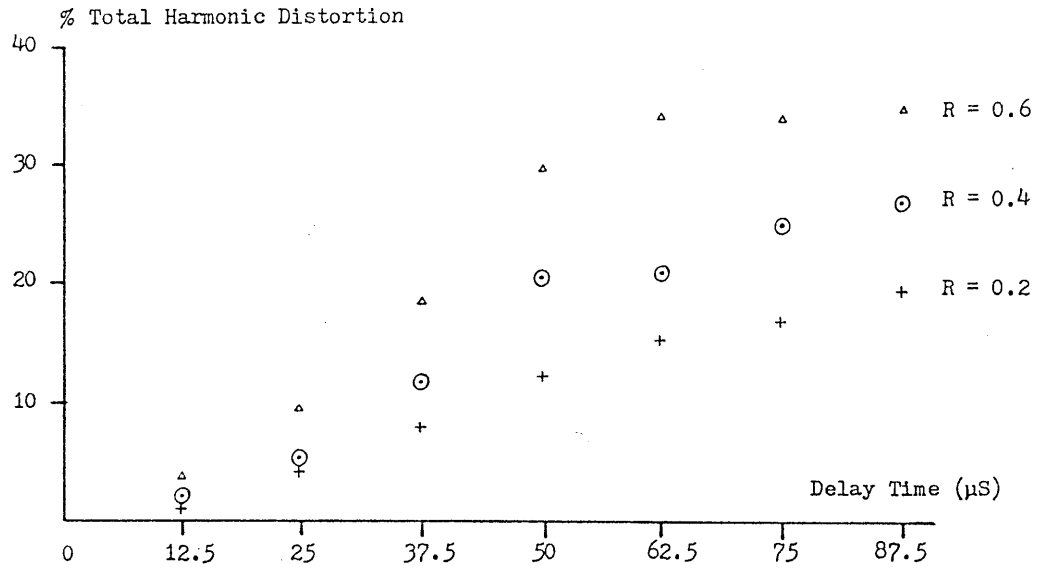

Figure 3.12 Influence of R on distortion-time delay curves

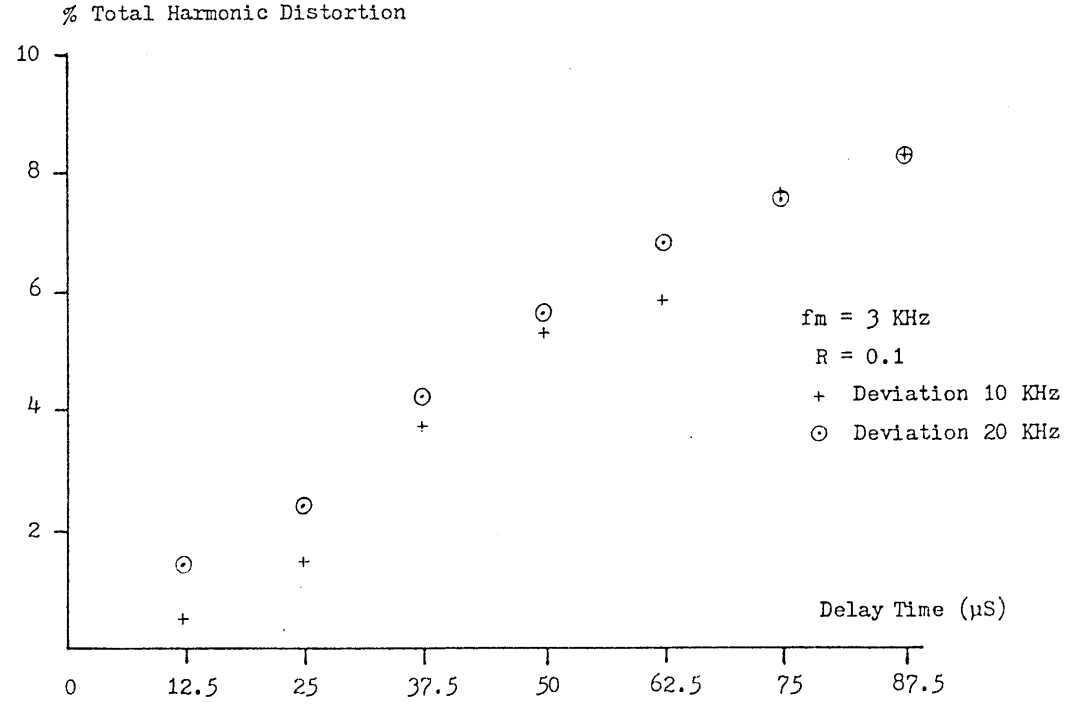

Figure 3.13 Influence of frequency deviation on the distortion-time delay curves

The effect of R is shown in the example of Figures 3.12 . As R is increased up to 0.6, the distortion increases in proportion. Above R = 0.6, however, values of distortion vary widely, with the distortion-time delay curves departing from their characteristic shape. Figure 3.13 shows the result of increasing the frequency deviation, f_d, of the transmitted signal.

In general, frequency deviation has little effect on the measured total harmonic distortion. It does, however, influence the bandwidth of the distortion components within the discriminator output signal, as shown in Figures 3.14 and 3.15 .

Figure 3.14 shows the frequency spectrum of the discriminator output signal with the transmission parameters shown and a transmitted frequency deviation of 10 kHz. In figure 3.15, the transmitted frequency deviation is increased to 20 kHz. Comparison of these figures reveals that this increase in frequency deviation has caused the bandwidth of the multipath distortion components to increase from approximately 20 kHz (Figure 3.14) to approximately 30 kHz (Figure 3.15), even though, as Figure 3.13 shows, the total harmonic distortion has increased less significantly from 5.2% to 5.7%.

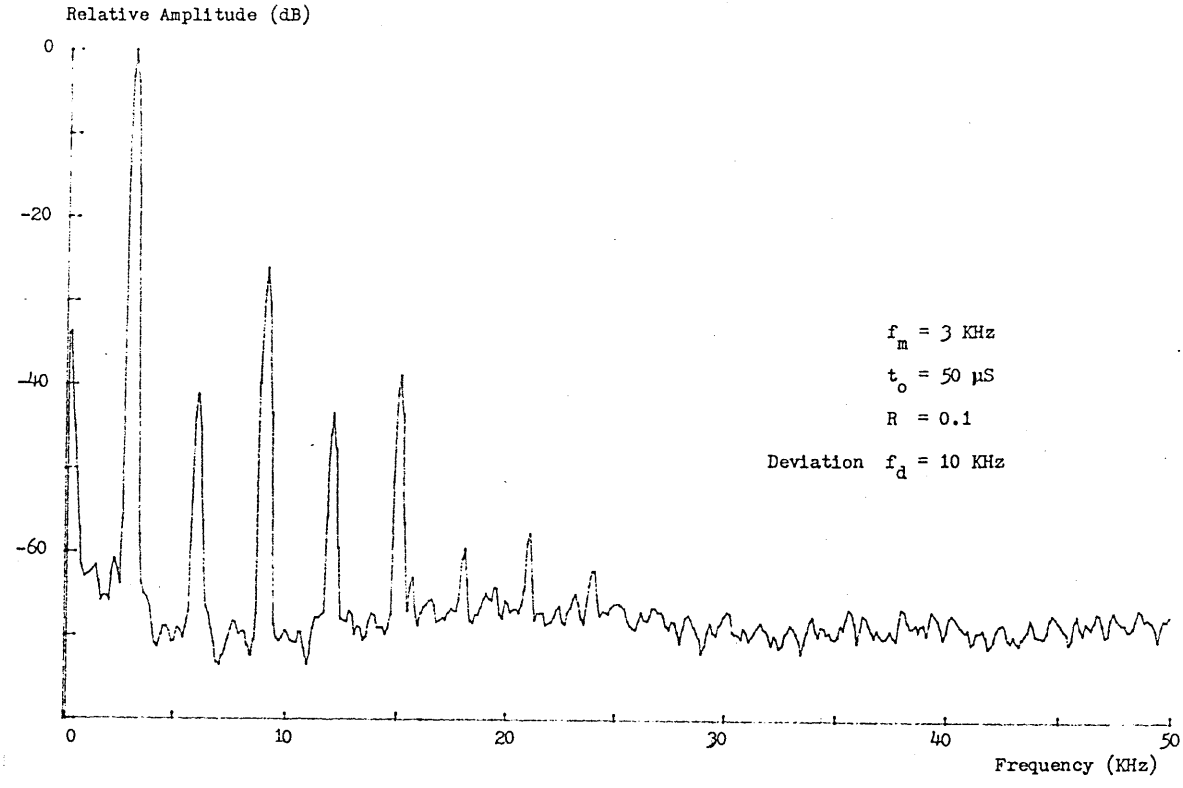

Figure 3.14 Frequency spectrum of discriminator output (f_d = 10 kHz).

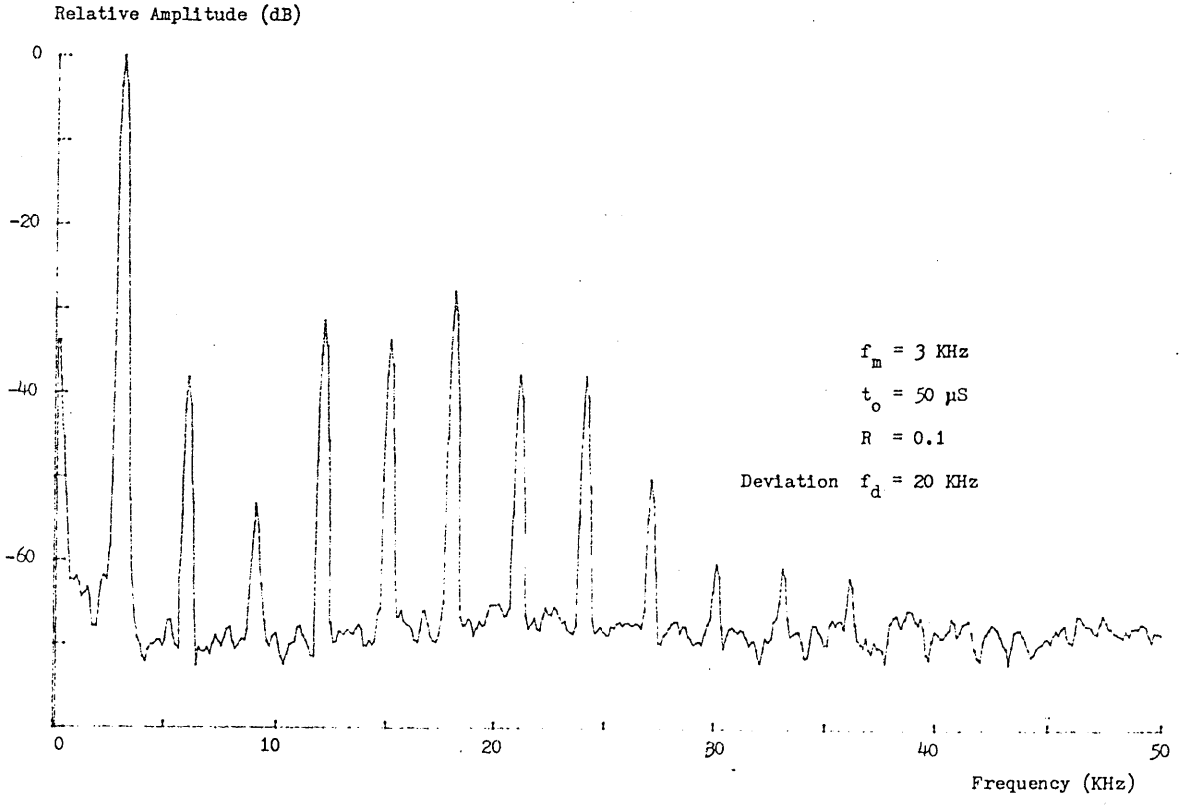

Figure 3.15 Frequency spectrum of discriminator output (f_d = 20 kHz).

The results of the test to examine the influence of the relative phase angle between the radio frequency carriers of the reflected and direct signals, show that, in general, the influence of this phase angle on total harmonic distortion is small except at high modulating frequencies with high values of R.

An example of the influence of the phase angle on the distortion is given in Figure 3.16 .

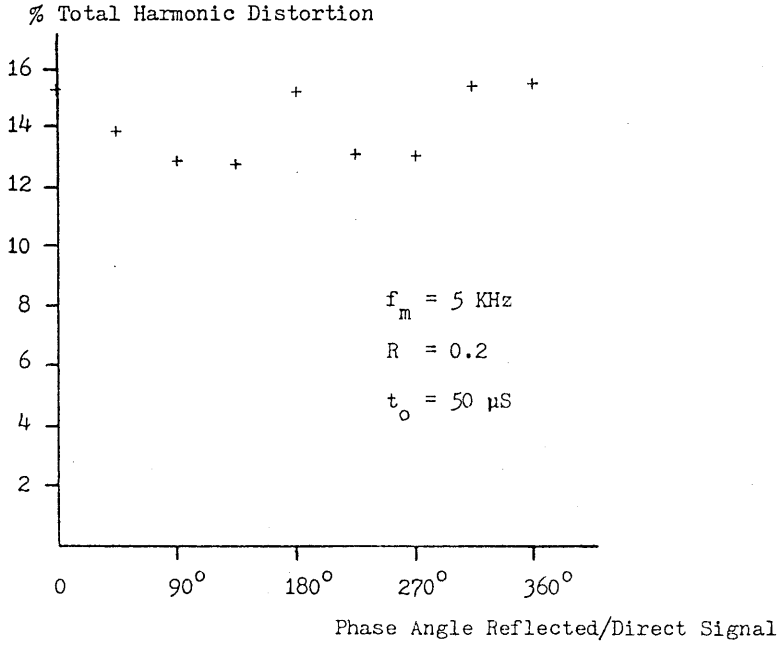

Figure 3.16 Influence of the relative phase angle between the carriers of the direct and reflected signals on the distortion

Conclusions

The practical examination of multipath propagation has shown the influence of the modulating frequency and delay time on distortion levels to be close to that described by equation (11) of Section 3.3.2,

and demonstrated in Figure 3.5 . The practical tests showed that equation (11) could be useful up to levels of R = 0.6 .

In addition, the simulation tests confirm that, for values of R up to 0.6 , distortion is proportional to R, and the frequency deviation of the transmitted signal has little effect on the total harmonic distortion relative to the desired signal level. However, increase in frequency deviation does produce a proportional increase in the bandwidth of the distortion components, as predicted by equation (11).

The influence of the relative phase of the carrier frequencies of the direct and reflected waves is small in comparison to that of other parameters.

3.3.4 General Methods of Reducing Multipath Distortion

The method most commonly recognised for the reduction of multipath propagation is the use of a well-sited directional aerial [15]. Such an aerial has the effect of reducing R by excluding the reflected wave, which in the majority of cases will have a different angle of incidence than the direct wave. The empirical study shows that a reduction in R will be accompanied by a proportional reduction in distortion.

The difficulty with this method of reduction is that the direction of the aerial for greatest multipath reduction does not always coincide with the direction giving maximum direct wave pickup [16]. As a result, significant residual levels of multipath distortion occur, even with the use of a highly directional aerial.

In addition to the use of a directional aerial, several electronic methods of multipath reduction have been proposed [17,18]. These methods use techniques, such as adaptive transversal filtering, to provide some cancellation of the multipath distortion components. In their present realisations, these methods are complex and, as a result, comparatively expensive to provide.

3.3.5 Multipath Distortion Reduction in Radiotext

For the accurate decoding of data signals, it is important that the integrity of the transmitted waveform is preserved. However, as Figure 3.4 shows, multipath propagation can result in severe waveform distortion. Thus, it is necessary to provide a system design, in terms of transmission parameter selection and circuit implementation, which minimises both the occurrence and effects of this distortion.

The methods used in Radiotext to reduce data errors caused by multipath distortion are given below.

(1) Use of a sinusoidal data waveform.

All the frequencies present in the data waveform produce harmonic distortion components when multipath propagation is experienced. By using a sinusoidal waveform for the data signal, many of the higher frequency components are removed, resulting in a significant reduction in the distortion.

(2) Use of band-pass filtering.

Since the data signal occupies only a portion of the available channel bandwidth, then suitable band-pass filtering at the

output of the receiver discriminator will further help to remove the resulting distortion components.

(3) Reduction in the frequency deviation of the transmitted signal.

The use of band-pass filtering is unfortunately less effective with stereophonic transmissions, where multipath propagation can cause crosstalk between the channels.

Harmonics of the distortion produced in the 'sum' channel may move into the 'difference' channel to appear, after decoding, in both the left and right channels. Consider, as an example, a data transmission using signalling frequencies between 7.2 kHz and 9.6 kHz in the left channel and an accompanying sound commentary in the right channel.

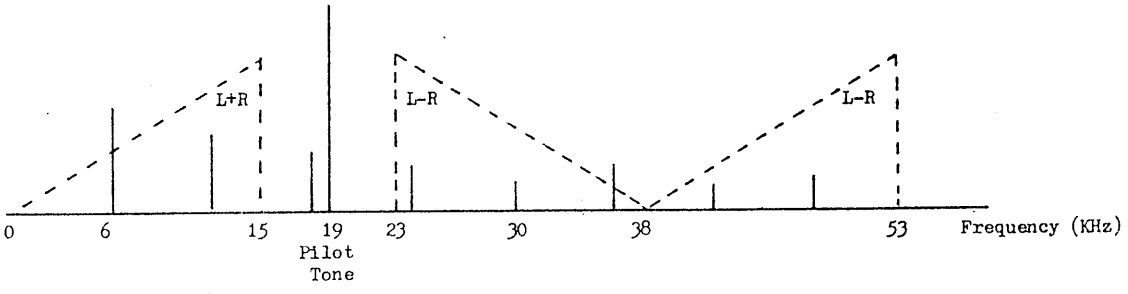

Figure 3.17 Frequency spectrum of a stereophonic transmission showing the harmonics of a 6 kHz component in the right channel following multipath propagation.

Figure 3.17 shows the harmonics, produced by multipath propagation, of a 6 kHz component in the sound commentary of the right channel. The fifth harmonic of this component at 30 kHz

appears in the 'difference' channel and will be decoded as a, (38 - 30), 8 kHz component in both channels. A band-pass filter, designed to accept the data signal in the left channel, will not remove this distortion component.

To remove the crosstalk between channels, it is necessary to keep the bandwidth of the distortion components as low as possible. Expression (11) of section 3.3.2 shows that this can be achieved by reducing the frequency deviation f_d of the transmitted signal. A reduction in deviation from the standard 75 kHz to 10 kHz produces a significant decrease in channel crosstalk, without reducing the signal to noise ratio to unacceptable levels.

(4) Use of low data signalling frequencies.

It was shown in sections 3.3.2 and 3.3.3 that multipath distortion is dependent on the frequency of the modulating signal. However, the relationship is not straightforward, being dependent on the time delay between the direct and reflected waves. For example, Figure 3.8 shows that, with a relatively short time delay of 25 μs, the distortion at 12 kHz is greater than that at 6 kHz. Whereas, Figure 3.9 shows that, with a longer delay of 75 μs, the distortion at 12 kHz is significantly less than at 6 kHz.

An important consideration here is that, although there is little evidence to suggest that a short time delay is more likely to occur than a long one, a reflected wave with a short time delay has travelled over a shorter path length and thus the resulting value of R is likely to be greater. In consequence, it is more

important to protect against the effects of short time delays than long ones. As Figure 3.8 shows, this is achieved by keeping the frequency of the data signal as low as possible.

3.4 The Effects of Noise

With the high signal to noise ratio of the broadcast channel, the probability of error in the transmitted data should be extremely low. However, particularly in urban areas, man-made noise sources produce high levels of impulse-type noise in their immediate environment [19,20]. The probability of data error may be significantly increased because of these noise impulses.

Skomal [21] gives a ranking of the sources of this type of noise, showing the main contributors to be automobiles, power distribution systems and domestic and industrial electrical equipment. To assess the extent of this noise, a survey was carried out with the help of 30 Open University students, spread across the country.

The survey made use of a 12-minute test tone of 880 Hz, transmitted at the end of the normal broadcasting schedule of a national radio station. At each location, the tone was recorded onto audio cassette tape for later analysis. Initial trial recordings showed that the majority of detected noise impulses appeared to arise from electrical appliances within the home. As a result, students were asked to note the appliances likely to be in operation, near the location of the receiver, during the time of the recordings.

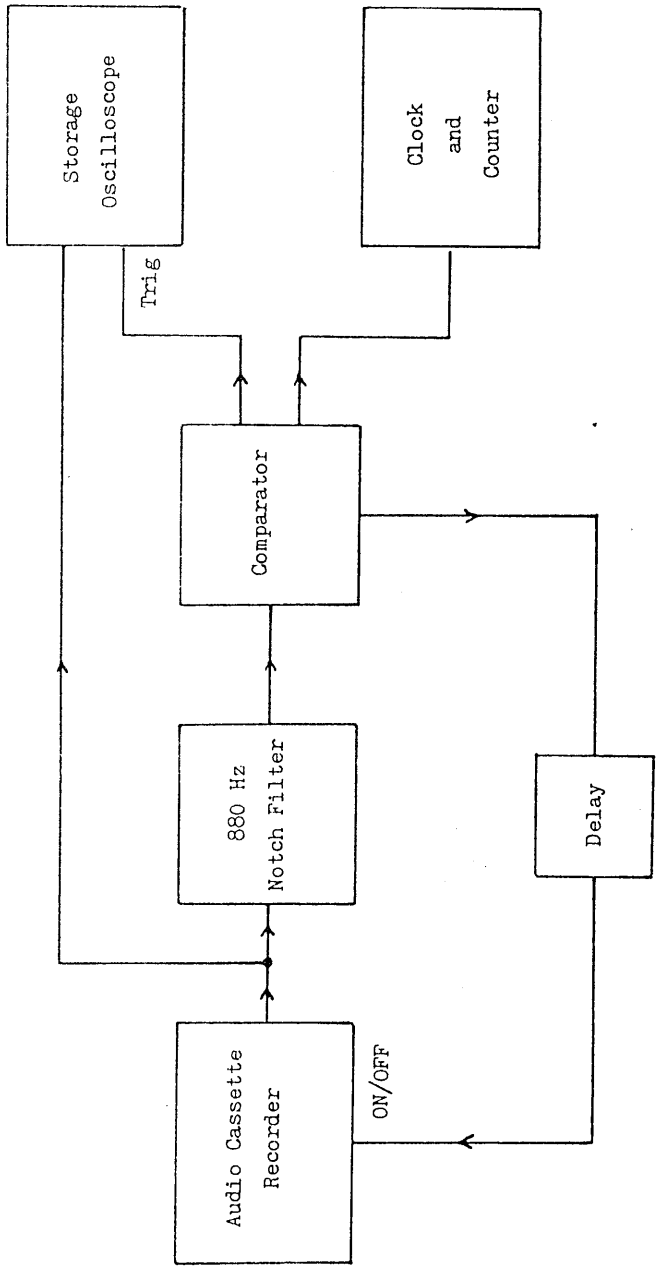

Figure 3.18 Schematic diagram of the circuit for the analysis of impulse-type noise on the radio broadcast path.

Figure 3.18 shows a schematic diagram of the circuit used for the analysis of the impulse noise occurring during reception of the test tone.

The output from the audio cassette recorder was taken to a storage oscilloscope and to a sharply-tuned notch filter. The notch filter removed the 880 Hz tone, leaving only the low level noise signals, which were compared to the reference level input of a comparator. The reference level was set at one half the amplitude of the test tone.

A noise impulse, with an amplitude greater than the reference voltage, caused the comparator to trigger the storage oscilloscope, and, after a short delay (1.5s), to switch off the recorder. In addition, a counter provided a record of the time duration of the impulse. In this way, the noise impulse could be both observed and timed. The recorder was then restarted and the test continued.

From observations of the particular signature of the impulse noise during closely monitored trials, the results of the survey could be interpreted to confirm that the majority of the noise results from appliances within the home, in particular those, such as refrigerators and freezers, which operate throughout the entire 24 hour period. Such appliances typically produce short duration multiple impulses which often go unnoticed during reception of conventional sound broadcasts.

The impulse noise distribution is shown in Figure 3.19 . The survey showed that, on average, a noise impulse is likely to occur once every 2 minutes 21 seconds. Although these noise impulses have little noticeable effect on sound broadcasts, they will cause data errors

which will be difficult to avoid.

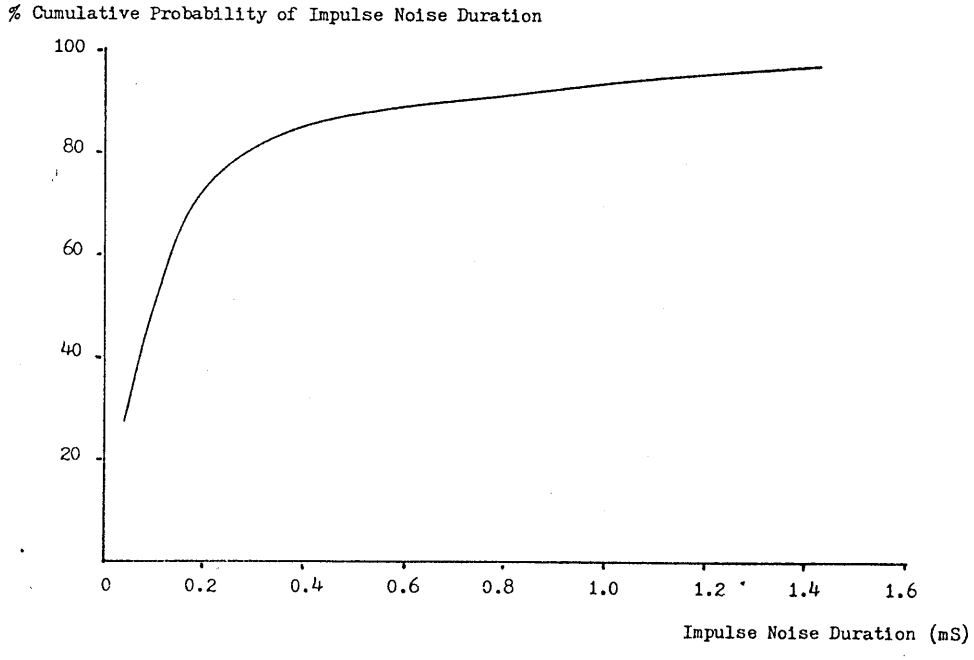

Figure 3.19 Distribution of impulse noise duration.

3.5 Choice of Channel Code (Modulation Method) for Broadcasting

The design constraints impose limitations on the choice of the modulation method used for data transfer over the broadcast link. Many of the limitations arise because use is made of the unmodified broadcast system. Should sufficient cooperation from the broadcasting authority be obtained, it might be possible to relax some of these limitations. In that case, it may prove valuable to reexamine the choice of modulation method with the aim of increasing the data rate without reducing reliability.

As previously explained in section 3.2 , the phase response of the transmission system cannot be predicted. Therefore, it is not possible

to correct for the lack of phase linearity by use of simple filtering methods. The provision of adaptive phase equalization at the display interface proved expensive to implement. As a result, the modulation method must be tolerant to phase distortion, ruling out the use of phase modulation and low redundancy pulse code techniques. A further significant reason for not using phase modulation is the unreliability of the required synchronous detection, in this application.

Frequency shift keying remains as the method of modulation least likely to be influenced by the system phase distortion. With frequency shift keying, however, it is still important to ensure that the signalling frequencies, for a given data rate, are sufficiently high to avoid intersymbol interference caused by the lack of phase linearity.

The necessity of recording the data signal on magnetic tape prior to transmission means that the modulation method used for data transmission over the broadcast link must also be suitable for magnetic recording. The use of frequency shift keying for data recording creates few problems, except that the signalling frequencies should be kept low to avoid the signal amplitude instability which occurs at high recording frequencies.

An additional constraint on the choice of signalling frequencies is a result of the need to avoid excessive distortion due to multipath propagation. In this case, the requirement is for the use of low signalling frequencies.

Consequently, choice of signalling frequencies is a compromise. They

must be sufficiently low to avoid both amplitude instability during recording and multipath propagation during transmission, but high enough to avoid excessive intersymbol interference caused by the lack of phase linearity. Signalling frequencies between 4.8 kHz and 9.6 kHz were selected for initial system trials.

A further contribution to the reduction of distortion due to multipath propagation is made by use of a sinusoidal waveform for the transmitted frequency-shift-keyed signal. In this way, the number of distortion products present in the received signal is reduced, with an accompanying reduction in channel crosstalk. Use of a sinusoidal signal has the added advantage of minimising intersymbol interference [22].

To enable a detector implementation which uses zero crossing information, the switching between signalling frequencies is made without phase discontinuity. This is important because, should a phase error occur at the time of switching, then the phase error will cause time jitter in the received data transitions [23].

It will be shown later that, in the student's home, it is possible to record the transmitted data onto audio cassette at a rate of 2400 baud. Therefore, this data rate was selected for implementation on the broadcast link, with the option of an increase to 4800 baud should intersymbol interference prove to be minimal. Circuits to provide phase-continuous frequency shift keying were designed for use at these data rates.

For system trials, two schemes were implemented. In the first,

non-harmonically related signalling frequencies of 7.2 kHz and 9.6 kHz were used. For the second, signalling frequencies of 4.8 kHz and 9.6 kHz were used, to allow some commonality between the broadcast channel decoder and that used for data storage at the display interface.

3.5.1 Encoder Circuit - Signalling Frequencies 7.2 kHz and 9.6 kHz

A schematic diagram of the method of signal generation is shown in Figure 3.20 . The frequency-shift-keyed signal is produced by using the data stream to switch between two sine wave oscillators. The oscillators are function generators which are locked in frequency and phase by being included in a phase-locked loop circuit. This circuit is fed from accurate frequencies produced by division of a stable clock. By producing a data clock from this same stable source, phase continuity is assured when switching from one signalling frequency to the other.

Figure 3.21 shows a full circuit diagram of the encoder. This circuit is suitable for use at a data rate of 2400 baud. At 4800 baud, however, the frequency shift keyed signal cannot be generated this way because an odd number of half cycles of the 7.2 kHz signalling frequency are transmitted during each bit period.

A circuit modification is required in which the signalling frequencies are generated by division of a stable clock as before, but then combined in logic circuitry, which is switched by the data stream, to produce a rectangular wave version of the output signal. A function generator is then phase locked to this signal to produce the equivalent sinusoidal

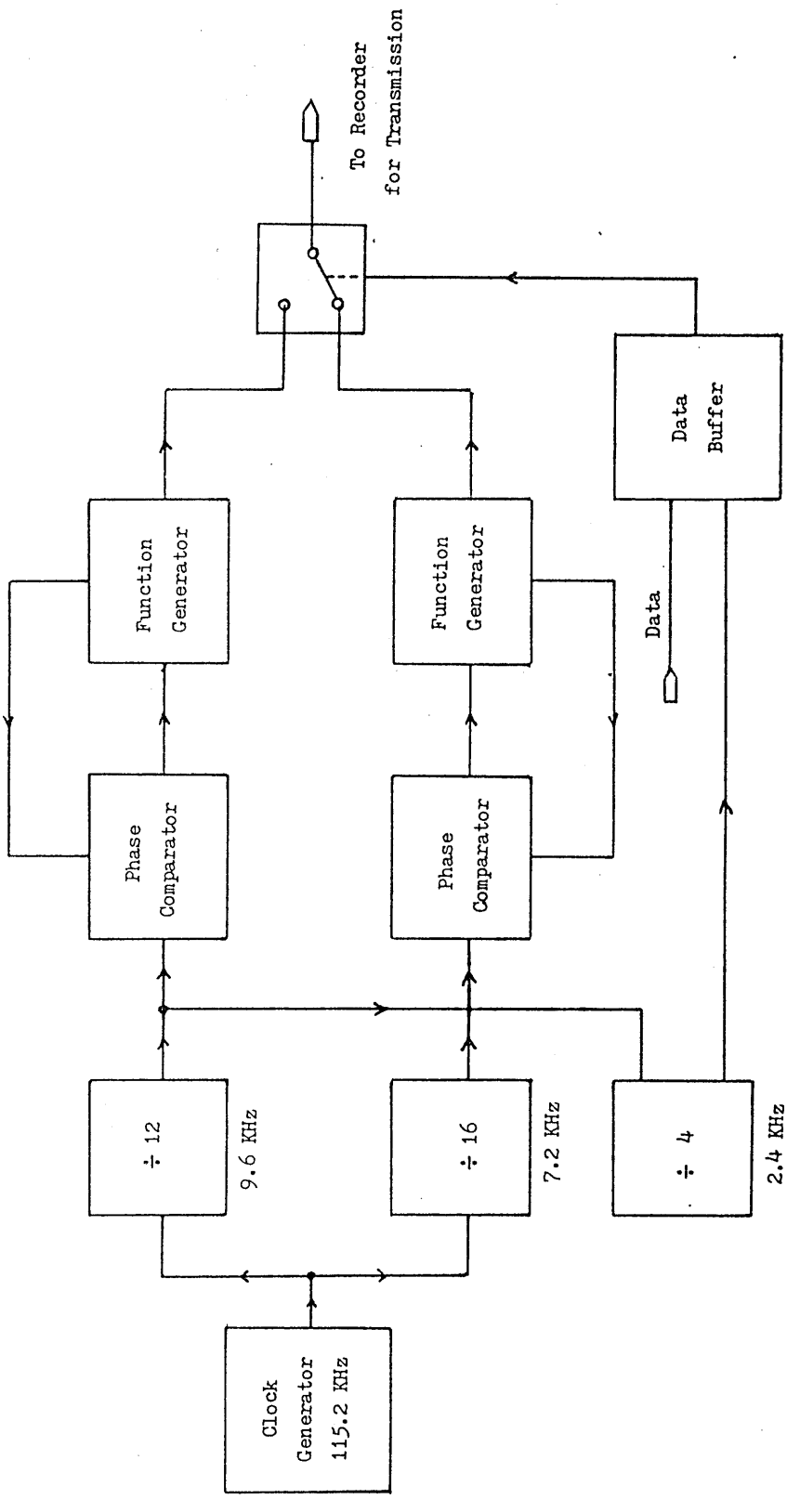

Figure 3.20 Schematic diagram of encoder - signalling frequencies 7.2 kHz and 9.6 kHz

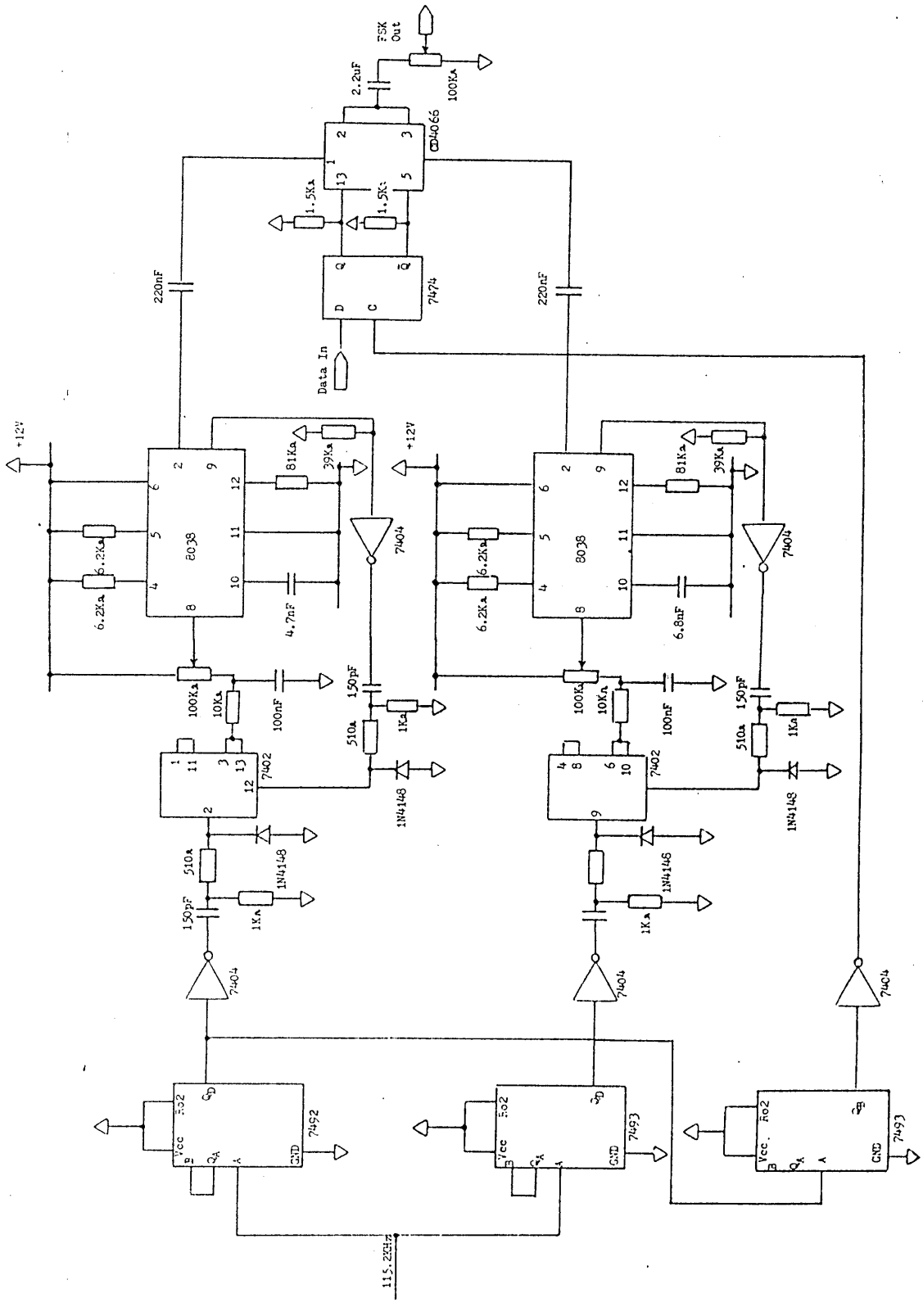

Figure 3.21 Encoder circuit diagram - signalling frequencies 7.2 kHz and 9.6 kHz (2400 baud)

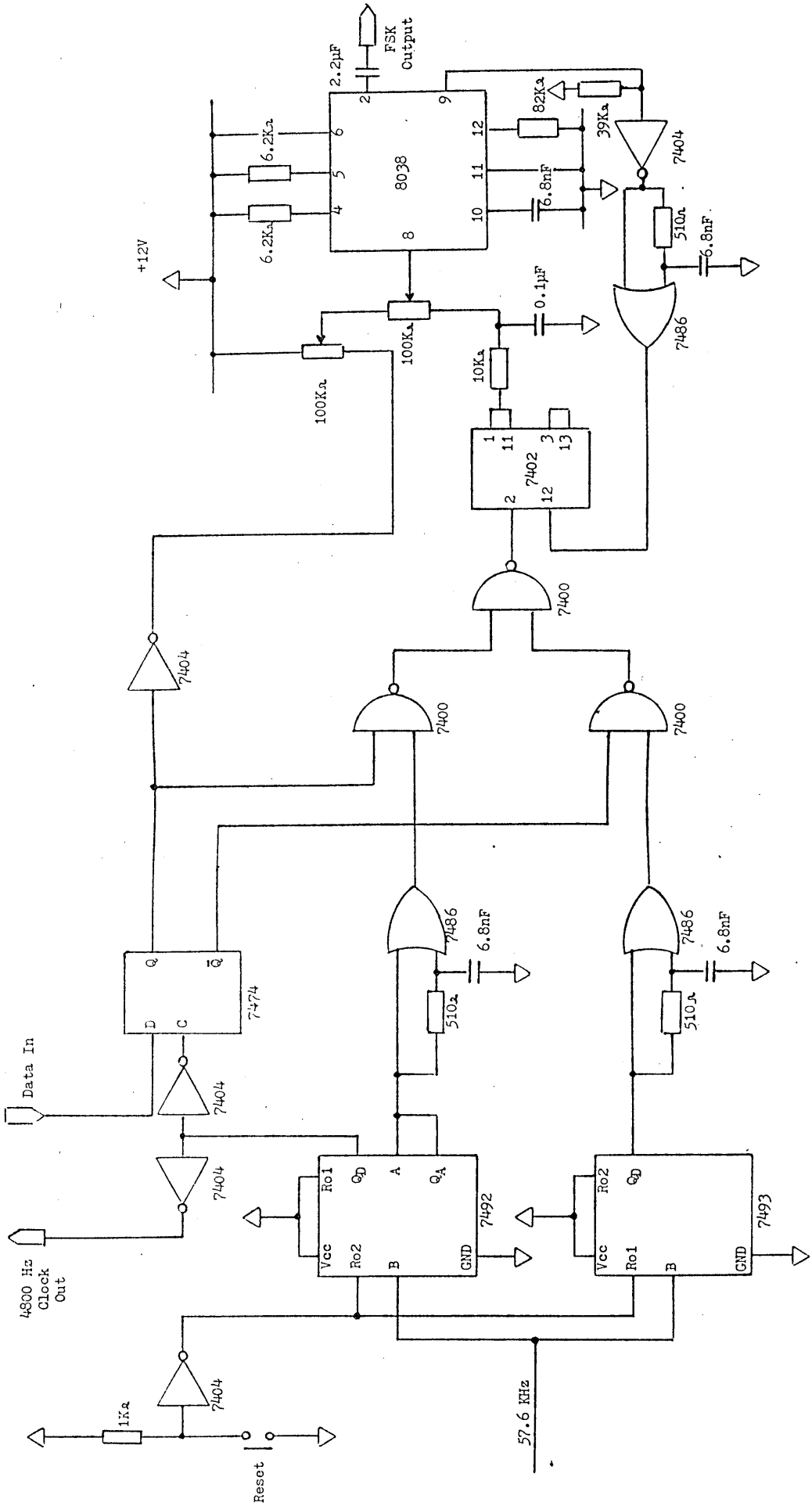

Figure 3.22 Encoder circuit diagram - signalling frequencies 7.2 kHz and 9.6 kHz (4800 baud)

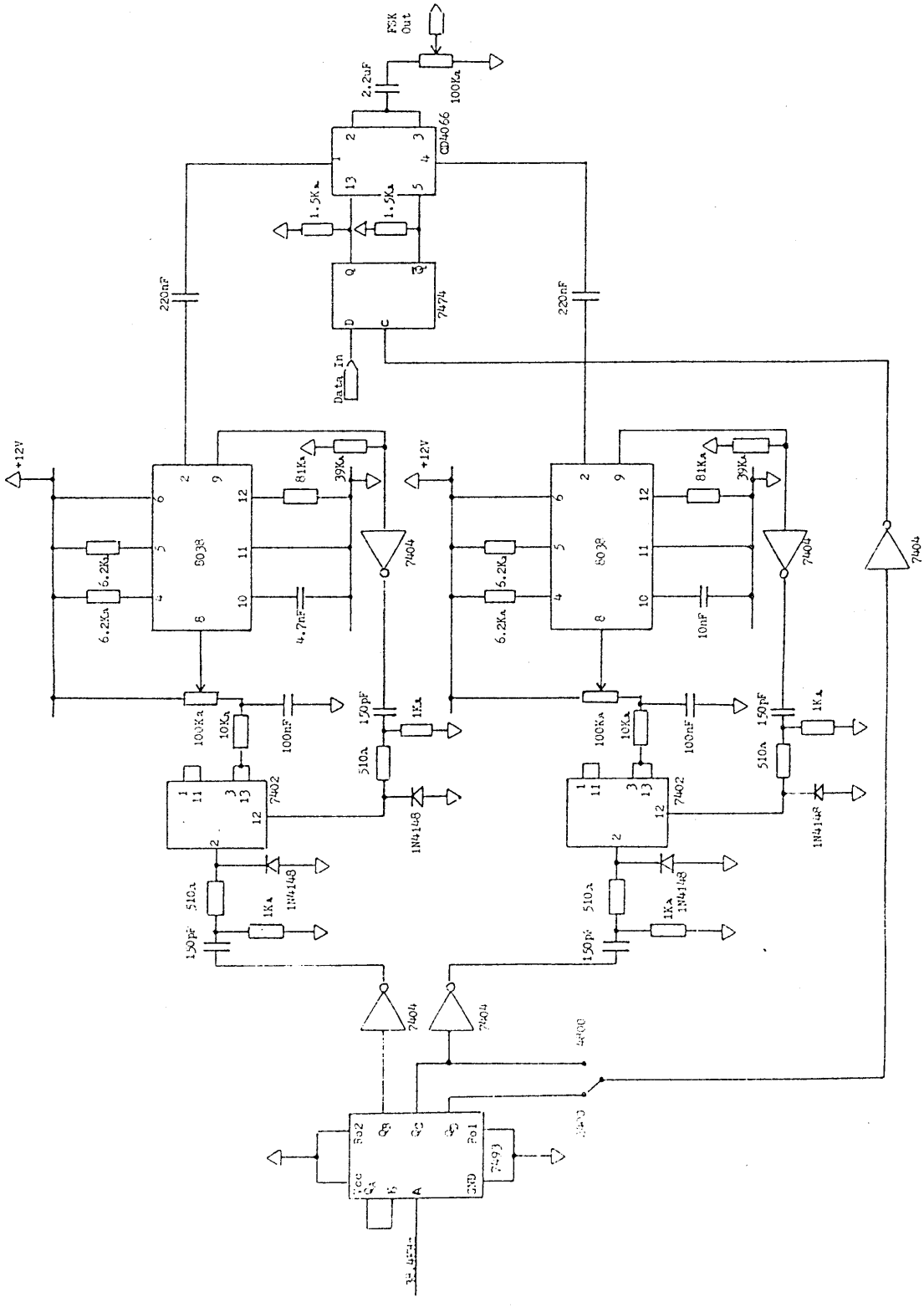

Figure 3.23 Encoder circuit diagram - signalling frequencies 4.8 kHz and 9.6 kHz (2400 and 4800 baud)

form. In this case, the function generator requires an additional suitably timed input, determined by the data stream, as shown in the circuit diagram of Figure 3.22 .

3.5.2 Encoder Circuit - Signalling Frequencies 4.8 kHz and 9.6 kHz

The encoder circuit for these signalling frequencies is very similar to the circuits of figures 3.20 and 3.21 . In this case, the data rate can be changed from 2400 baud to 4800 baud with little circuit modification, as shown in Figure 3.23 .

3.5.3 Decoder Circuits

In terms of performance in the presence of noise, synchronous or coherent methods of detection are to be preferred to non-coherent techniques. Attempts to use synchronous detection on the transmitted frequency-shift-keyed signal proved to be extremely successful when the signal from the encoder was transmitted directly. However, once this signal was recorded on magnetic tape prior to transmission (following the procedure of the proposed system), variation in the recorder speed (wow and flutter) made it impossible to generate carrier frequencies in the decoder with sufficiently accurate frequency and phase. Consequently, it was necessary to use non-coherent detection techniques.

Two methods of detection were selected for trial. In the first, filtering and envelope detection are employed, and in the second, the detector output is determined by zero crossing timing. The first method is used with transmitted signalling frequencies of 7.2 kHz and 9.6 kHz, and the second with frequencies of 4.8 kHz and 9.6 kHz.

3.5.4 Decoder Circuit - Filtering and Envelope Detection

A schematic diagram of the decoder circuit, designed for this application, is shown in Figure 3.24 . The incoming frequency-shift-keyed signal is filtered by sharply tuned band-pass filters and the resulting signalling frequencies applied to a full wave rectifier and low-pass filter, for envelope detection. The rectified and filtered outputs are then compared to determine the binary value of the output data.

To improve the performance of the envelope detector, additional rectified peaks of the signalling frequencies are provided by a 90^{o} phase shift circuit in each signal path. These additional peaks have the effect of doubling the ripple frequency of the rectifier output. In this way, reliable operation at a data rate of 4800 baud is achieved which, otherwise, would not be possible.

The full circuit diagram is shown in Figure 3.25 .

3.5.5 Decoder Circuit - Zero Crossing Detection

In this case, the designed decoder circuit relies on timing the intervals between transitions of the received signal. The interval between transitions of the 4.8 kHz signal is twice that of the 9.6 kHz signal. A schematic diagram of the decoder circuit is shown in Figure 3.26 .

The frequency-shift-keyed signal is filtered by stagger-tuned band-pass filters, tuned to the signalling frequencies. Following this filtering, the signal is limited and short duration pulses, coincident with the

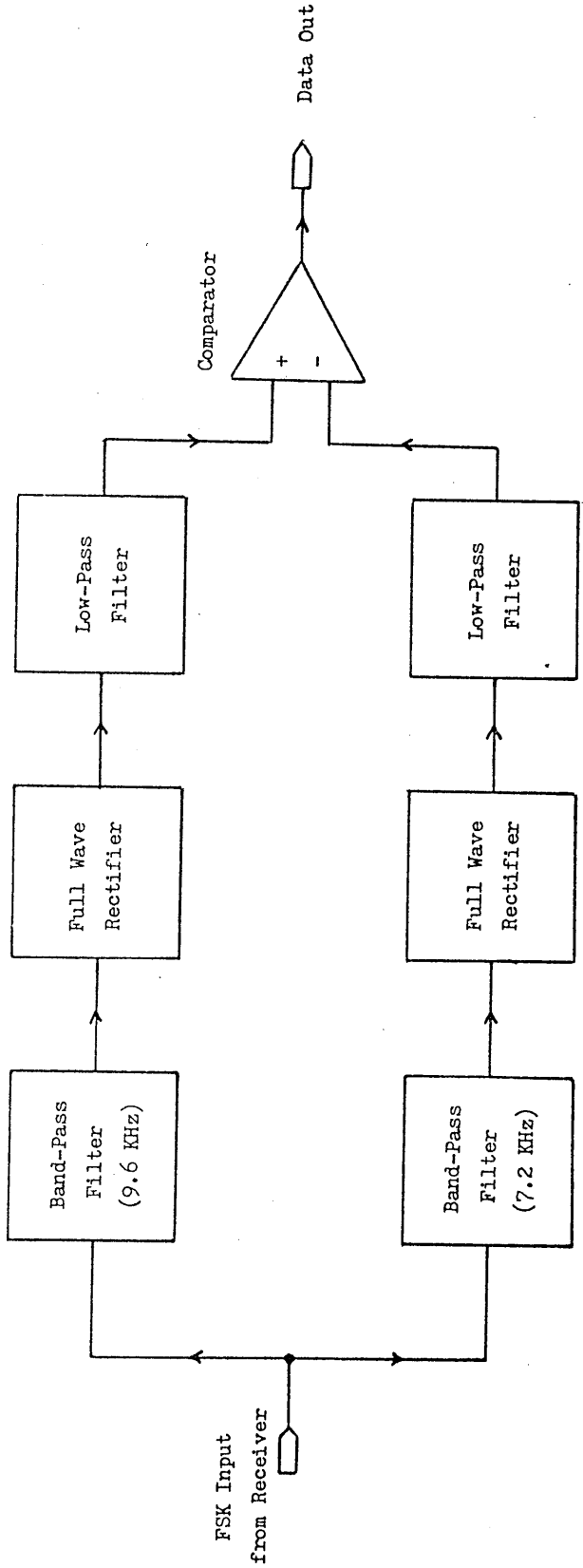

Figure 3.24 Schematic diagram of decoder - filter and envelope detection.

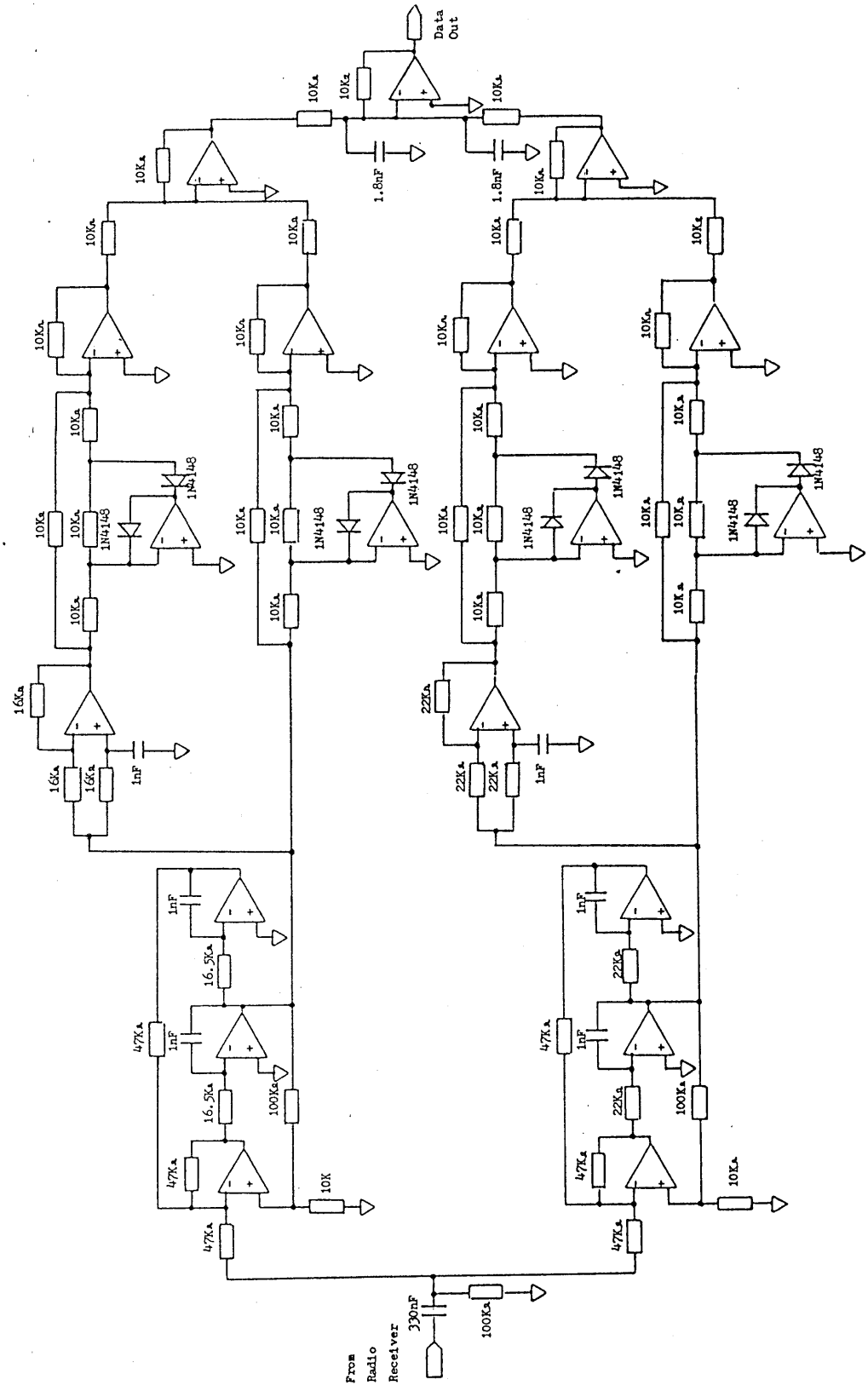

Figure 3.25 Decoder circuit diagram - filtering and envelope detection.

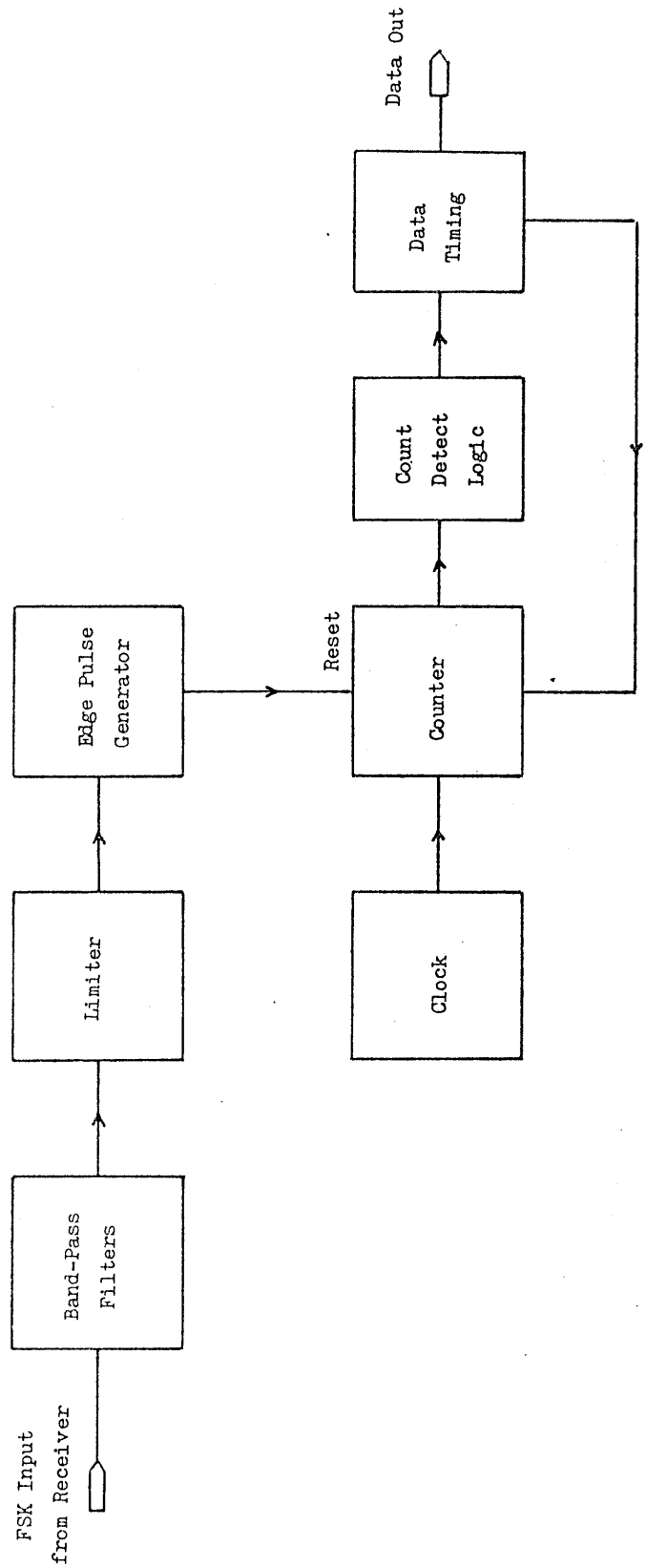

Figure 3.26 Schematic diagram of decoder - zero crossing timing.

zero crossings of the signal (termed edge pulses in Figure 3.26), are produced.

These pulses are used to reset the counter, which is receiving clocking pulses from a highly stable clock generator. The frequency of the clock pulses determines the resolution with which the zero crossing intervals are measured and, therefore, a relatively high clock frequency of 307.2 kHz is used. The state of the counter before each reset will depend upon the time interval since the previous zero crossing, and so will indicate the frequency of the input signal. Count detect logic determines the state of the counter and from it produces the decoded data stream.

At these signalling frequencies, the decoder circuit differs only slightly from the decoder used for the storage of data on audio cassette (this circuit will be described in detail later). A band-pass filter and suitable clock signal are the only additions required to enable the audio cassette decoder to be used to decode the broadcast data signal.

3.5.6 Comparison of Decoding Methods

Laboratory tests were carried out to compare the performance of these two methods of data decoding. The radio broadcast path was simulated by use of the multipath simulator previously described.

The two methods performed well in both conditions of weak signal strength and high levels of multipath propagation. Use of non-harmonically related signalling frequencies for the filter-envelope decoding method provided slightly higher immunity to multipath effects.

On the other hand, this decoding method had a tendency to produce an asymmetrical data stream when used with some radio receivers, because, with these receivers, the amplitude of the output at 9.6 kHz was less than that at 7.2 kHz.

From the results of the tests and because the circuit could also be used for data storage, the zero crossing decoding method, with signalling frequencies of 4.8 kHz and 9.6 kHz, was chosen for use on the radio broadcast link. Duplication of the purpose of this circuit also gives rise to a valuable reduction in system cost.

4. DISPLAY INTERFACE

A schematic diagram of the display interface is shown in Figure 4.1 . The major components are a time clock, broadcast channel decoder, data storage encoder and decoder and essentially a simple microcomputer made up of microprocessor, memory, display generator and output devices. It is intended that the interface will be available either as a 'stand-alone' model, which will be completely self contained, or as an 'add-on' to a microcomputer. In the latter case, the microprocessor, memory and display generation facilities of the microcomputer will replace those of the 'stand-alone' interface.

The interface has two modes of operation. In the 'receive' mode, the interface and the radio receiver are remotely switched on by the time clock at the appointed time for the transmission. The broadcast signal is decoded in the broadcast channel decoder and the resulting data passed to the microcomputer. In the microcomputer, the header code of each transmitted 'page' is compared with the identifier code previously entered by the student, and where appropriate, the contents of the 'page' are loaded into memory. Following error correction on the completed 'page', the audio cassette recorder is remotely switched on and, after a pause to allow the recorder speed to stabilise, the received 'page' is reformatted and applied to the data storage encoder and on to the recorder. At the end of the transmission time period,

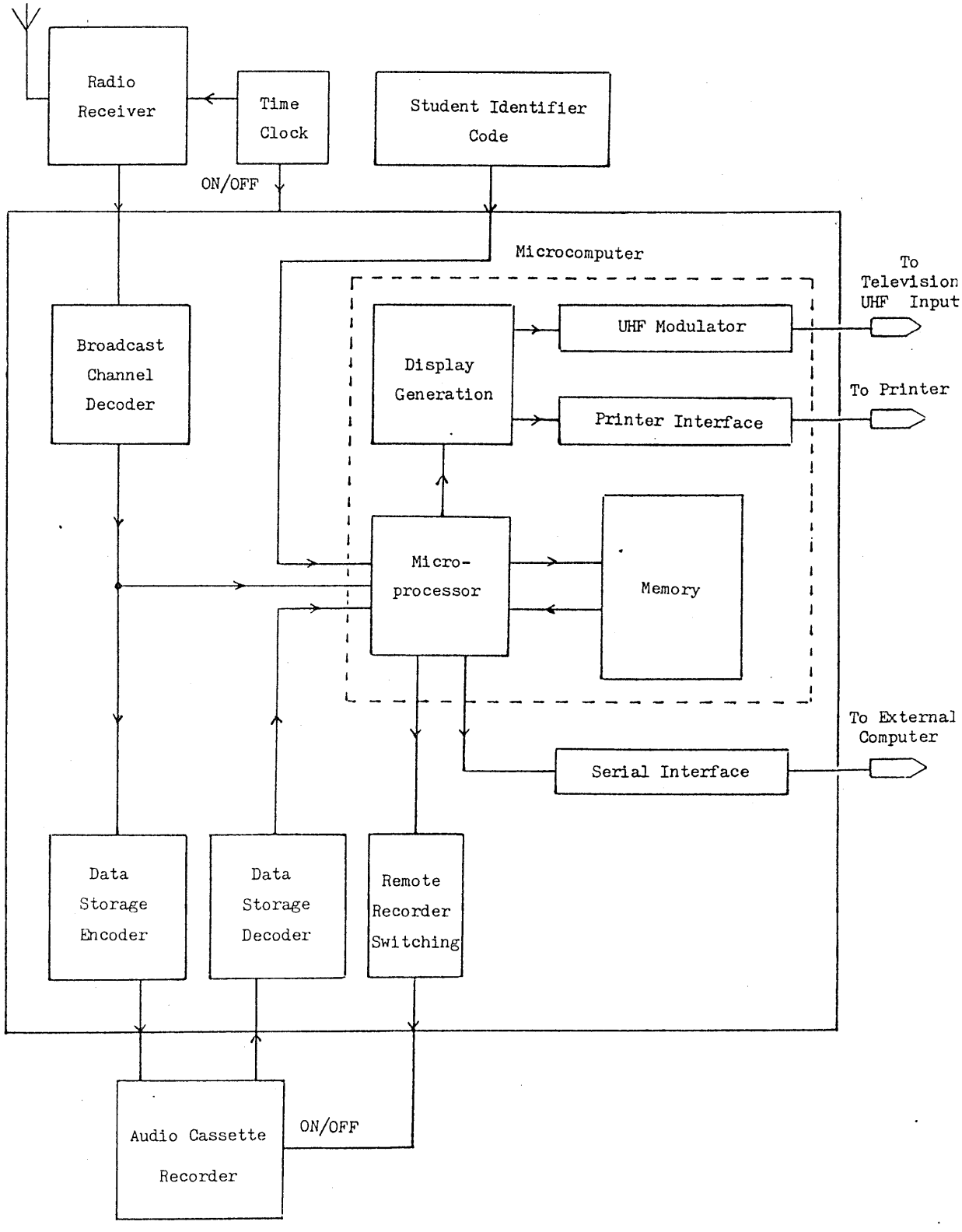

Figure 4.1 Schematic diagram of the display interface.

the receiver and interface are switched off by the time clock.

In the 'display' mode, the audio cassette recorder is remotely switched on by the interface. The output signal of the recorder is decoded in the data storage decoder and passed to the microcomputer. As each 'page' is loaded into memory, error correction takes place. A memory size of 20 Kbytes enables 2 low resolution (1 Kbyte) and 2 high resolution (8 Kbyte) 'pages' to be stored for display. The recorder is switched off when the memory area is full. Once a 'page' has been displayed, then its memory area is available for reuse and, provided the next 'page' to be loaded is in the appropriate display mode, the recorder is switched on once again. The additional 2 Kbytes of memory are required for error correction. The use of internal memory in this way, provides uninterrupted access to the transmitted material with minimum delay when switching from one item to the next.

5. DATA STORAGE

Inherent in the concept of Radiotext is the need to store data. Besides making unattended reception possible, data storage enables the student to select the most convenient time to view the received material. It may be studied at any desired rate, with repetition if necessary.

Open University students make use of audio cassette recorders in their conventional study programme. In keeping with the overall system design aim of minimising cost, a study was made to provide a method of fast and reliable data storage using these recorders.

For some time, audio cassette recorders have been used as storage devices for microcomputers. In that type of application, reliable data storage has been achieved only at low data rates [24,25]. In general, the operation at higher data rates has required the use of good quality and so more expensive recorders [26]. Low data rates could impose a severe constraint on the volume and type of data to be handled (the cassette recorder is the component with the slowest data rate in Radiotext), and in consequence an effort was made to maximise the data rates obtained.

The study involved an examination of the properties of such audio cassette recorders to identify characteristics relevant to data

storage (5.1 - 5.4). Then followed the selection of a suitable channel code (5.5), and finally the production of an interface design (5.6 - 5.9).

5.1 The Recording-Playback Process

The signal to be recorded is applied as a current to the windings of the record head (which, in many audio cassette recorders, is also used for playback), together with a high frequency bias current which aids linearity [27]. These currents cause an external magnetic field to be developed across a narrow gap in the record head, as shown in Figure 5.1 .

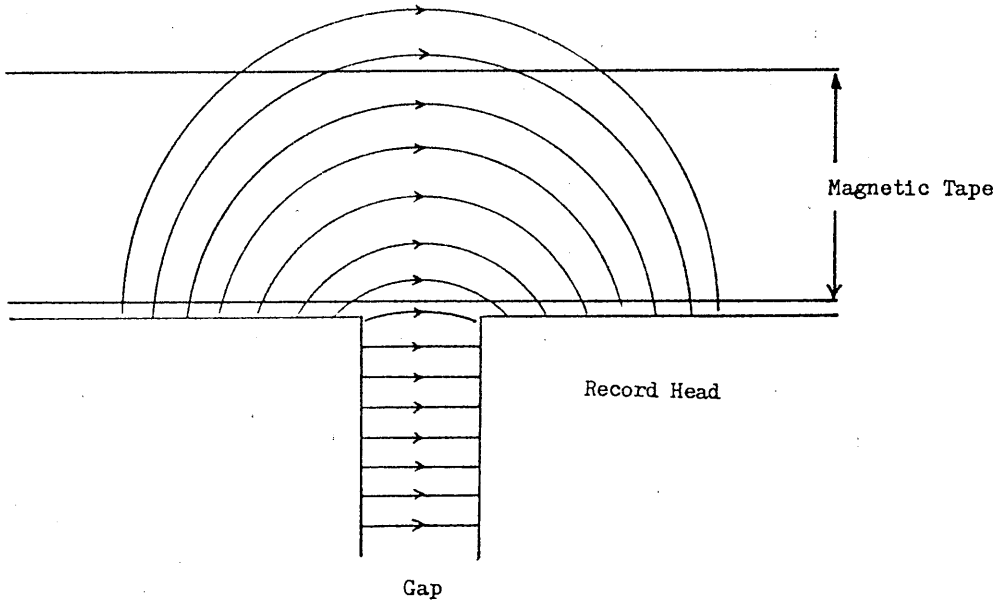

Figure 5.1 Flux distribution across the pole tips of the record head.

When the magnetic tape passes through this field, the bias current causes it to undergo cycles of magnetization. As the tape leaves the gap field, these cycles gradually diminish until, at some point beyond

the gap, the tape is left with a surface magnetization which is approximately proportional to the signal current.

On playback, the recorded tape is passed over the playback head. The surface magnetic flux of the tape passes through the low reluctance ferromagnetic core of the head. A voltage, which is proportional to the rate of change of this magnetic field, is induced into the windings around the core. Hence, a playback voltage is produced which is approximately proportional to the rate of change of the recorded waveform.

For a recorded sine wave, $A \sin\omega t$ (A is amplitude, ω is angular frequency), the playback voltage is nearly proportional to $A\omega \sin(\omega t + \frac{\pi}{2})$. Thus, for the recording of a variable frequency sine wave with constant recording current, the playback voltage will increase linearly with frequency. The phase response is such that the playback voltage has a constant $+90^{\circ}$ phase shift which is independent of frequency, being due to the $\frac{\pi}{2}$ term in the expression for the playback voltage.

In practice it is found that the playback amplitude variation with frequency is as shown in Figure 5.2 . In addition to the 6 dB/octave rise in amplitude with frequency, losses occur at high and low frequencies. It is these losses which determine the bandwidth of the recording process [28]. The most relevant losses are described below.

5.1.1 At Low Frequency

At low frequencies the wavelength of the signal on tape becomes very long when compared to the dimensions of the playback head. As a

result, not all the surface magnetic flux of the tape links with the core of the playback head, and so the playback voltage falls accordingly. The rate of fall is determined to a major extent by the shape of the playback head and, as a result, varies from machine to machine.

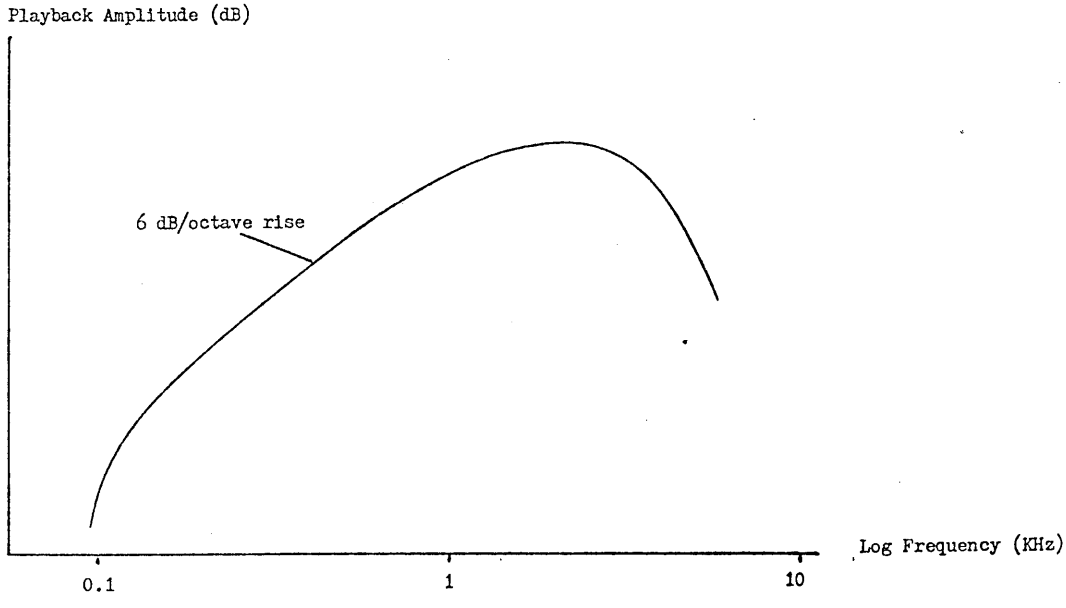

Figure 5.2 Typical amplitude/frequency response with constant current recording.

5.1.2 At High Frequency

Gap Loss

As the signal frequency increases and its wavelength on tape reduces to approach the length of the playback head gap, the resultant magnetic flux through the playback head core reduces. Eventually, at what is termed the 'extinction frequency', the head gap covers one full cycle of the recorded signal causing the resultant flux through

the head core to fall to zero and remain so, as the tape moves across the head.

The effect of gap loss is shown in Figure 5.3 .

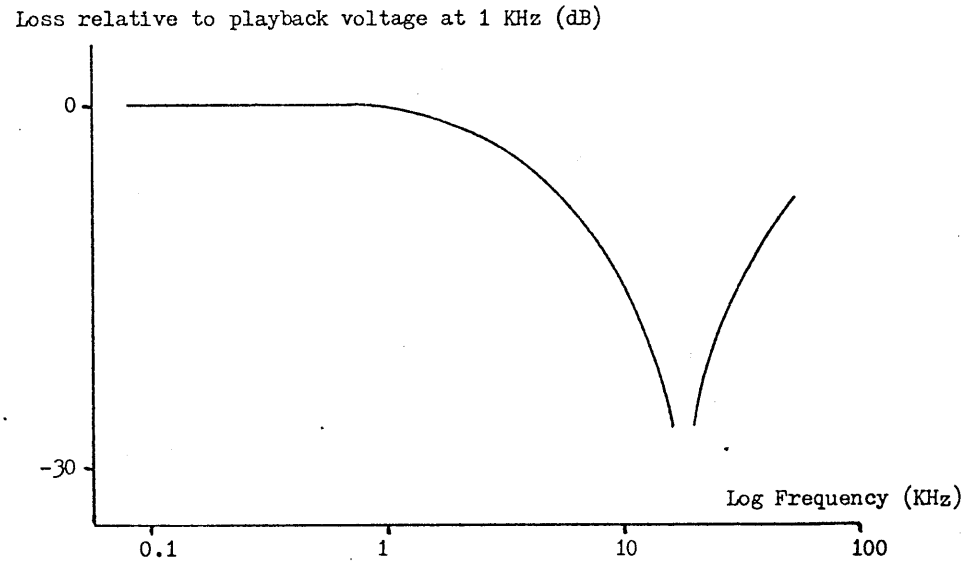

Figure 5.3 Effect of gap loss on playback signal.

This amplitude response is closely represented by

$$\frac{\sin\left(\frac{\pi b}{\lambda}\right)}{\left(\frac{\pi b}{\lambda}\right)}$$

where, b is gap length (mm)

λ is wavelength (mm).

To reduce the effects of gap loss, the 'extinction frequency' must be made as high as possible. This is achieved by making the head gap as short as possible consistent with other constraints in the design of the playback head.

Spacing Loss

If intimate contact between the tape surface and playback head is lost, the resulting high reluctance air gap significantly reduces the tape flux reaching the head core. In consequence a playback voltage loss occurs. The loss is severe for even small separations and is proportional to frequency.

An empirical formula for the loss was demonstrated by R.L. Wallace Jr. [29].

$$\text{Loss in dB} = 54.6\ \frac{d}{\lambda}$$ where, d is separation (mm)
λ is wavelength (mm).

This loss may also occur during the record process. In this case, loss in recording effectiveness with separation is related to the ratio of separation to record head gap length and does not depend upon the wavelength of the recorded signal [30].

The most common causes of increase in head to tape separation are:

(1) irregularities in the surface coating of the magnetic tape,
(2) dust, such as tape oxide, interposed between the head and tape surface,
(3) deficiencies in the tape transport mechanics resulting in loss of tape tension.

Therefore, spacing loss will vary from recorder to recorder and from tape to tape. It is characterised by short-duration severe losses in amplitude, commonly termed 'drop-outs'. The occurrence of spacing loss

in audio cassette recording was investigated using a selection of commonly available recorders and tapes. The investigation and conclusions are given in Section 5.2 .

Penetration or Thickness Loss

At high frequencies, the remanent flux of the tape may not penetrate the full depth of the oxide coating. Consequently the reduction in volume of magnetised material reduces the playback voltage.

Moreover, a frequency dependent spacing loss occurs on playback due to the separation between the head and the magnetic flux which has penetrated the oxide coating [31].

$$\text{Thickness loss in dB} = 20 \log_{10} \frac{2\pi T/\lambda}{1 - e^{-2\pi T/\lambda}}$$

where, T is tape thickness (mm)

λ is wavelength (mm).

Head Losses

These are fundamental high frequency hysteresis and eddy current losses in the ferromagnetic circuit of the tape head.

Head Alignment Losses

The record and playback heads (or the combined head in most audio cassette recorders) should be aligned to the tape correctly. The five positional adjustments of the audio head are shown in Figure 5.4 .

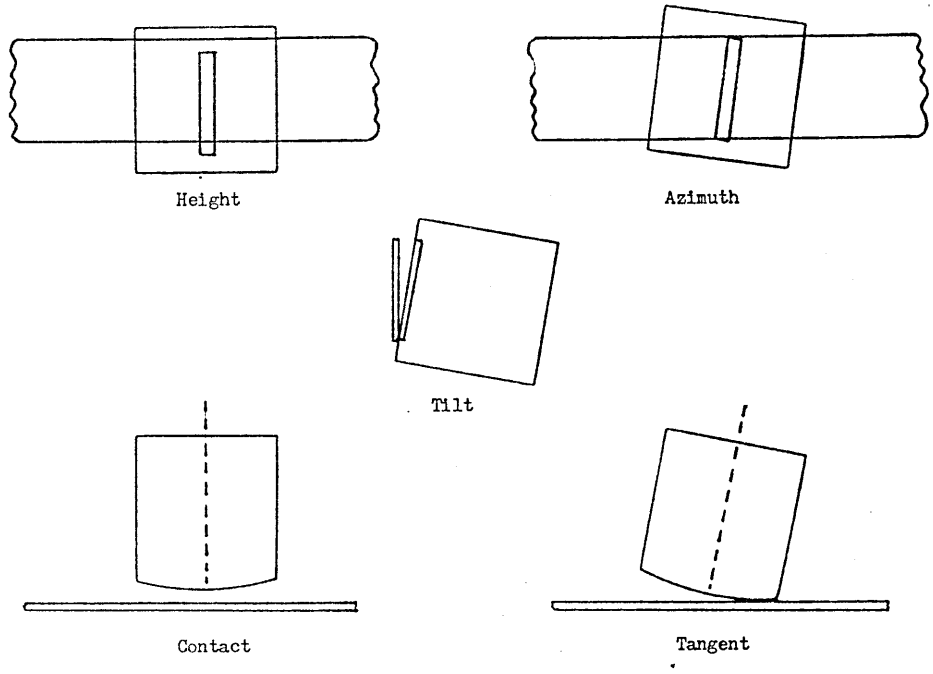

Figure 5.4 The positional adjustments of the audio head.

During the life of the recorder, misalignment of the heads may occur [32]. Misalignment of tilt, tangent and contact all affect proper head to tape contact, resulting in increased spacing loss. Misalignment of height causes mis-tracking with resultant loss of signal and crosstalk from neighbouring tracks.

Azimuth misalignment is, however, the major cause of signal loss. Its result is to increase the effective playback head gap length so increasing gap loss and reducing the 'extinction frequency'.

Figure 5.5 shows the effect of azimuth misalignment in greater detail.

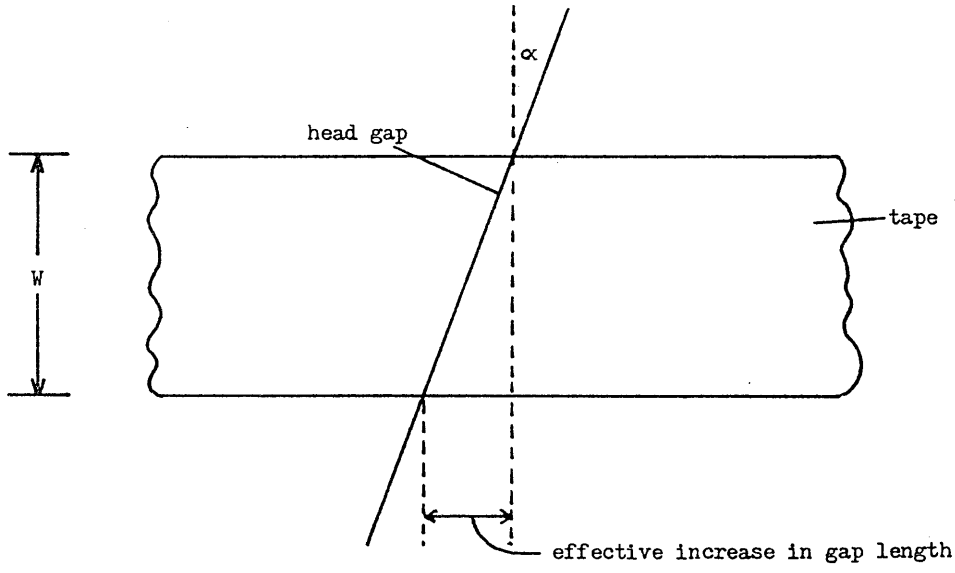

Figure 5.5 Azimuth Misalignment

If a tape is recorded with a correctly aligned record head, but on playback the head is set at an angle α , then a phase difference will exist between the tape flux at the top of the gap and that at the bottom. In effect the gap length has been extended by W tan α , where W is the recorded track width and α the angle of azimuth.

$$\text{Azimuth loss in dB} = 20 \log_{10} \left[\frac{\sin \left(\frac{\pi W \tan\alpha}{\lambda} \right)}{\frac{\pi W \tan\alpha}{\lambda}} \right]$$

where, W is track width (mm)

α is angle of azimuth (degrees)

λ is wavelength (mm).

The sensitivity of the playback process to azimuth misalignment can be shown by a calculation of the 'extinction frequency' for an angle

of misalignment of say 0.5 degree. For an audio cassette recording with track width 0.66 mm the gap length is extended by 0.006 mm. The 'extinction frequency' is therefore the frequency which has a wavelength on the tape of this length i.e. approximately 8 kHz.

Azimuth misalignment loss occurs whenever there is misalignment between record and playback heads. Where a single head is used for both record and playback the effect of misalignment is considerably reduced and may only be noticeable on playback of a tape recorded on a different recorder.

To assess the degree of azimuth misalignment likely to be found in practice and its effect on the data recording process, samples of audio cassette tapes recorded on a wide variety of recorders were tested. These tests and the results are described in Section 5.3 .

5.1.3 Effective Recorder Bandwidth

In order to provide an overall flat amplitude/frequency response, from the response shown in Figure 5.1, an amplitude equalization filter is normally provided within the recorder amplifier circuitry. The major amplitude equalization circuit provides a 6 dB/octave fall in amplitude with frequency, up to the point where high-frequency losses take effect. The filter characteristic is then designed to give increasing amplitude with frequency to combat these losses. The frequency at which the equalization filter characteristic is changed is standardized at 1330 Hz (time constant 120 μs) for ferric tapes and 2270 Hz (time constant 70 us) for chrome tapes.

The bandwidth of a low-cost audio cassette recorder is typically

150 Hz to 6 kHz. In data storage applications, the effective bandwidth has to be reduced to avoid use of the higher frequencies because these frequencies are more susceptible to spacing loss and azimuth misalignment.

5.2 'Drop-Out'

Introduction

As explained in Section 5.1.2, 'drop-outs' are short duration severe losses in playback signal caused by spacing loss. Although, in sound recording, they are almost imperceptable to the ear, 'drop-outs' are likely to be a major cause of error during data recording.

An experiment was set up to examine the frequency of occurrence and length of 'drop-outs' that might be expected to occur.

Experimental Procedure

A constant amplitude tone, at a known frequency, was recorded. On playback each half cycle of the recorded signal was examined and its peak value compared with the long-term average peak value. Each time the peak value fell below a pre-determined threshold level a counter was incremented.

A schematic diagram of the test circuit is shown in Figure 5.6, and the expected waveforms at various points in the circuit in Figure 5.7 .

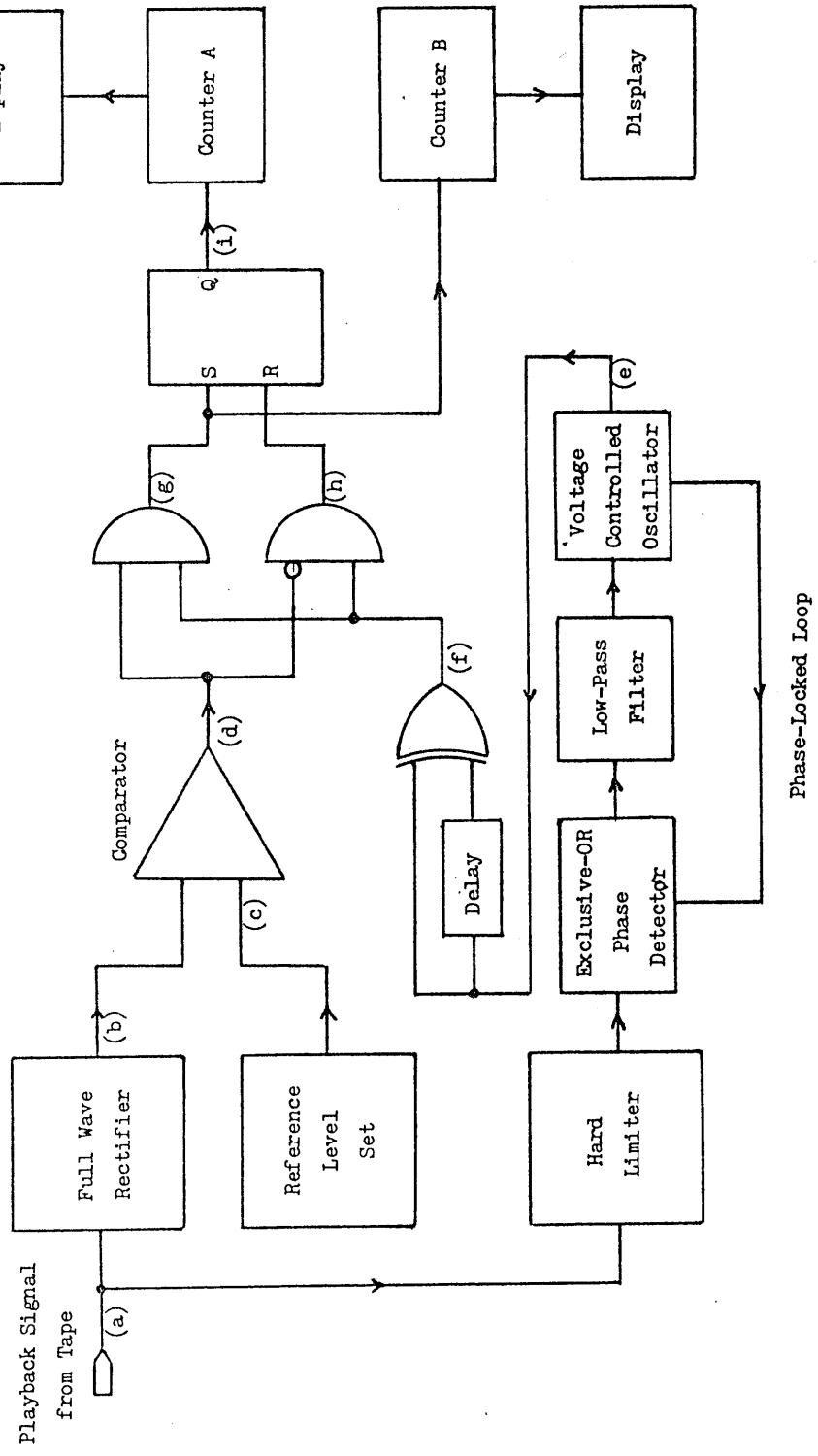

Figure 5.6 Schematic diagram of test circuit.

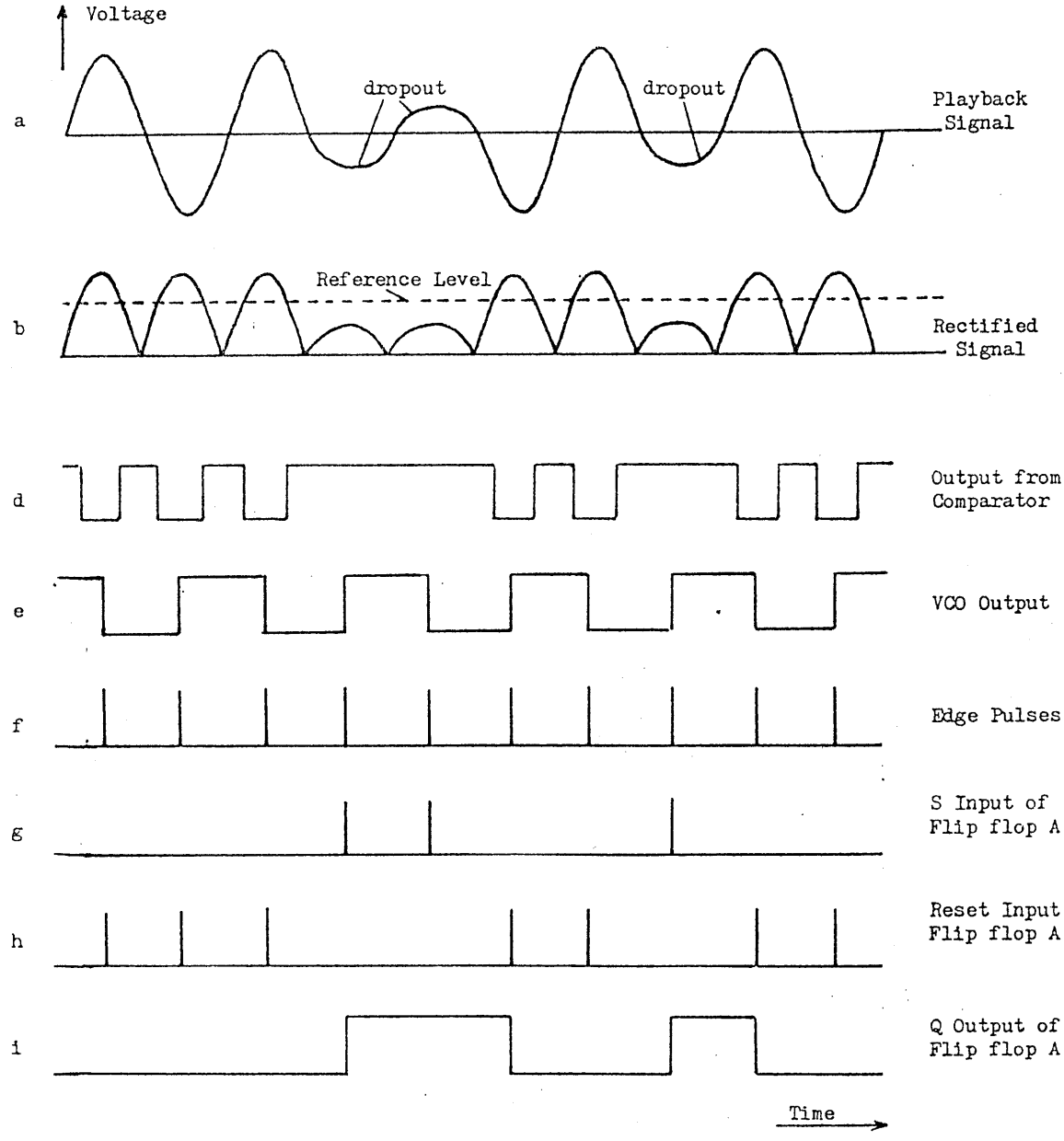

Figure 5.7 Waveforms at points in circuit of Figure 5.6 .

The playback signal is rectified and then compared with a fixed d.c. reference voltage set at some proportion of the long term signal peak level. The output of the comparator is low for the time that the incoming half cycle exceeds the threshold reference voltage. Should a 'drop-out' occur, such that the incoming half cycle does not reach the reference voltage, then the comparator output remains high.

Additionally, a phase-locked loop is locked to the playback signal. It is arranged that the output from the voltage-controlled oscillator of the loop is in phase quadrature with the playback voltage (the phase detector is the Exclusive-OR type). Short duration 'edge' pulses are generated from the voltage-controlled oscillator output. These pulses are gated by the output of the comparator to two counters.

Counter A counts the number of times flip-flop A has been 'set' and so gives the total 'drop-out' count. Counter B counts the total number of edge pulses and hence the number of half cycles of recorded signal that occur during the time the signal drops below the selected threshold level.

The time constant of the phase-locked loop is made sufficiently long to enable accurately timed edge pulses to be produced during a short-term (less than one second) complete loss of playback signal. To reduce the time taken to carry out the tests the comparator and counter circuits were duplicated to give simultaneous 'drop-out' counts at four threshold levels.

Results

Three audio cassette recorders were used together with five commonly

available brands of audio cassette tape. The recorders had been in use for some time and were first tested in this condition before being thoroughly cleaned and tested once again. The tapes were selected to cover the price range of those available for domestic use. The tests were carried out at frequencies of 3 kHz and 5 kHz with threshold levels between 20% and 80% of long-term peak value of the playback signal.

Figure 5.8 shows a plot of the number of 'drop-outs' per 80 metres of tape (approximately one side of C60 tape) against threshold level, as a percentage of long-term signal peak level, for each of the five tapes. Curve A is the average number of 'drop-outs' occuring for the six recordings (two with each recorder) and curve B is the worst-case 'drop-out' count.

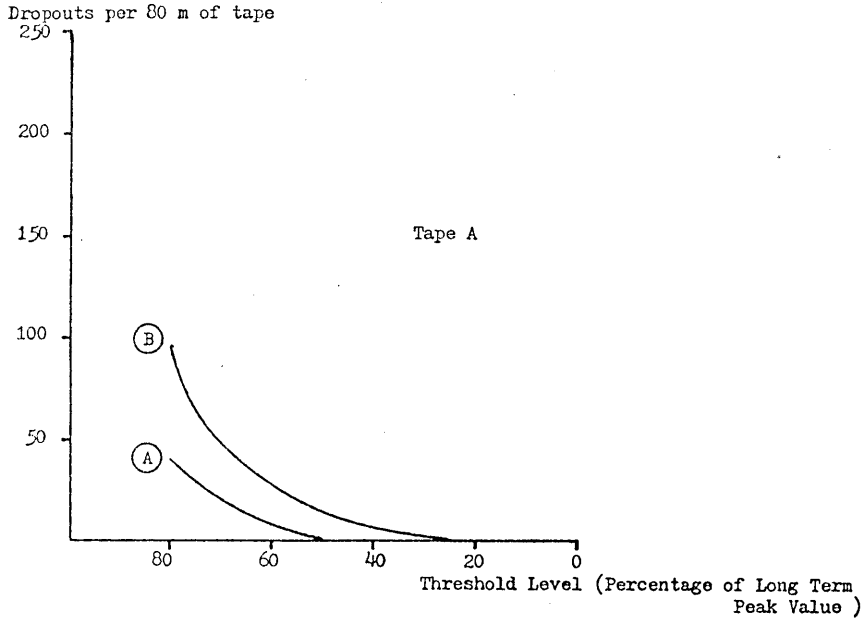

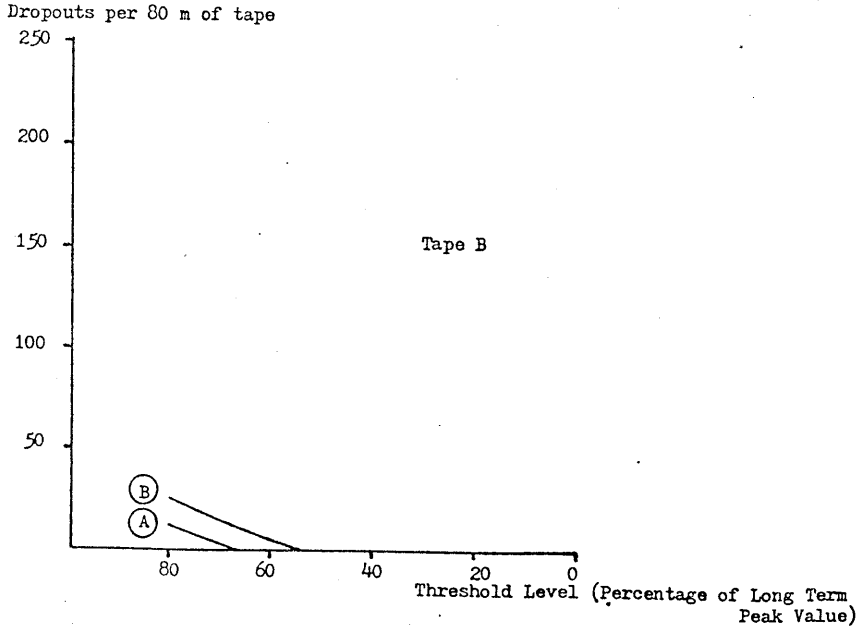
Dropouts per 80 m of tape
250
200
150
100
50
Tape B
B
A
80
60
40
20
0
Threshold Level (Percentage of Long Term Peak Value)

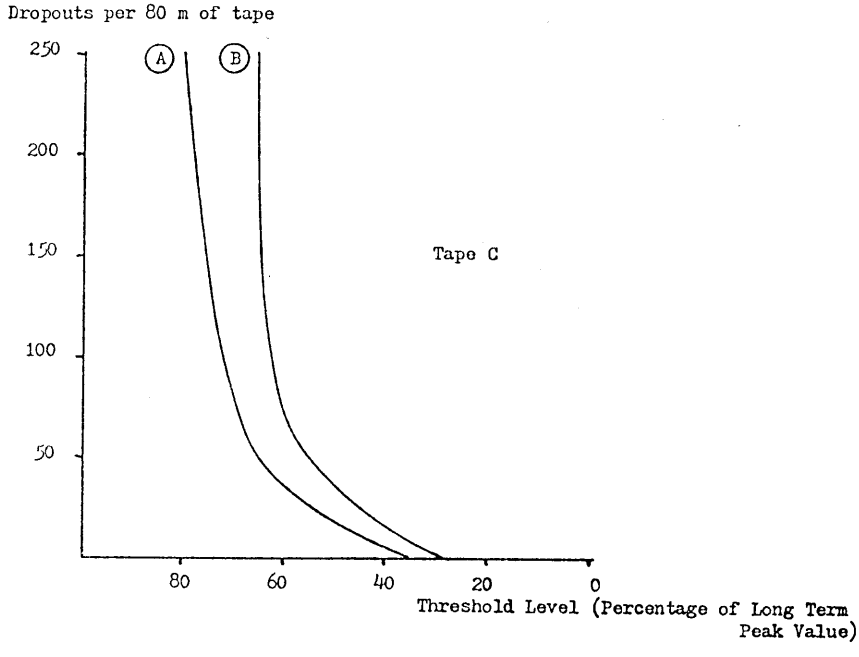
Dropouts per 80 m of tape
250
200
150
100
50
A
B
Tape C
80
60
40
20
0
Threshold Level (Percentage of Long Term Peak Value)

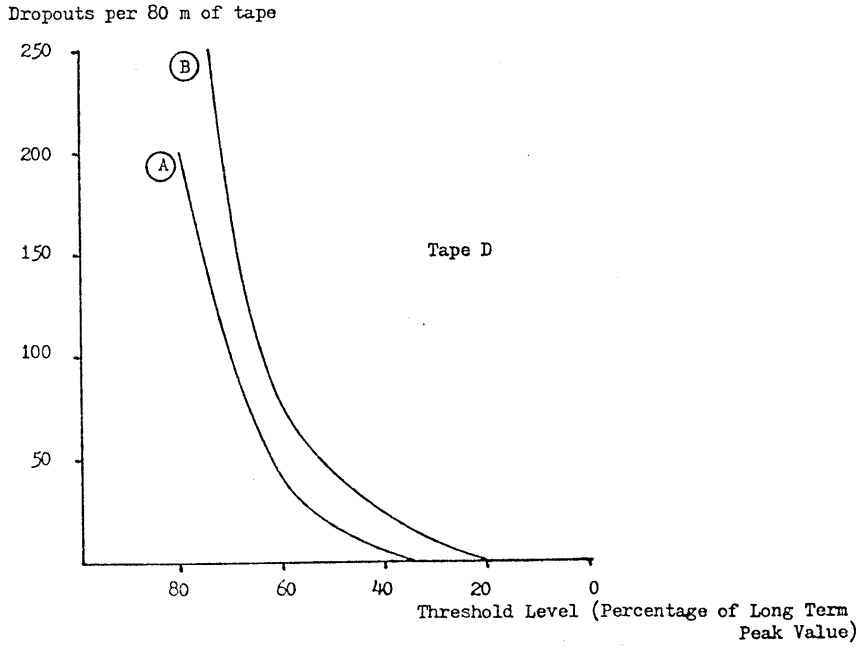

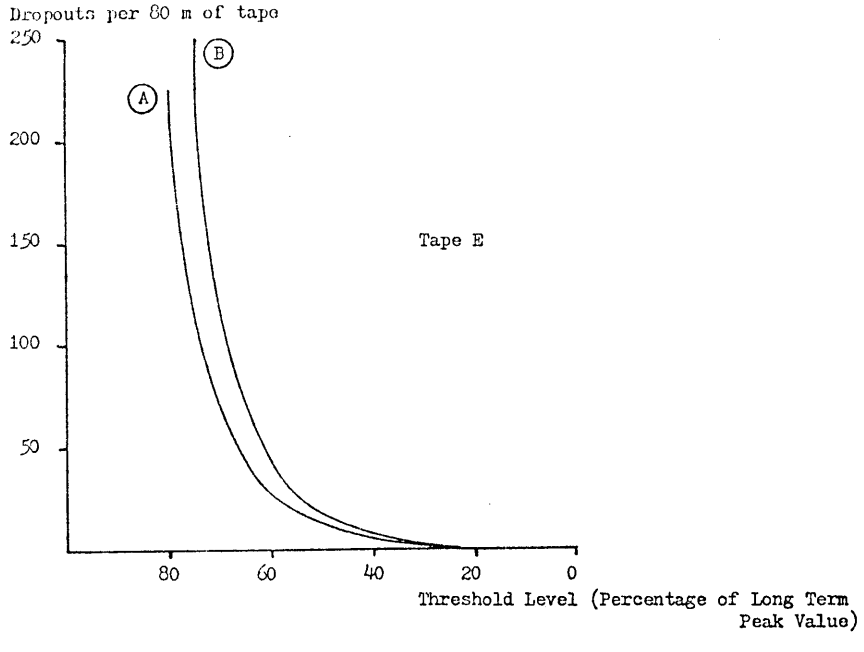

Figure 5.8 'Drop-out' count compared to threshold level for the audio cassette tapes used in the test - frequency 3 kHz.

The effect of the recorded frequency is shown in Figure 5.9 . Curve A shows the worst-case 'drop-out' count for tape A at 3 kHz, and curve B the worst-case 'drop-out' count at 5 kHz.

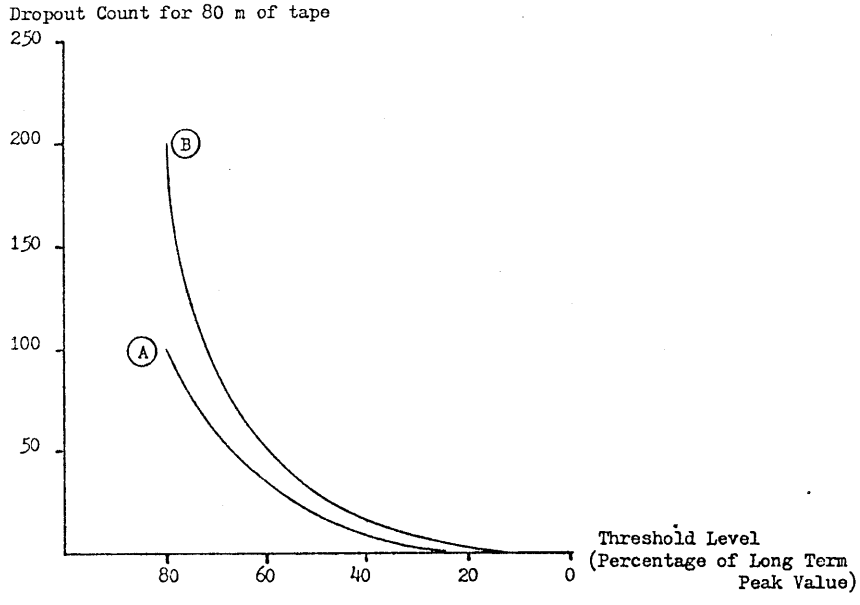

Figure 5.9 Effect of frequency on 'drop-out' count.

The duration of each 'drop-out' was measured using counter B. The 'drop-out' length distribution is shown in Figure 5.10 .

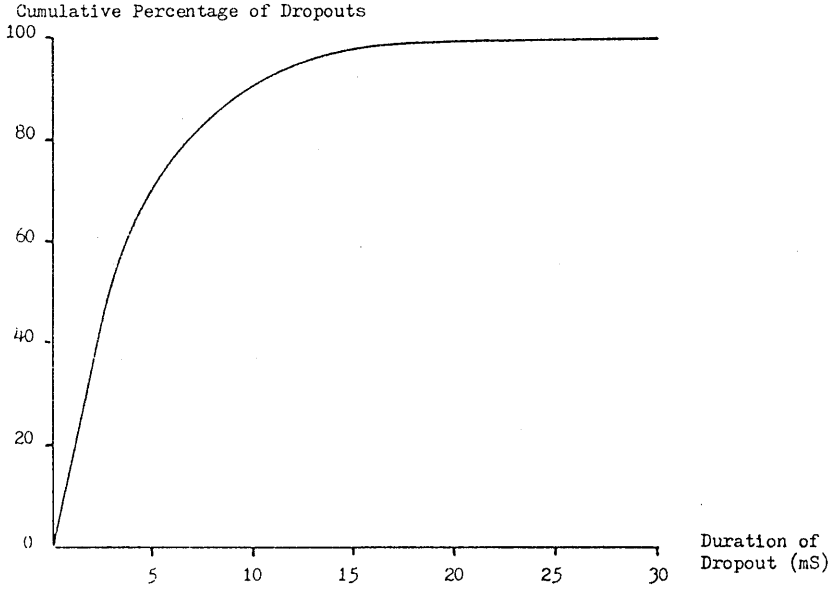

Figure 5.10 Length distribution of 'drop-outs' - frequency 3 kHz.

Conclusions

1. There is an almost continuous rapid variation in amplitude of the playback signal. The amplitude commonly varies between 100% and 80% of its normal long-term value. Falls to lower levels are much less frequent. With a recorded frequency of 3 kHz, the playback signal did not fall below 20% of peak value at any time during the tests. Therefore, it should be possible to provide essentially 'drop-out' free data storage provided the detection of the recording code can be made sufficiently insensitive to amplitude variation.

2. The single most important factor in determining 'drop-out' performance is the quality of the recording tape, in as much as, tapes A and B, which gave the lowest 'drop-out' figures were samples of higher priced tapes. There was little difference in performance between the remaining three tapes. Further tests of other samples of tapes A and B have shown that the results obtained are fairly consistent.

3. The number of 'drop-outs' at each threshold level increased with increase in recorded frequency. It is to be expected that data recording which avoids the use of the higher frequencies will be less prone to 'drop-out' induced errors.

4. 90% of all 'drop-outs' are less than 10 ms in duration (0.5 mm of tape).

5. There is little evidence to suggest that tests carried out once the tape recorders had been cleaned gave any improvement in terms of protection against 'drop-out'.

Notes

1. The tapes used in the test were new and previously unused. Therefore, the results do not reflect the possibility of 'drop-out' caused by damage to the tapes due to mishandling, etc. Simulation tests show that, where there is visible tape damage, it may be accompanied by severe 'drop-out'.

2. Since the tests were made, a sample of an untested tape was found to contain two segments, each of approximately 1 mm in length, where complete signal loss occured. Clearly, therefore, not all tapes can be predicted to be free of 'drop-outs' below 20% of peak.

5.3 Azimuth Misalignment

Introduction

Section 5.1.2 described the loss in signal caused by azimuth misalignment. In order to assess the extent of this misalignment in typical audio cassette recorders, the alignment of a wide range of recorders was examined.

The method employed avoided the need to bring the recorders to be tested into the laboratory or to limit the test to those recorders which provided a convenient method of azimuth adjustment.

Experimental Procedure

A precision head-alignment tape was used to adjust the alignment of a recorder used as a laboratory standard. A recording of a test tone was then made on one of the recorders to be tested. The recording was

used to readjust the alignment of the standard recorder to give maximum playback signal. The degree of adjustment required was directly related to the head alignment of the tested recorder. The process was repeated for each of the recorders.

Accurate mechanical measurement of the required adjustment proved difficult. In consequence, the peak playback level of the head-alignment tape, in the two head positions, was used as an indicator of the error in azimuth. The sense of the error was recorded separately as either positive or negative.

$$\text{Azimuth alignment factor} = \frac{\text{peak level at test tape alignment position}}{\text{peak level at correct alignment position}}.$$

Results

A total of 20 recorders were tested, selected as typical of those already used by students. The azimuth alignment factor for each recorder and the sense of the misalignment are shown in Table 5.1 . The head-alignment tape, used to produce the values in the table, was recorded at 3 kHz.

Recorders 5 and 11 show the largest misalignment. In this case, the alignment factor of 0.5 shows that the recorders are misaligned to an extent that would reduce a 3 kHz tone to half the amplitude it would have at correct alignment. The sense of the misalignment in recorder 5 is opposite to that in recorder 11 and consequently a recording made on recorder 5 would suffer severe loss on playback by recorder 11 and vice versa.

Test	Sense	Alignment Factor	Test	Sense	Alignment Factor
1	+	0.9	11	+	0.5
2		1.0	12	-	0.9
3	+	0.9	13		1.0
4	-	0.95	14	+	0.85
5	-	0.5	15	+	0.9
6		1.0	16		1.0
7	-	0.9	17	-	0.7
8	+	0.95	18	+	0.9
9	+	0.8	19	+	0.95
10	+	0.9	20	+	0.8

Table 5.1 Azimuth alignment factor for each of the tested recorders.

Table 5.2 shows the effect of head misalignment on test tones at different frequencies within the bandwidth of the recorders.

Alignment Factor

Test	1 kHz	2 kHz	3 kHz	4 kHz	5 kHz	6 kHz
1	0.8	0.66	0.5	0.27	0.11	0.10
2	0.95	0.8	0.5	0.25	0.15	0.1
3	0.8	0.6	0.5	0.3	0.1	0.05

Table 5.2 Effect of head misalignment on alignment factor at different frequencies.

Conclusions

The tests show that, although the majority of the tested recorders had correctly aligned heads with only a small margin of error, some recorders had quite severe head alignment error. The effect of the alignment error increases with signal frequency.

The solution to azimuth misalignment adopted by several microcomputer manufacturers, is to provide an alignment tape to enable the head alignment of the recorder to be checked and, if necessary, corrected [33]. The difficulty here is that the adjustment of head alignment is not a simple procedure in the majority of recorders. In most cases, it requires the removal of the outer case of the recorder and often some desoldering of connecting wires. Clearly, this solution can only be adopted where the technical skill of the user is known to be adequate.

If azimuth misalignment cannot be corrected easily, then its effects have to be minimised. Table 5.2 shows that the level of misalignment found in practice has far less effect on the playback signal amplitude at frequencies below 3 kHz, than at higher frequencies. Therefore, to minimise the effects of azimuth misalignment, use of the higher frequencies within the passband of the recorder must be avoided.

5.4 Tape Speed Variation

Introduction

In addition to bandwidth considerations, the choice of channel code is determined by timing stability. This is dependent upon the ability of the recorder to maintain constant tape speed, because variation in tape speed affects the relationship between the wavelength of the signal on tape λ and the frequency f of the original record and playback signals (f = tape speed/λ) [34].

The ability of the transport mechanisms of typical audio cassette recorders to provide constant tape speed was examined in a simple experiment.

Experimental Procedure

A 3 kHz tone was recorded on a selection of tapes, by each of three recorders. The tapes were then played back on the recorders, in turn. The playback signal, in each case, was applied to an oscilloscope and to a phase-locked loop. The filtered error voltage of the phase-locked loop was monitored on a previously calibrated chart recorder. A schematic diagram of the test circuit is shown in Figure 5.11 .

Short-term speed variation (e.g. variation over a time duration of less than 100 ms - 'flutter' in audio recording applications) was determined by measurement of the maximum variation in the time period of repeated cycles of the playback signal, as displayed on the oscilloscope. Medium-term speed variations (e.g. variations over a time duration of between 100 ms and 1 s - 'wow' in audio recording) and longer-term

speed variations were evident in changes of the phase-locked loop error voltage as displayed on the chart recorder.

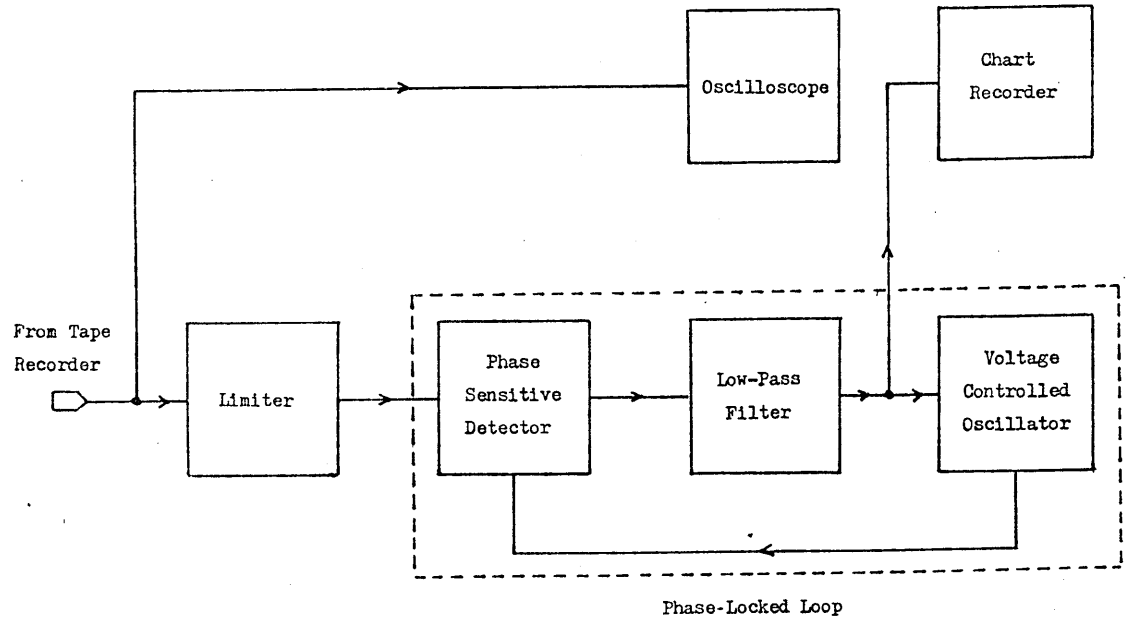

Figure 5.11 Schematic diagram of tape speed test circuit.

Results

The worst case short-term speed variations found in the tests, expressed as a percentage of the long-term tape speed, are shown in Tablet 5.3 . Results indicate that the audio cassette tape in use has a significant effect on the short-term speed variation of the recorder (through frictional effects inside the cassette).

Tape Recorder	Worst case short-term tape speed variation
A	± 3.1 %
B	± 1.9 %
C	± 3.2 %

Table 5.3 Worst case short-term speed variations of tested recorders.

Figure 5.12 shows two typical chart recordings and indicates the resolution and response time obtained from them.

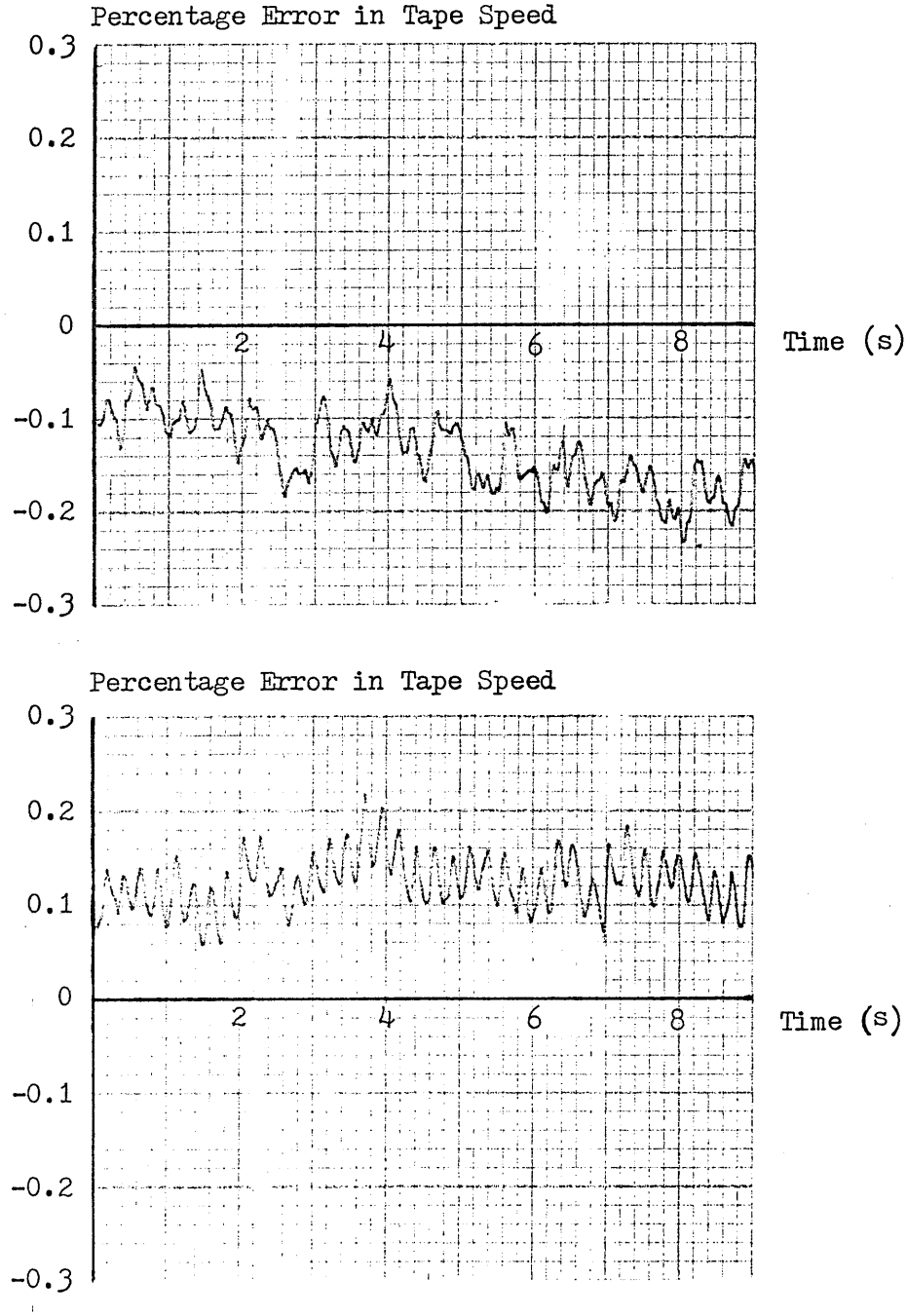

Figure 5.12 Example chart recordings of tape speed monitoring procedure.

The chart recordings were used to calculate medium and long-term speed variations. Medium-term speed variation was calculated over one second sample periods, and long-term speed variation over the 30 minute duration of the tape. Worst case speed variations for each of the tested recorders are given in Table 5.4 .

Tape Recorder	Worst case medium-term speed variation	Worst case long-term speed variation
A	± 1.1 %	± 2.0 %
B	± 0.9 %	± 2.2 %
C	± 2.1 %	± 5 %

Table 5.4 Worst case medium and long-term speed variations of the tested recorders.

Conclusions

Unlike many digital cassette storage systems, which are hub driven [35], the audio cassette recorder has capstan and pressure roller drive which gives superior tape speed control. However, even in this case, a long-term tape speed error of 10% may still be encountered when tapes are interchanged from recorder to recorder. In addition to this variation, the short-term speed variations of recorders are likely to cause significant timing jitter in the playback signal.

The two most common causes of tape speed variation are worn and slipping drive belts and flaws in the pressure roller. During use within the Radiotext system, recorders will be left in the record mode with the motor switched off. As a result, the capstan may cause a temporary indentation in the pressure roller with some subsequent

variation in tape speed [36]. It is important, therefore, to recognise that protection against tape speed variation of greater than 10% may be required.

5.5 Alternative Channel Codes

5.5.1 Introduction

The audio cassette recorder is essentially a band-pass channel which suffers amplitude instability, particularly at higher frequencies, with time jitter due to tape speed variation. The channel code used to store data should modify it in such a way as to provide reliable recording at the highest data rate possible, given the limiting characteristics of the recorder.

The major requirements of a suitable channel code are that it should:

(1) be free of any d.c. content,

(2) efficiently utilise the bandwidth available,

(3) be self clocking to protect against time base error, and subsequent loss of bit synchronization, due to tape speed variation,

(4) be insensitive to amplitude instability.

5.5.2 Review of Existing Recording Codes

Many channel codes have been and are used for data storage on digital recorders. Some of them have been used to store data on audio cassette recorders. In addition, other codes have been specifically developed for use with audio cassette recorders.

The major channel codes used for data storage are reviewed below.

Return to Zero RZ

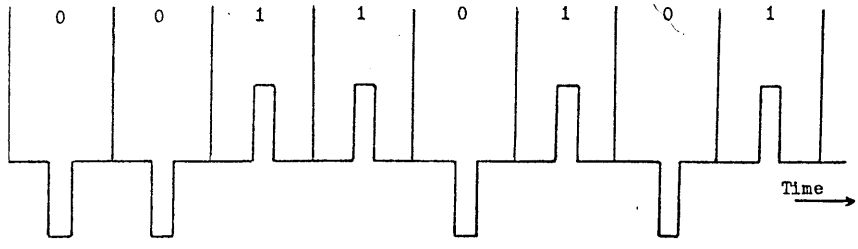

Figure 5.13 Return to Zero Code.

In this code a data '1' is represented by saturating the tape in one direction for a short period and data '0' by saturating the tape in the opposite direction. Between pulses the tape remains unmagnetized [37].

(1) D.C. content - Yes

(2) Bandwidth (expressed as highest frequency content within code) - greater than twice data rate.

(3) Self clocking - Yes

Return to Bias RB

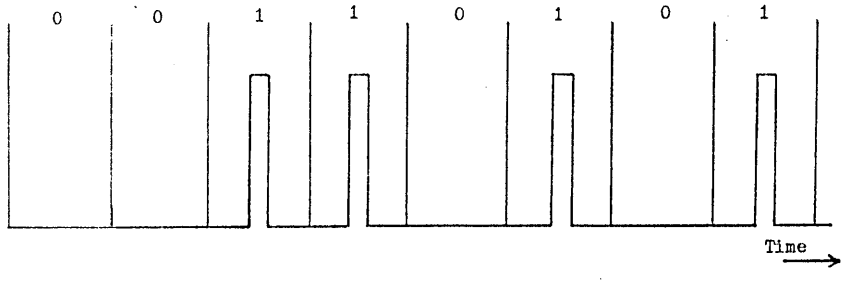

Figure 5.14 Return to Bias Code.

The tape is normally biased to saturation. A data '1' magnetizes the tape in the opposite direction for a portion of the bit cell. The reproduced voltage at the playback head in approximately double that of

RZ coding, because of the change in magnetization from saturation to saturation [38, 39].

(1) D.C. content - Yes

(2) Bandwidth - greater than twice data rate

(3) Self clocking - No

Return to bias RB with complementary code RB-S on second track

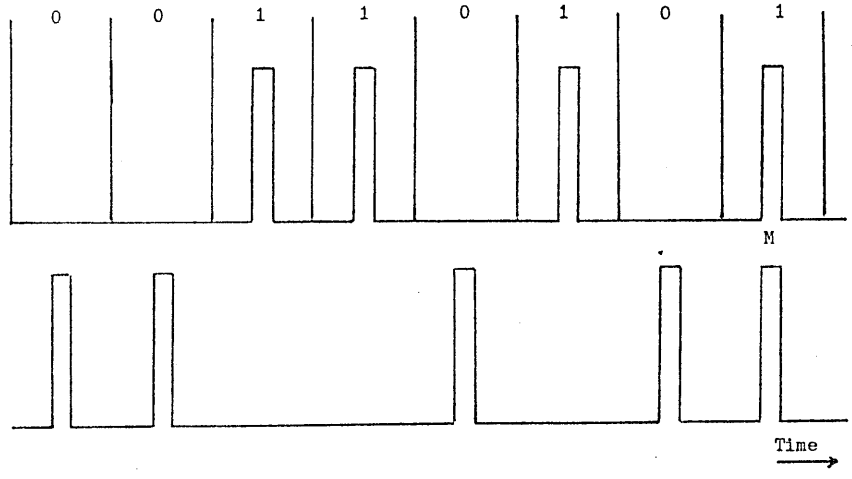

Figure 5.15 Return to bias with complementary code on second track.

RB code is used in low-cost digital cassette drives where clock information is obtained by writing the complement of RB, RB-S, on a second track [40]. A framing mark (M) can be provided by causing a transition to occur on both tracks simultaneously. Error checking is possible by counting clocks between framing marks.

(1) D.C. content - Yes

(2) Bandwidth - greater than twice the data rate

(3) Self clocking - Yes

Return to Bias - Pulse Ratio

(similar codes are speed tolerant recording, pulse duration modulation and pulse width encoding)

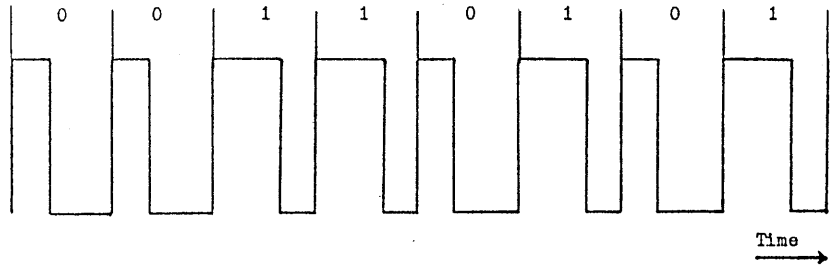

Figure 5.16 Return to Bias - Pulse Ratio Code.

The bit cell is divided into three parts. There is always a transition at the beginning of the cell to provide a self clocking characteristic. Data '0' is indicated by a transition at 1/3 of the bit cell and a data '1' is indicated by a transition at 2/3 of the bit cell [41].

This code has the advantage of being extremely speed tolerant and has been applied to low-cost digital cassette systems with reel to reel drives lacking capstan speed control [42].

(1) D.C. content - Yes

(2) Bandwidth - greater then twice the data rate

(3) Self clocking - Yes

Non Return to Zero NRZ (also called NRZ-Level)

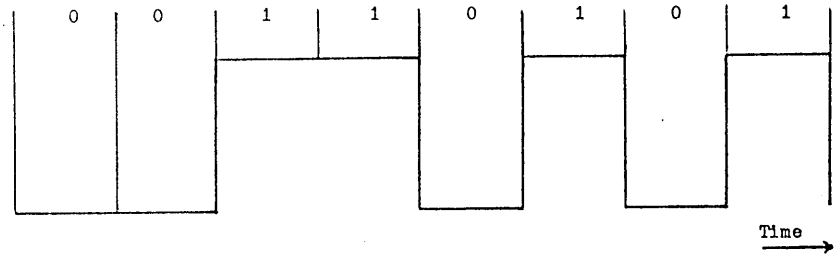

Figure 5.17 Non Return to Zero Code.

Data '1' is represented by saturation in one direction and data '0' by saturation in the other [43,44,45,46].

(1) D.C. content - Yes

(2) Bandwidth - up to data rate

(3) Self clocking - No

Non Return to Zero-Inverted NRZ-I (also called NRZ-Mark)

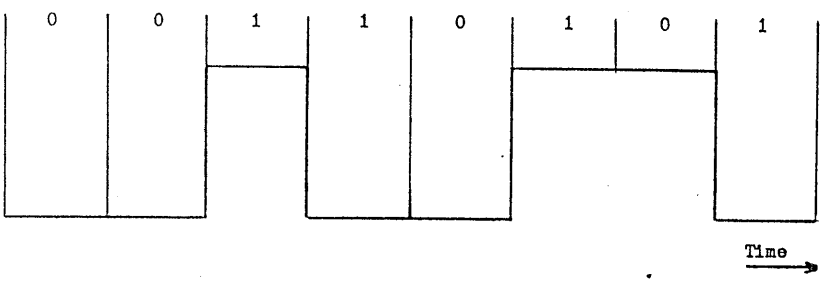

Figure 5.18 Non Return to Zero-Inverted Code

NRZ-I has a transition for each data '1' and no transition for data '0'. It is not self clocking. However, with the use of multitrack recording of parallel data words, and odd parity, there will always be an odd number of data ones across the tape to be used for clocking [47,48,49].

(1) D.C. content - Yes

(2) Bandwidth - up to data rate

(3) Self clocking - No, unless used in multitrack applications

Non Return to Zero-Inverted with complementary code NRZ-S on second track

Some digital cassette recorders use NRZ-I on one track and its complement, NRZ-S, on the other. The clock information is contained within the two tracks [50,51].

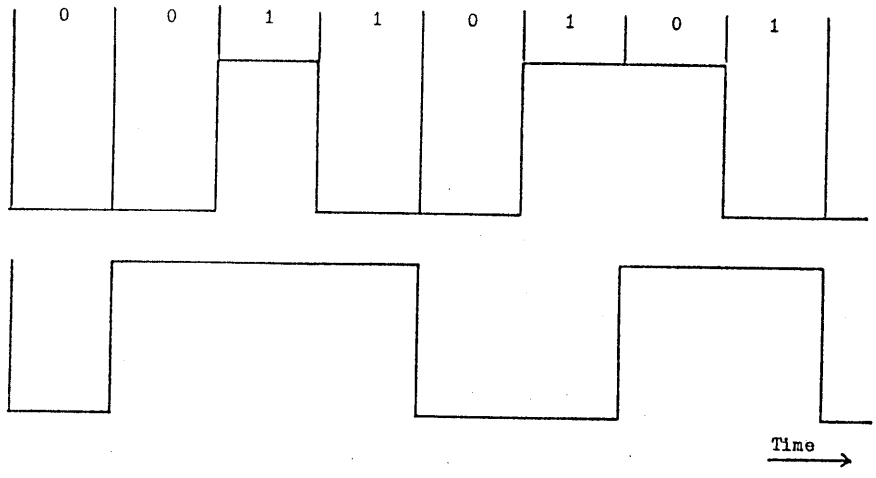

Figure 5.19 Non Return to Zero-Inverted with complementary code on second track

(1) D.C. content - Yes

(2) Bandwidth - up to data rate

(3) Self clocking - Yes

Phase Encoding Bi ∅ M (also called Manchester Code)

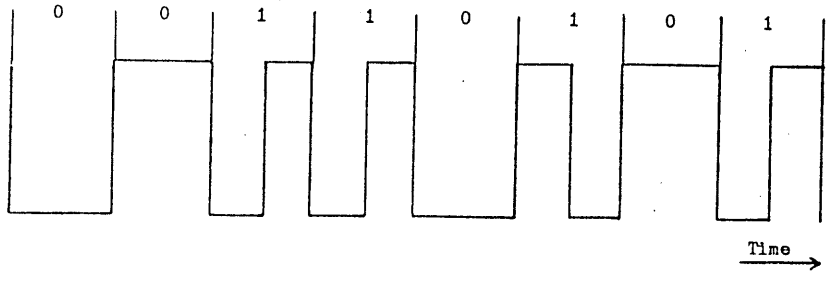

Figure 5.20 Phase Encoding Bi ∅ M

A transition occurs in the code at every bit edge, with an extra transition midway through the bit period when the data is '1' to distinguish it from data '0' 52,53,54,55,56.

(1) D.C. content - No

(2) Bandwidth - up to twice the data rate

(3) Self clocking - Yes

Phase Encoding Bi ∅ L

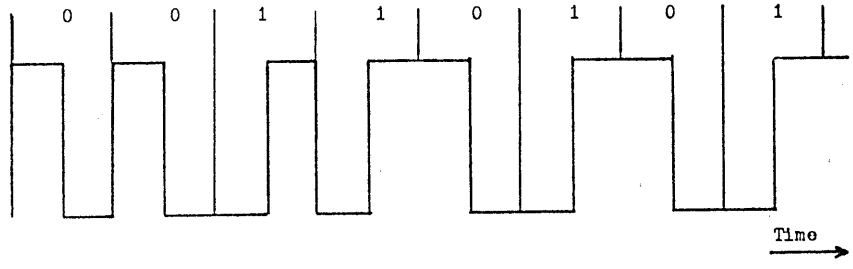

Figure 5.21 Phase Encoding Bi ∅ L

For data '0', the flux transition within the bit cell is 'negative' and, for data '1', it is 'positive'. If two similar bits follow each other, there is an interbit transition at the boundary of the bit cell [57,58,59,60].

(1) D.C. content - No

(2) Bandwidth - up to twice data rate

(3) Self clocking - Yes

Miller Code

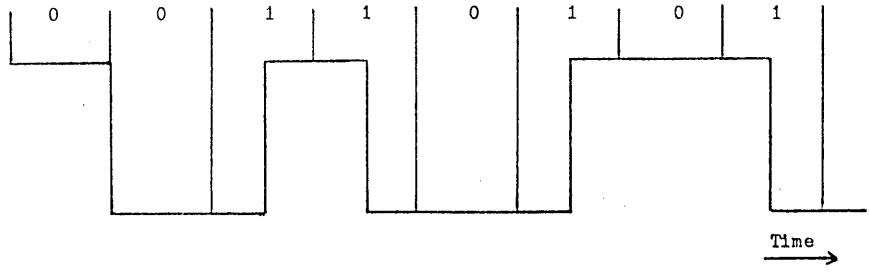

Figure 5.22 Miller Code

Data '1' is coded with a flux transition in the middle of the bit cell. An isolated data '0' is ignored. Transitions are inserted at the beginning of the bit cell between pairs of data '0's. Coding requires

a comparison of adjacent bits and therefore a single bit store in the encoding circuitry [61,62,63].

(1) D.C. content - Yes

(2) Bandwidth - slightly above data rate

(3) Self clocking - Yes, but since transitions have to be identified at the beginning and middle of bit cells, only certain bit patterns provide clock synchronization.

M^2 and Zero Modulation

Miller code can be made d.c. free by modifying the coding of those data bit sequences which would otherwise produce a d.c. component. Coding in this way requires look-forward and look-backward memories to identify problem sequence boundaries [64,65,66,67].

(1) D.C. content - No

(2) Bandwidth - slightly above data rate

(3) Self clocking - Yes (given correct bit pattern)

Group Coding (including Run Length Coded NRZ and Enhanced NRZ)

Group encoding involves slicing the data to be recorded into groups and transforming the groups into longer 'code words', which are then recorded in NRZ-I. Extending the length of the data groups in this way (by the addition of extra bit cells) enables use to be made of only those code words with little or no d.c. content [68,69].

(1) D.C. content - No, although some group codes, e.g. Enhanced NRZ, still retain a d.c. component.

(2) Bandwidth - greater than data rate to a degree determined by

coding technique.

(3) Self clocking - No, unless used in multitrack applications.

Tone Burst Modulation

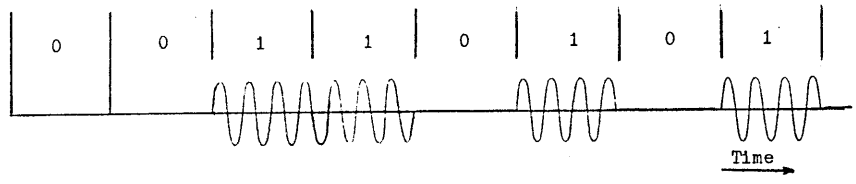

Figure 5.23 Tone Burst Modulation

A tone burst represents data '1', and absence of a burst indicates data '0'. Like all amplitude modulation schemes this code is susceptible to errors caused by amplitude instability and noise. Detection requires several tone cycles per bit cell [70,71].

(1) D.C. content - No

(2) Bandwidth - greater than twice the data rate

(3) Self clocking - No

Pulse Width Carrier Modulation

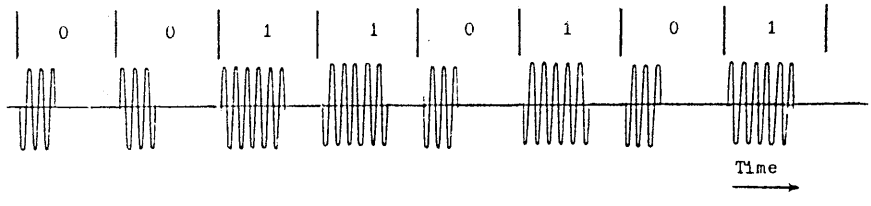

Figure 5.24 Pulse Width Carrier Modulation

A short tone burst within the bit cell represents data '0', and a longer burst represents data '1'. This code can be detected in such a way as to make it independent of amplitude variation [72].

(1) D.C. content - No

(2) Bandwidth - greater than twice the data rate

(3) Self clocking - Yes

Frequency Shift Keying (FSK)

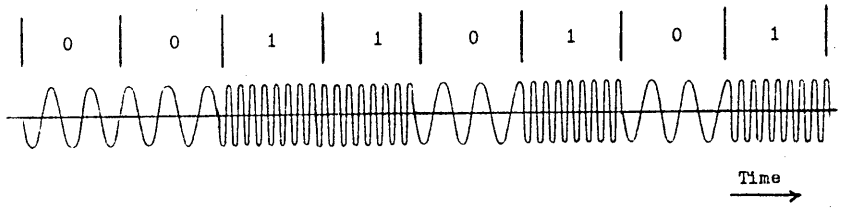

Figure 5.25 Frequency Shift Keying

A data '0' is represented by one signalling frequency, and a data '1' by another. The deviation between the signalling frequencies must be sufficient to protect against decoding errors due to tape speed variation [73,74].

(1) D.C. content - No

(2) Bandwidth - greater than twice the data rate

(3) Self clocking - No, unless an effort is made to synchronize the signalling frequencies to the data rate, or pulse width FSK is used

5.5.3 Choice of Channel Code for Radiotext

The review of channel codes in Section 5.5.2 shows that many channel codes do not fulfil the requirements of a suitable code for data storage on audio cassette. This is because, in many digital applications, the requirements placed on the channel code may be relaxed. For example, multitrack recording, with use of a parallel

clock track, removes the need for the code to be self clocking. Additionally, in some digital storage systems, the worst effects of baseline shift and pattern sensitivity, caused by the d.c. content of a code, may be reduced by trapping the worst case or 'pathological' data sequences, and by use of d.c. restoration in the decoder circuitry [75].

Of the reviewed codes, those which do fulfil the necessary channel code requirements are listed below in order of least bandwidth requirement for a given data rate.

Zero Modulation and M^2 Code

Phase Encoding Bi Ø M

Phase Encoding Bi Ø L

Pulse Width Carrier Modulation

Frequency Shift Keying

Zero Modulation and M^2 code are used in high-density digital recording applications (Zero Modulation in the I.B.M. 385 Mass Storage System [76], and M^2 code in the Ampex 'Electronic Still Store' [77]). The penalty for the economy of bandwidth provided by these codes is in the complexity and resultant high cost of the encoding and decoding circuitry. The relative cost of implementation of these channel codes is inappropriately high when viewed in terms of the overall system cost requirements of Radiotext.

Therefore, phase encoding remains as the most bandwidth efficient method of channel coding which can be implemented at realistic cost. In

existing microcomputer data storage applications, phase encoding is rarely used because available circuit implementations have been unable to provide consistently reliable operation. As a result, the majority of microcomputers employ frequency shift keying techniques at low data rates. For example, the 'Kansas City' or 'C.U.T.S.' standard for data storage uses frequency shift keying with synchronized signalling frequencies at a data rate of 300 baud [78].

Phase encoding offers the promise of substantially higher data storage rates (2400 baud) than frequency shift keying (300 baud). A study was undertaken to examine the difficulties encountered in the use of phase encoding, and to provide solutions in the form of a highly reliable encoder/decoder circuit design.

Of the two phase encoding techniques, Bi ϕ M was chosen for this application. Unlike Bi ϕ L, Bi ϕ M is unaffected by signal phase inversion which occurs in some makes of audio cassette recorder. The result of signal phase inversion on Bi ϕ L is to complement the decoded data stream. In addition, Bi ϕ M does not require the synchronizing data sequence necessary for Bi ϕ L, and therefore recovery from failure is more rapid, without any need to resynchronize data and clock transitions.

5.6 The Phase Response of the Audio Cassette Recorder

When a Bi ϕ M coded signal is recorded using a digital recorder, the playback waveform consists of well-defined peaks coincident with transitions in the recorded waveform. These peaks are used in decoding the waveform. In audio cassette recording, the effect of the amplitude

equalization filter, provided to give an overall flat amplitude-frequency response, is to cause the peaks to be less well defined and not necessarily coincident with the recorded transitions. As a result, detection must rely on timing the intervals between zero crossings of of the playback signal.

In order to preserve the waveform of the Bi ϕ M coded signal and so enable zero crossing timing detection to be used, phase linearity within the recording channel is essential, i.e. the channel phase change should be small enough to be neglected, or else, as far as possible it should be proportional to frequency. Because the human ear is fairly insensitive to the relative phases of the frequency components within a signal, the manufacturers of low-cost audio cassette recorders make little attempt to linearize the phase response. Due to the absence of abrupt changes in the amplitude response of these recorders, the phase or delay distortion should be moderate as compared to the delay distortion introduced by the sharp filtering in many communication channels [79]. Therefore, provided the phase response is sufficiently consistent, it should be possible to provide overall phase linearity by use of external circuitry.

The characteristic nature of the playback waveforms, produced from 'square' wave recordings at various frequencies, demonstrates this consistency in the phase response. Figure 5.26 shows such a typical playback waveform from a recorded 'square' wave at 1 kHz. By far the majority of recorders produced such a waveform.

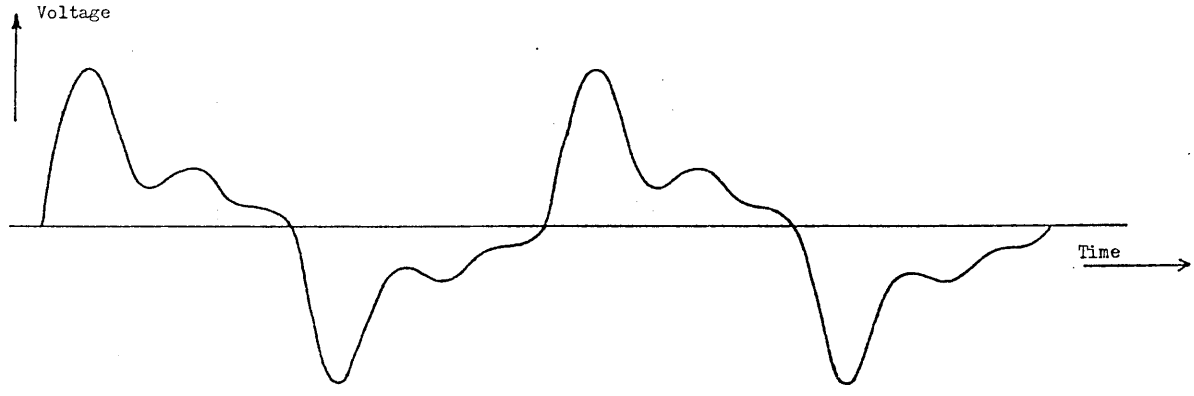

Figure 5.26 Characteristic playback waveform produced by a 'square' wave recorded signal at 1 kHz.

Phase response is difficult to measure because of the discontinuous nature of the recording process. Overall recorder response was estimated by measurement of record and playback amplifier phase responses and by measurement of the relative phase of frequency components within the playback signals of recorded 'square' waveforms at various frequencies. Additionally, the phase response of the recorder was modelled, the expected response to selected waveforms calculated and comparison made between the calculated response and that found in practice.

A typical recorder phase response, ignoring the time displacement between record and playback, is shown in Figure 5.27 . The extent of the variation from this typical response is indicated by the dotted curves. Below 800 Hz, there is wide variation in the phase response.

The response is essentially that of the $+90^{o}$ shift, independent of frequency, produced at the playback head, with a lag caused by the low-pass characteristic of the amplitude equalization filter at lower frequencies and the lead caused by the high-pass characteristic of

this filter at higher frequencies.

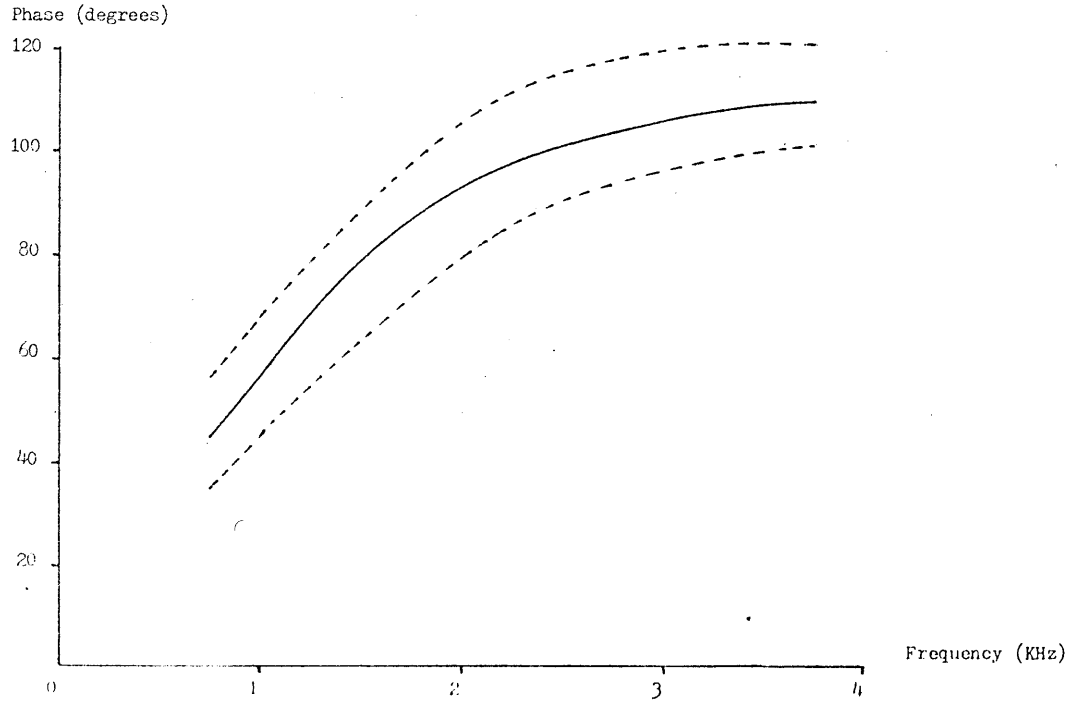

Figure 5.27 Typical phase response of audio cassette recorder. Dotted curves indicate the extremes of phase response experienced in practice.

The effect of the phase response on Bi ∅ M coded data is shown in Photograph 5.1 . The upper trace shows the playback waveform at a data rate of 2400 baud. The lower trace is a hard limited version of this playback waveform to enable zero crossing intervals to be seen more clearly.

In addition to a reduction in the ratio between zero crossing intervals of data '0' and data '1', there is considerable droop in the waveform during data '0'. This droop reduces the immunity of the code to amplitude instability and can result in the occurrence of spurious zero crossings.

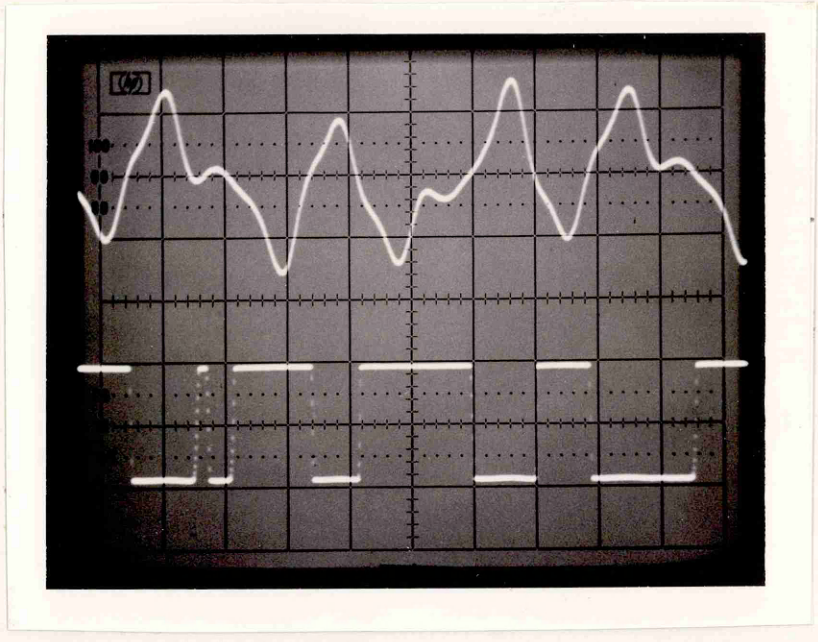

Timebase ≃ 250 us/div

Photograph 5.1 Playback waveform of Bi Ø M coded data at 2400 baud.

5.6.1 Phase Equalization - low-pass pre-filtering

In existing interface designs for phase encoding, the method most commonly employed to provide phase equalization is to include a first order low-pass filter in the encoder circuitry [80,81,82,83]. The filter produces a phase lag which increases with frequency to counteract the phase lead produced by the recorder. The effect of such a filter, with a break point or cut-off frequency of 1 kHz, is shown in Figure 5.28 . Curve A is the phase response of the recorder and curve B that of the filter. Curve C shows the resultant phase response in which the phase lead is approximately proportional to frequency.

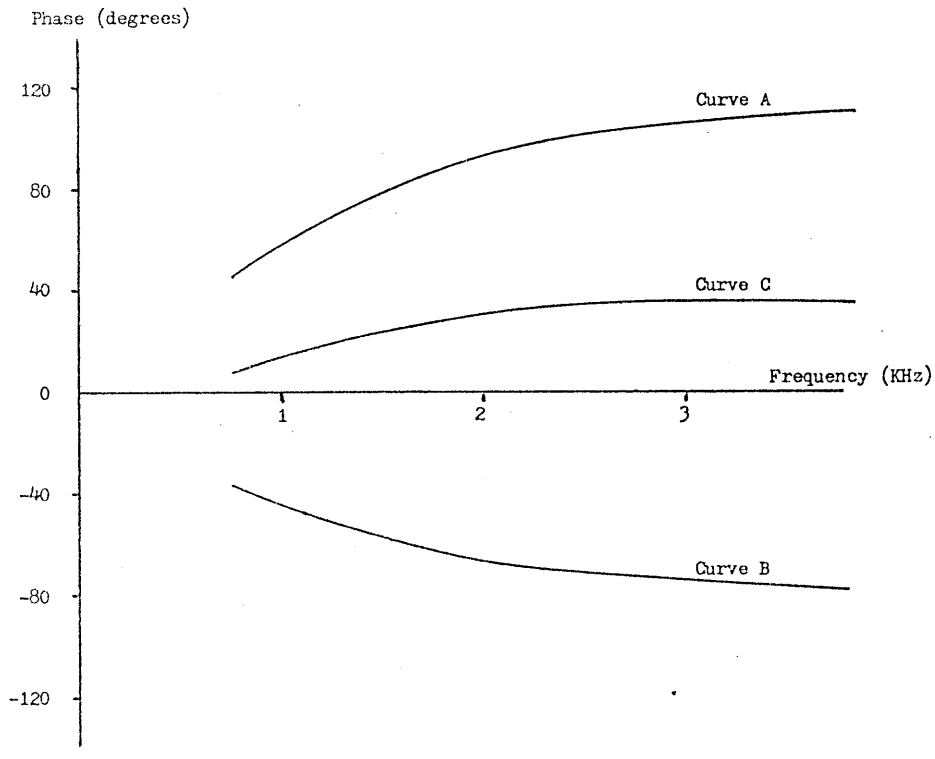

Figure 5.28 Phase response of recorder (curve A), low-pass filter (1kHz) (curve B) and their combined response (curve C).

The major difficulty with this method of phase equalization is the effect of the low-pass filter on the amplitude of the waveform to be recorded. Figure 5.29 shows the result of the use of such a filter (with cut-off frequency 1 kHz) on example Bi ϕ M coded data at a data rate of 2400 baud.

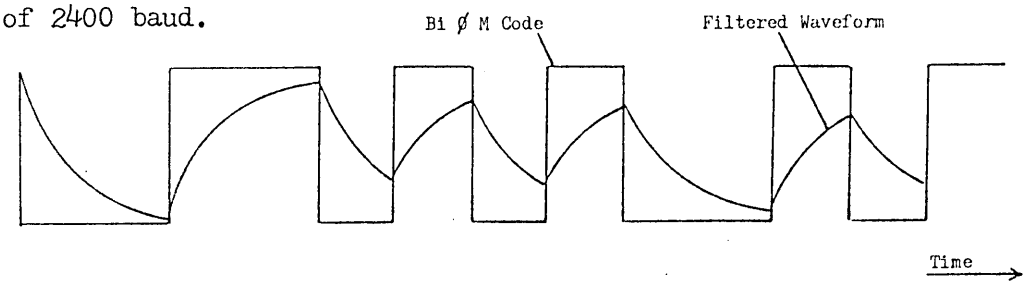

Figure 5.29 Effect of a low-pass filter (cut-off frequency 1 kHz) on Bi ϕ M coded data at 2400 baud.

The reduced amplitude of the higher frequency components of this waveform causes baseline shift and data pattern sensitivity in the playback signal. In consequence, the zero crossing intervals are highly inaccurate, as shown in Photograph 5.2 .

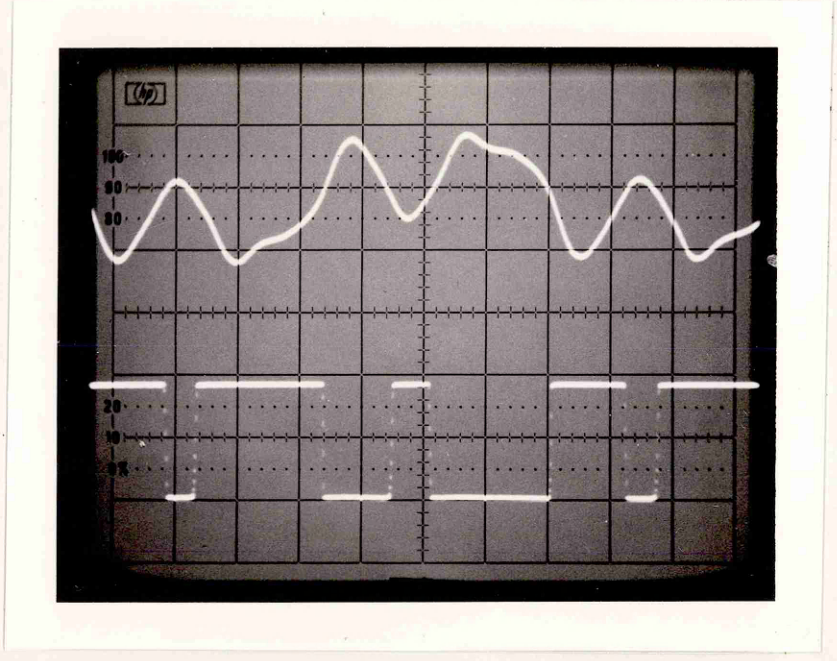

Timebase ≃ 250 us/div

Photograph 5.2 Playback waveform of Bi Ø M coded data with low-pass pre-filtering.

If the cut-off frequency of the filter is increased to reduce its effect on the amplitude of the phase encoded data, the filter becomes less effective in providing system phase linearity, as shown in Figure 5.30 .

So the choice of the cut-off frequency for the low-pass filter is usually a compromise. It has to be low enough to provide sufficient phase linearity, yet high enough to avoid prohibitive amplitude reduction of the higher frequency components within the coded waveform.

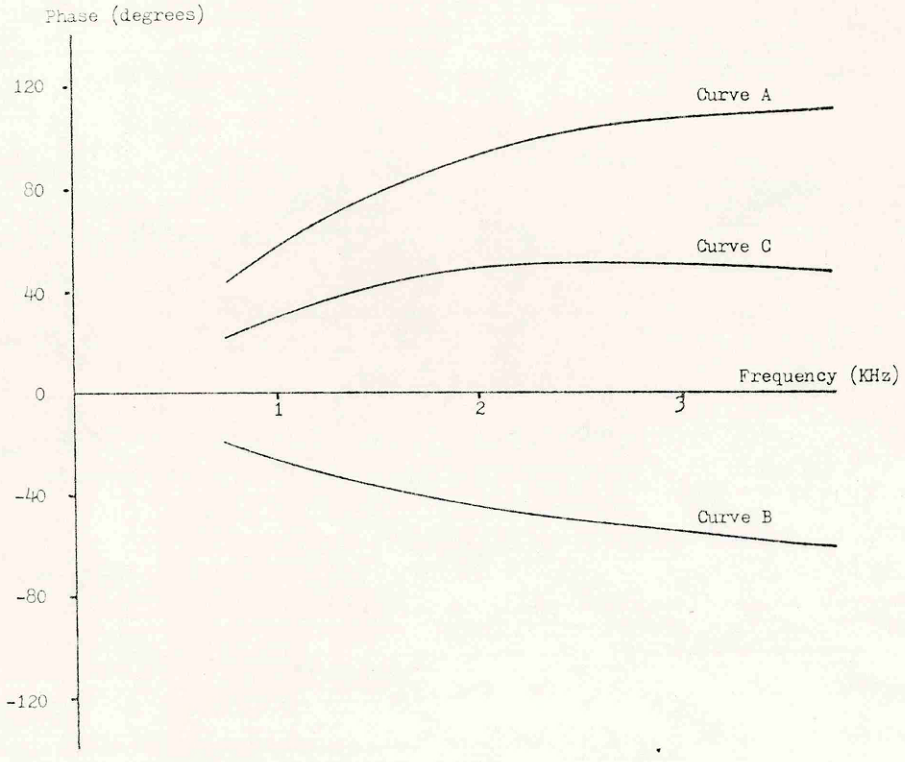

Figure 5.30 Phase response of recorder (curve A), low-pass filter (2kHz) (curve B) and their combined response (curve C).

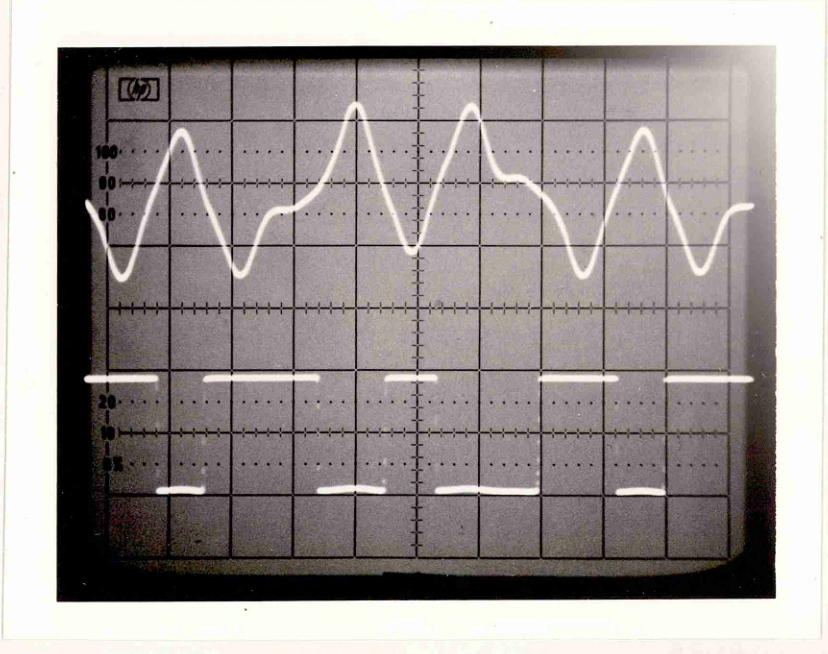

Timebase ≃ 250 μs/div

Photograph 5.3 The playback waveform of Bi Ø M coded data with a compromise low-pass filter cut-off frequency (1.5 kHz).

The result is a playback waveform typified by that of Photograph 5.3 . The margin for protection against amplitude instability remains small and appreciable inaccuracy remains in the zero crossing interval timing.

It is the difficulty of decoding such a waveform in the presence of timing jitter and amplitude instability which results in the low reliability of existing interface designs.

For reliable operation, it is necessary to provide phase linearity without influencing the amplitude of the coded data. Techniques were investigated to achieve this at low cost. Two solutions, switched pre-filtering and use of an all-pass filter, resulted from this investigation and were developed for further test and performance evaluation.

5.6.2 Phase Equalization - switched pre-filtering

In this method, a switched first order low-pass filter is used in the encoder circuit. The data stream is used to switch the filter, so that the cut-off frequency is doubled during the signalling of data '1' compared to that during data '0'. In this way, the filter can be adjusted to provide sufficient phase linearity to remove much of the droop experienced during signalling of data '0', without the accompanying reduction in amplitude when data '1' is signalled.

The effect of switched pre-filtering on the playback waveform is shown in Photograph 5.4 . The zero crossing interval ratio is very close to the 2:1 ideal. Droop during the signalling of data '0' is reduced so enabling reliable detection of the waveform to be achieved.

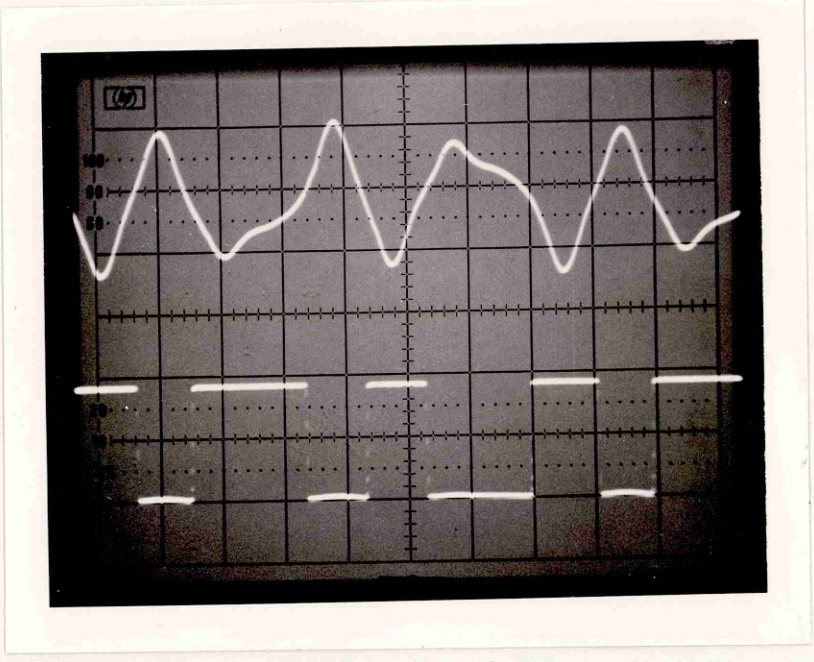

Timebase ≃ 250 μs/div

Photograph 5.4 The playback waveform of Bi Ø M coded data with switched pre-filtering.

5.6.3 Phase Equalization - all-pass filter

In this case, phase equalization is provided by an active all-pass filter to which the playback signal is applied before decoding. Figure 5.31 shows the circuit of a simple all-pass filter suitable for use in this application.

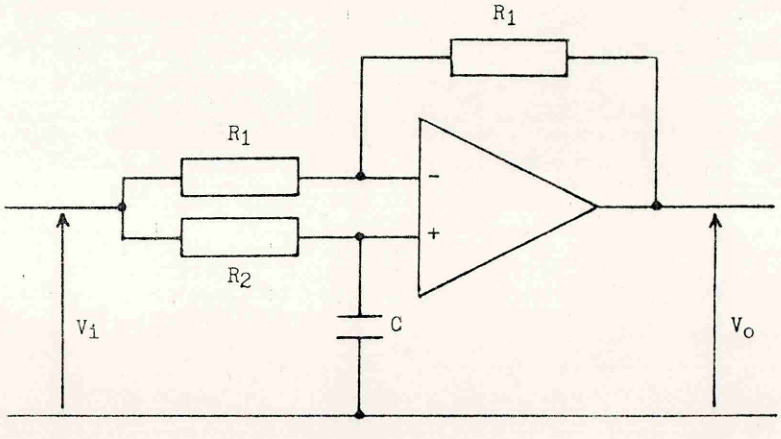

Figure 5.31 Active all-pass filter.

The voltage transfer function of this filter is

$$\frac{V_o}{V_i} = \frac{1 - j\omega CR_2}{1 + j\omega CR_2}$$

with modulus = 1 and angle = $-2 \arctan \omega CR_2$.

As a result, the filter provides a frequency dependent phase lag without influencing the amplitude of the input signal in any way. The phase lag is twice that which would be expected from first order low-pass filter CR_2 within this circuit.

Figure 5.32 shows how the use of a suitably designed all-pass filter can result in a significant improvement in the overall system phase linearity. The overall phase change throughout the frequency range of interest is very small and consequently produces little phase distortion. Curve A is the response of the recorder, curve B that of the all-pass filter and the combined response of recorder and filter is given in curve C.

The effect of the all-pass filter on the playback signal is shown in Photograph 5.5 . The phase corrected waveform is very close to that of the original Bi $\emptyset$ M coded data. The difference is due to the band-limiting characteristic of the recorder. Zero crossing intervals are very accurate and remain accurate in the presence of severe amplitude instability.

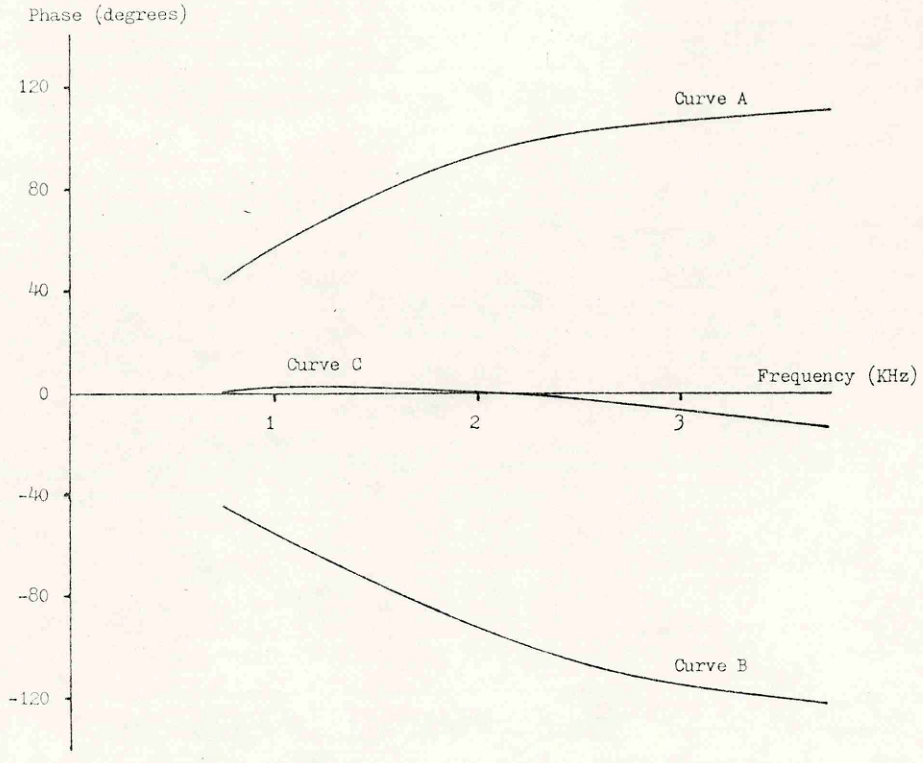

Figure 5.32 Phase response of recorder (curve A), all-pass filter (curve B) and their combined response (curve C).

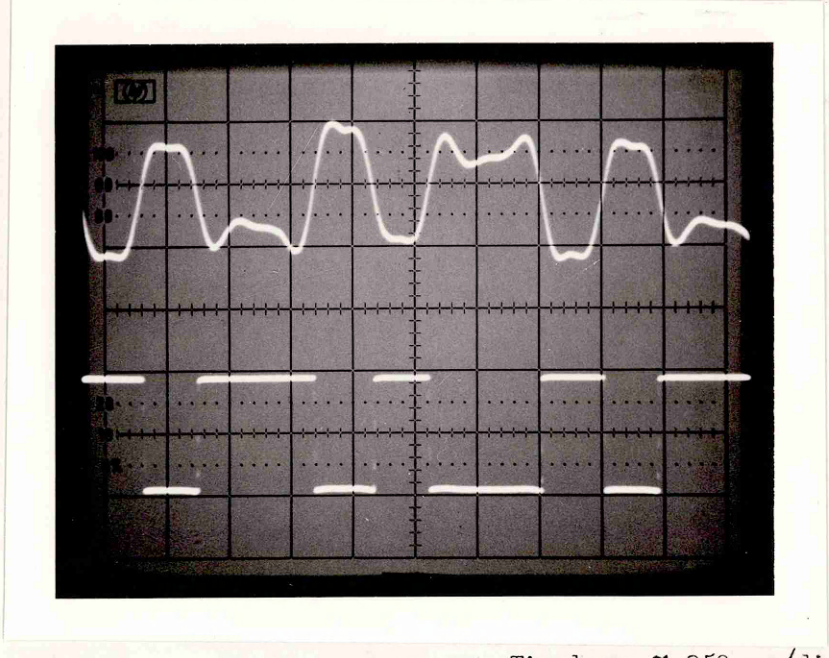

Timebase ≃ 250 μs/div

Photograph 5.5 The playback waveform of Bi Ø M coded data with phase equalization provided by an active all-pass filter.

5.7 Encoder

5.7.1 Introduction

With the use of Bi Ø M coding, it is possible to provide a data rate of 2400 baud within the effective bandwidth of the recorder. At this data rate the effects of spacing loss and azimuth misalignment should be minimal. In addition to this 'standard' data rate, it was considered desirable to provide the option of a higher rate of 4800 baud should this prove to be reliable in individual cases. The encoder and decoder circuits are therefore designed to provide both data rates. Description of the circuits will assume operation at 2400 baud. The modifications required for 4800 baud operation will follow the circuit description.

The data is provided to the encoder in serial format. It is delivered, together with a X16 data-rate clock, from an asynchronous communications interface adaptor.

5.7.2 Encoder Circuit Description

(a) Basic Circuit

A circuit diagram of the encoder is shown in Figure 5.33 .

IC1 divides the X16 data-rate clock frequency to provide the 4.8 kHz clock required by IC2. Flip-flops IC2a and IC2b produce the coded data. The output of IC2b is reduced to a suitable level (approximately 450 mV) for application to the auxiliary input of the audio cassette recorder. The output is filtered using a first order low-pass filter (approximate cut-off frequency 4.5 kHz) to avoid 'ringing' which occurs with some

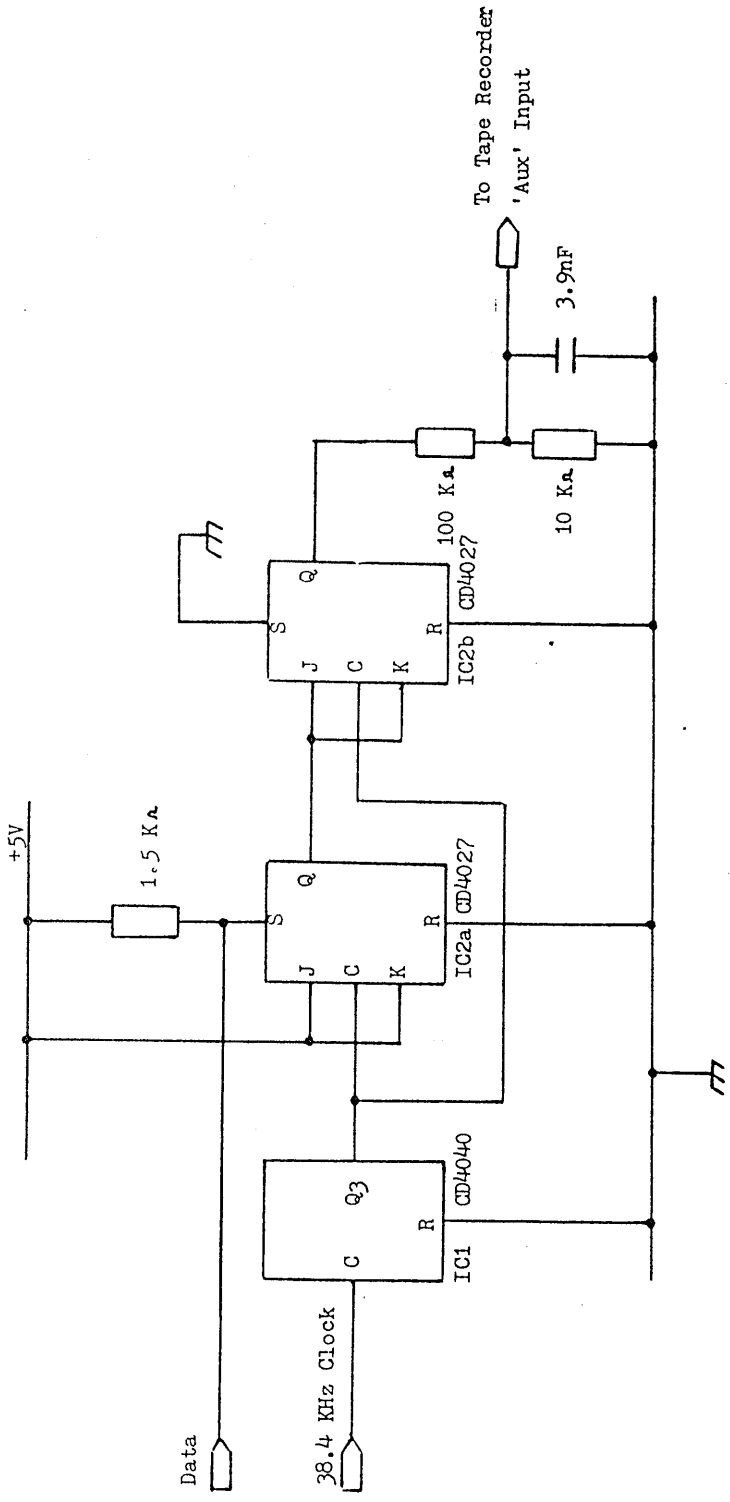

Figure 5.33 Basic encoder circuit.

record amplifiers.

The waveforms applicable to the various points within the encoder are shown in Figure 5.34 .

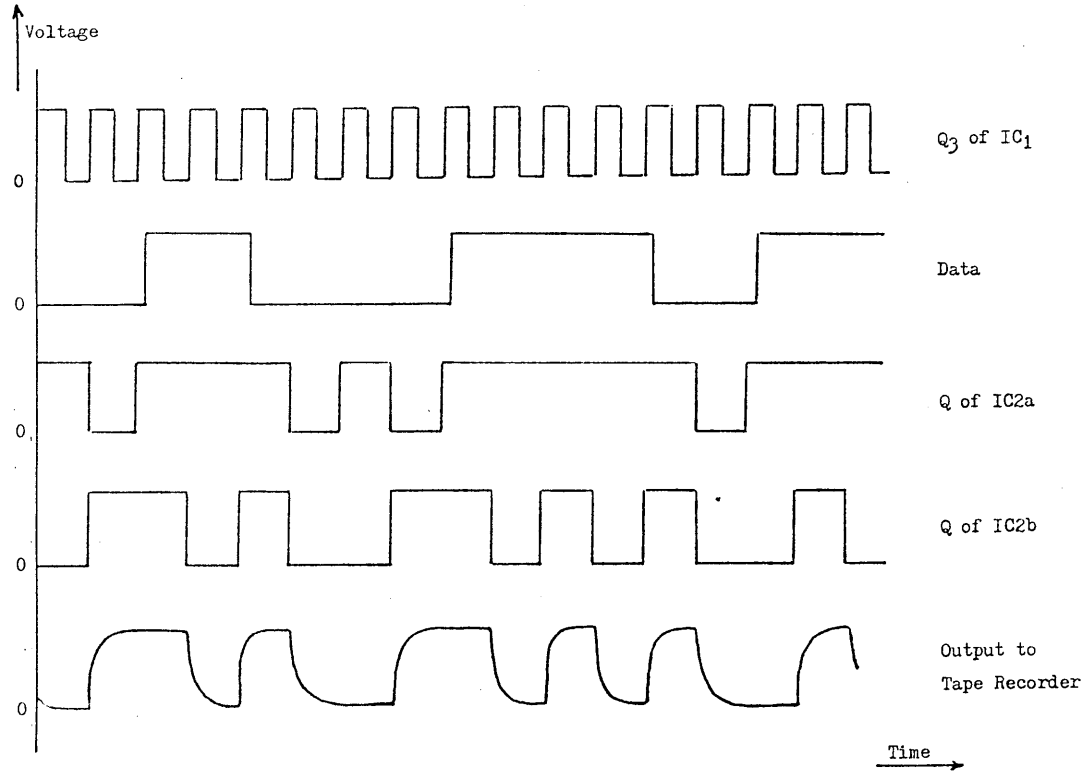

Figure 5.34 Waveforms in basic encoder circuit.

This basic encoder does not require modification for 4800 baud operation.

(b) Encoder with Switched Pre-filtering

In this case, the basic circuit of Figure 5.33 requires some modification, as shown in Figure 5.35 .

Flip-flops IC2a and IC2b produce the encoded data which is then pre-filtered before recording. Filter switching is provided by an analogue switch IC4 driven by flip-flop IC3. During data '0', IC4b switches

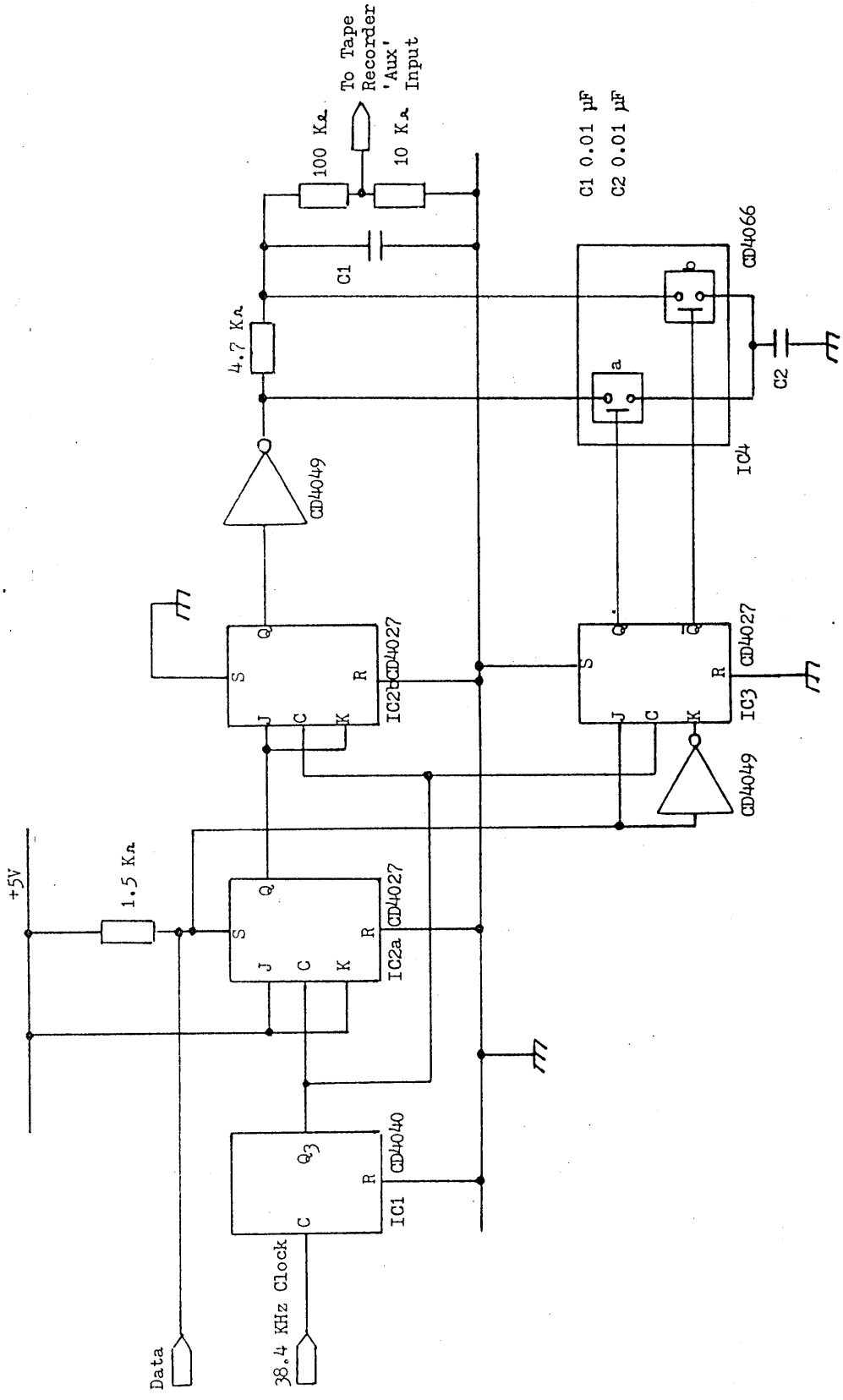

Figure 5.35 Encoder circuit with switched pre-filtering.

additional capacitor C2 into the filter circuit to appropriately reduce the cut-off frequency. Switch IC4a, working in opposite sense to IC4b, ensures that C2 is fully charged when switched into a high logic level and fully discharged when switched into a low level. For 4800 baud operation, the filter resistor of 4.7 Kn is reduced to 2.2 Kn . Circuit waveforms are shown in Figure 5.36 .

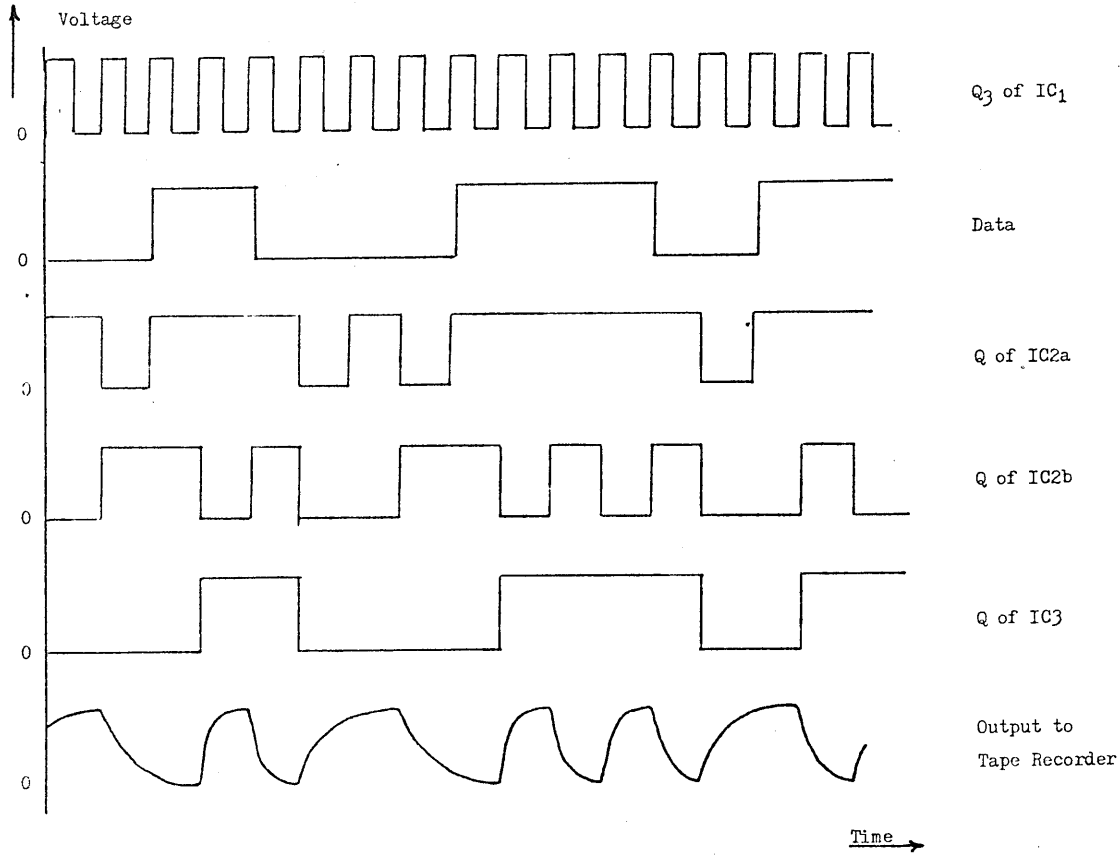

Figure 5.36 Waveforms in switched pre-filter encoder circuit.

5.8 Decoder

Decoding of the coded data relies on timing the interval between transitions of the playback signal. If the interval between transitions is greater than 3/4 of the duration of the bit cell, then the signal is decoded as a data '0', otherwise it is decoded as data '1'. It is

important that the threshold timing interval should remain at 3/4 of the bit cell duration, even though this duration may change due to variation in tape speed.

In the decoder circuit of Figure 5.37 , the timing is achieved by use of counter IC5. The clock input to IC5 is derived from the incoming playback signal by phase-locked loop IC7, and so accurate decoding is independent of tape speed. Very few of the existing interface designs for data storage on audio cassette make any attempt to use the self-clocking property of the code in this way [84].

IC1, an active all-pass filter, provides phase equalization of the playback signal as described in section 5.6.3 . The alternative input arrangement, for use when phase equalization is provided by switched pre-filtering, is shown by the dotted lines. The playback signal is hard limited by IC2 and 'squared' to logic levels by IC3a. It is then passed to Exclusive-OR gate IC4a, with a delayed version of itself, to produce a narrow pulse. This pulse is used to reset counter IC5.

The clock frequency for IC5 (76.8 kHz at correct tape speed) is provided by phase-locked loop IC7 and divider IC8. The count between resets should be 16 for data '1' and 32 for data '0'. IC3c output goes low after count 24, the threshold count midway between the two extremes. Flip-flops IC6a and IC6b, together with Exclusive-OR gate IC4b, provide a symmetrical data stream.

Variable resistors at pins 11 and 12 of IC7 are used to give a phase-locked loop range of approximately 120 kHz to 180 kHz. The 4.8 kHz output at Q5 of IC8 is locked to the 4.8 kHz output of IC5. The output frequency of the phase-locked loop, given accurate tape speed, will be

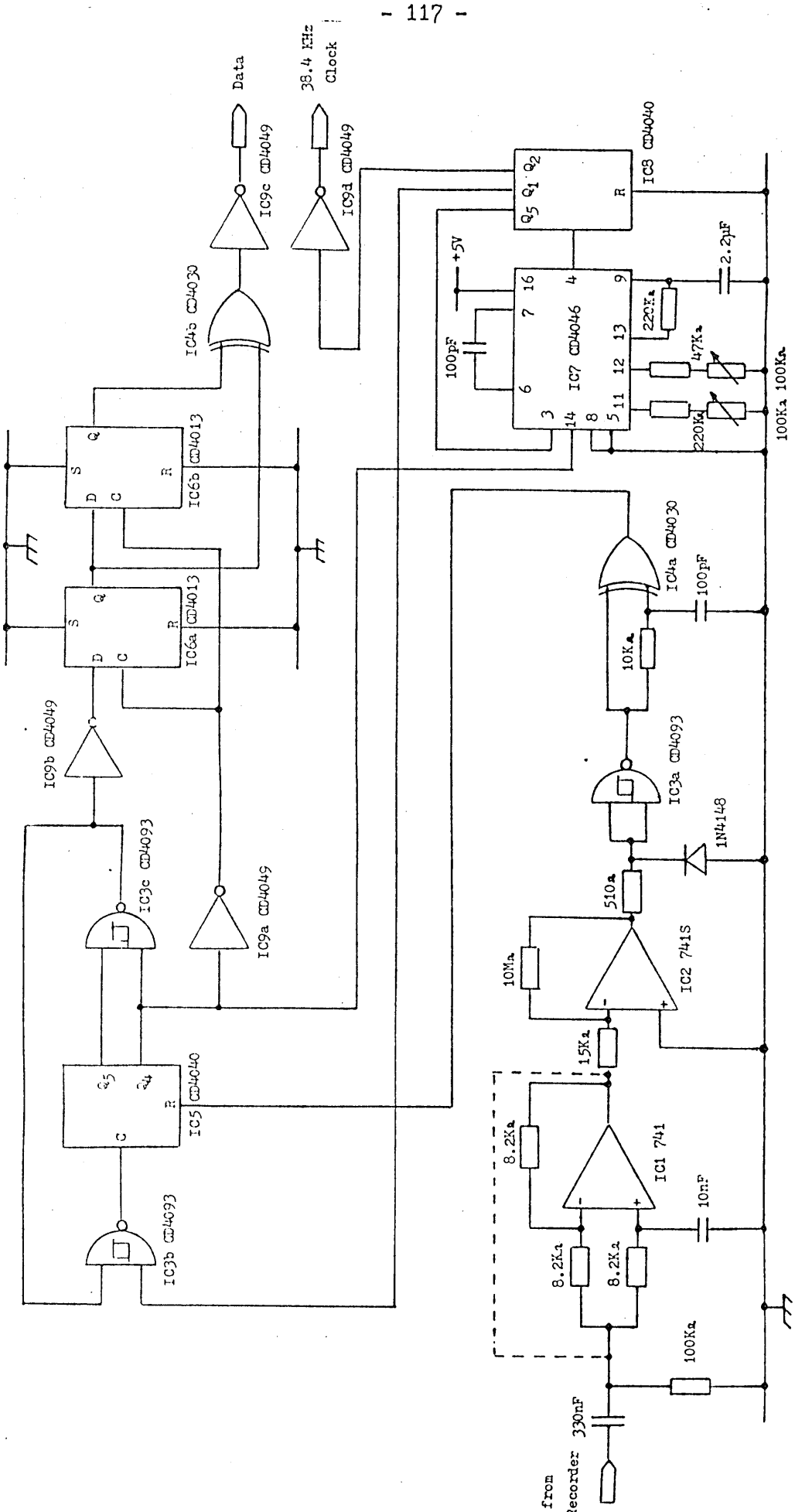

Figure 5.37 Decoder circuit.

153.6 KHz.

The data stream and a X16 data-rate clock, from Q2 of IC8, are applied to an asynchronous communications interface adaptor for conversion to parallel format. Waveforms throughout the decoder circuit are shown in Figure 5.38 .

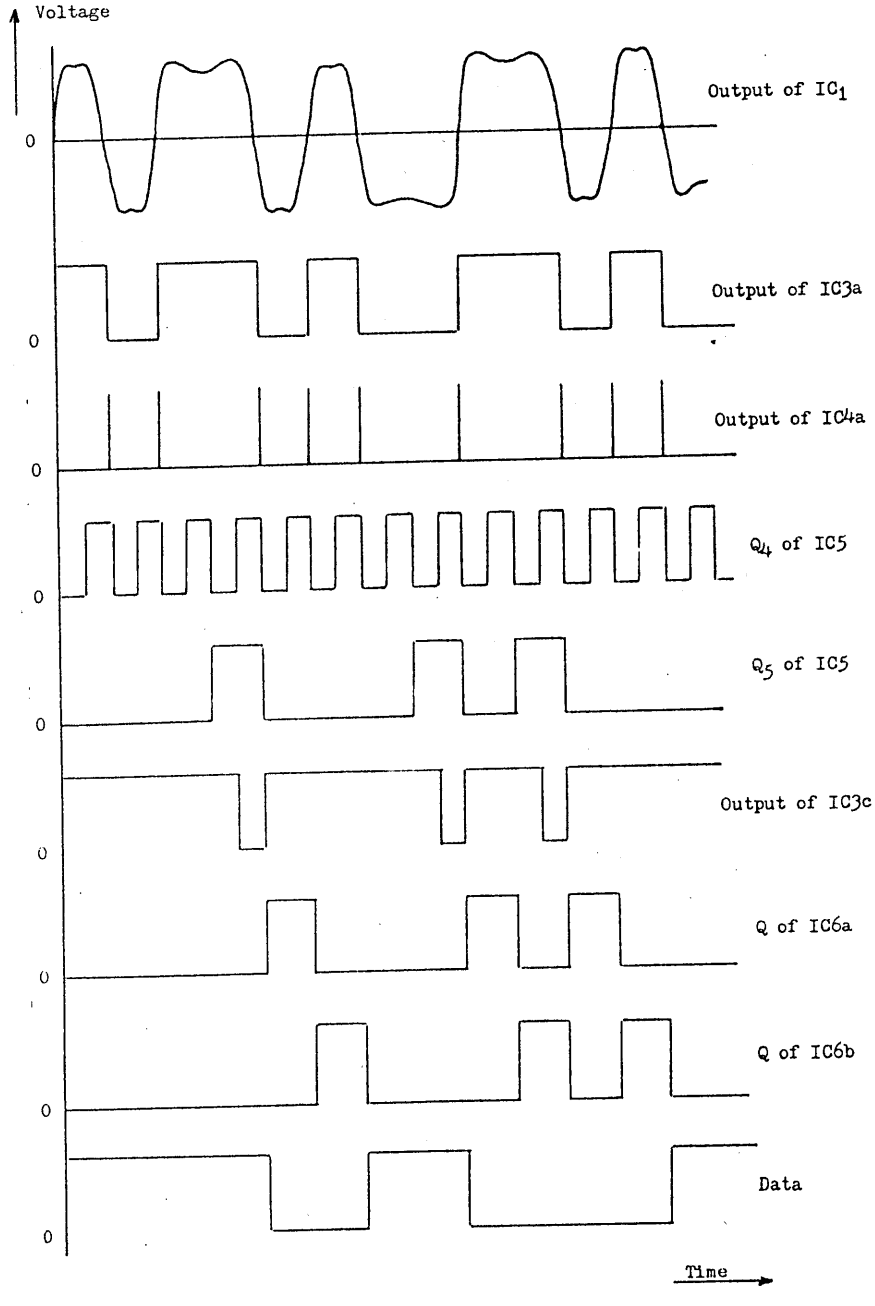

Figure 5.38 Waveforms in decoder.

For circuit operation at 4800 baud, a doubling in frequency of the outputs of IC8 is required. Therefore, it is necessary to modify the decoder, as shown in Figure 5.39 .

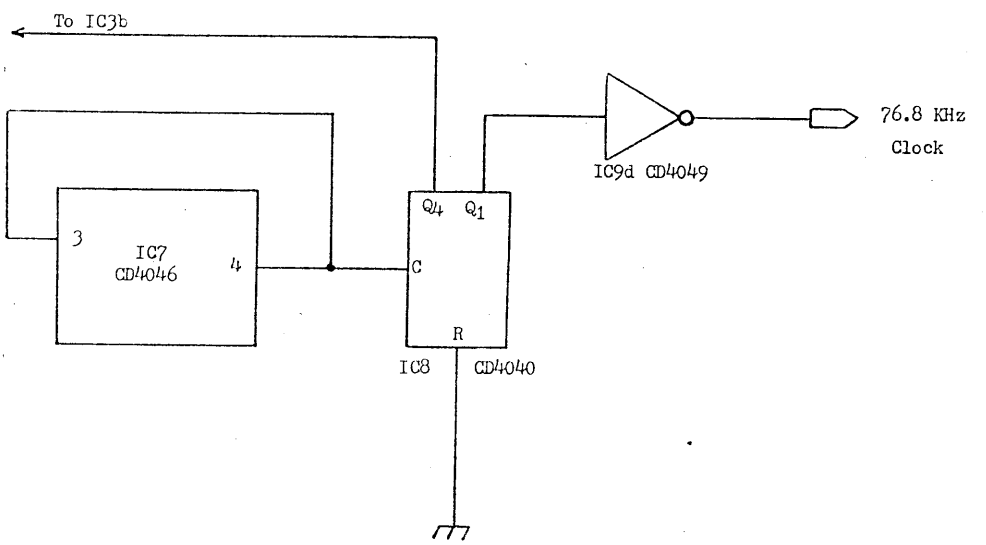

Figure 5.39 Modifications required for decoder operation at 4800 baud.

To simplify the switching that is required to change data rates, IC8 is wired permanently for 4800 baud operation. The simple circuit of Figure 5.40 is then used to halve the frequency of the input to IC8, when 2400 baud operation is required.

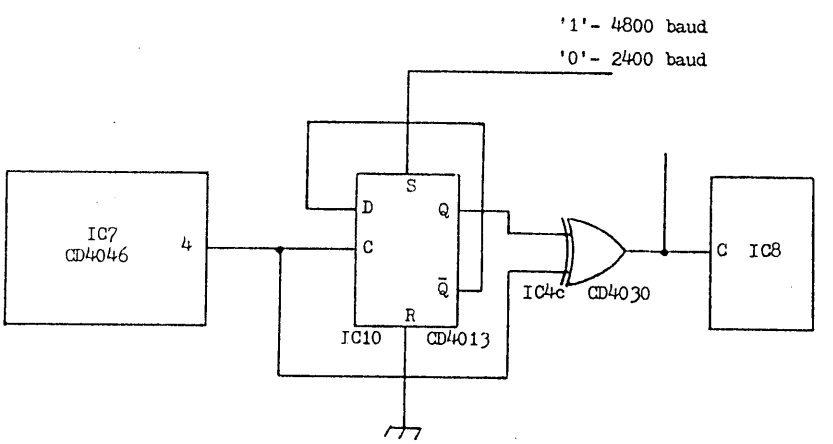

Figure 5.40 Circuit of switchable divider for baud rate selection.

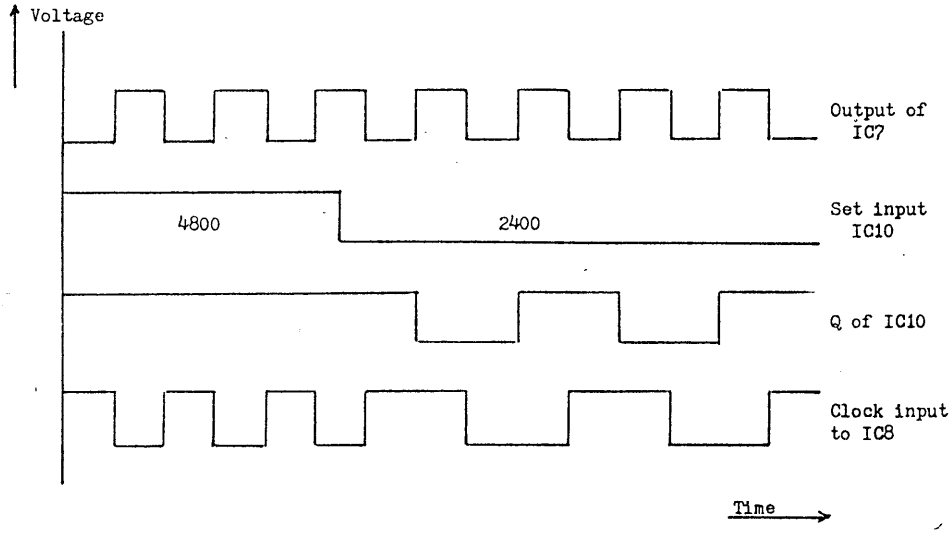

Figure 5.41 Waveforms of switchable divider circuit.

5.9 Circuit Testing

The encoder and decoder circuits described in sections 5.7 and 5.8 were subjected to testing with a varied selection of audio cassette recorders and tapes.

During testing, the normal precautions that would be taken in any magnetic recording procedure were observed. In particular, the recorders were regularly cleaned and care was taken to avoid damage to the surface of the tape. However, no attempt was made to correct for head misalignment in any of the tested recorders.

A method of automatic error checking was used for the majority of the tests. This involves the repetitive recording of a 16-bit pseudo-random sequence throughout the full length of the tape. On playback, the data is clocked into a 16-bit shift register. Then, comparison is made between the data bit about to be clocked into the register with

bit 16, which is about to be clocked out. In effect, the compared bits are the same bits of two successive and identical 16-bit sequences. Therefore, they should have the same data values when compared in an Exclusive-OR gate, as shown in Figure 5.42 .

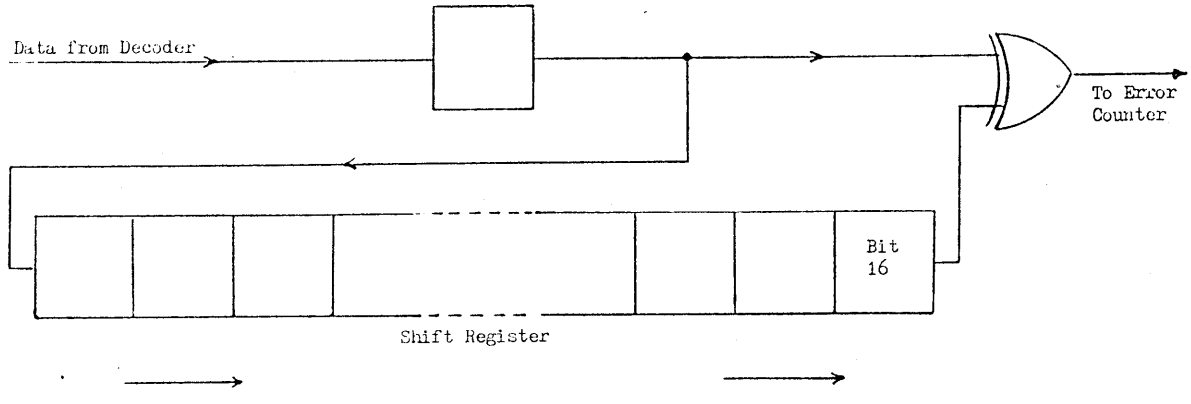

Figure 5.42 Error detector.

For equal data values, the output of the Exclusive-OR gate remains low. Should an error occur in the input bit, then the Exclusive-OR output will go high for one bit period. A bit in error is actually compared twice, as shown in Figure 5.43, and so the output of the Exclusive-OR gate is divided by two to obtain the error count.

The disadvantage of this method is that it does not respond to systematic errors that may occur in the same bit position of successive data sequences. In consequence, testing was extended by making use of a microcomputer memory verify routine. This routine was used to compare blocks of sample data recorded onto tape with those decoded on playback.

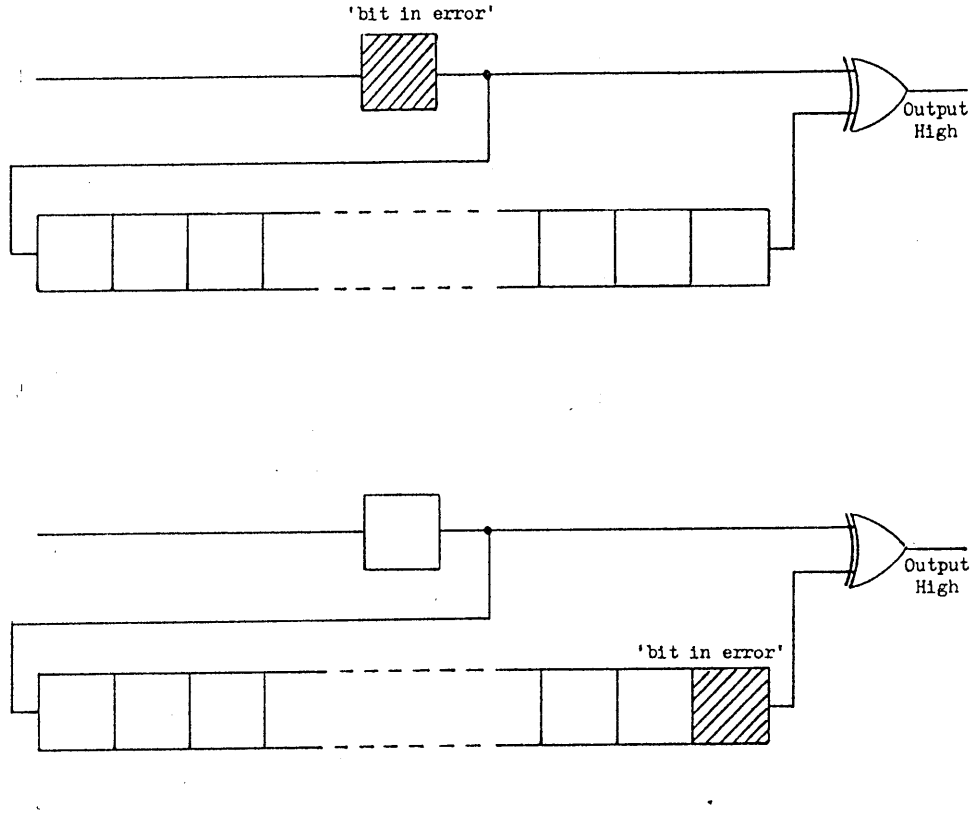

Figure 5.43 A single bit in error is compared twice.

	4800 Baud	Tape 1	Tape 2	Tape 3	Tape 4	Tape 5	Tape 6
Switched-Filtering	Recorder 1	0	0	0	0	0	>999
	Recorder 2	0	0	0	78	0	>999
	Recorder 3	0	0	0	3	0	>999
	Recorder 4	>999	>999	>999	>999	>999	>999
	Recorder 5	0	0	0	0	0	>999
All-pass Filter	Recorder 1	0	0	0	0	0	>999
	Recorder 2	0	0	0	0	0	>999
	Recorder 3	0	0	0	0	0	>999
	Recorder 4	0	0	11	0	0	>999
	Recorder 5	0	0	0	0	0	>999

Table 5.5 Test Results (errors recorded during 30-minute test).

At 2400 baud, there were no recorded errors in any of the tests. However, as Table 5.5 shows, at 4800 baud use of the switched pre-filter circuit produced excessive errors on recorder 4, with all the tested tapes. Tape 6 proved to be completely unusable at the higher data rate.

On the basis of these tests and the comparison of the margin for error, as indicated by the 'eye diagram' of the decoder signal (examples of which are given in Photographs 5.6 and 5.7), the active all-pass filter technique was adopted to provide phase equalization within the recording system. The tests confirmed the superior performance of good quality tape and the feasibility of using 4800 baud as an optional storage rate with most recorders.

There followed prolonged testing to ensure the reliability of the chosen encoder and decoder designs, at the 'standard' data rate of 2400 baud. A total of 200 30-minute test recordings were made. During these tests, two error bursts were detected. Both bursts occurred with samples of the same low-cost tape and both were due to clearly visible tape defects. Otherwise, the circuits proved to be consistently reliable. The encoder and decoder design proved insensitive to the normal listening range of volume control settings, to the use of automatic record level control and to variations in tape speed.

5.10 Audio Cassette Tape

From the testing procedures of Sections 5.2 and 5.9, it is possible to compare the relative performance of the various brands and formulations of audio cassette tape for use in this application.

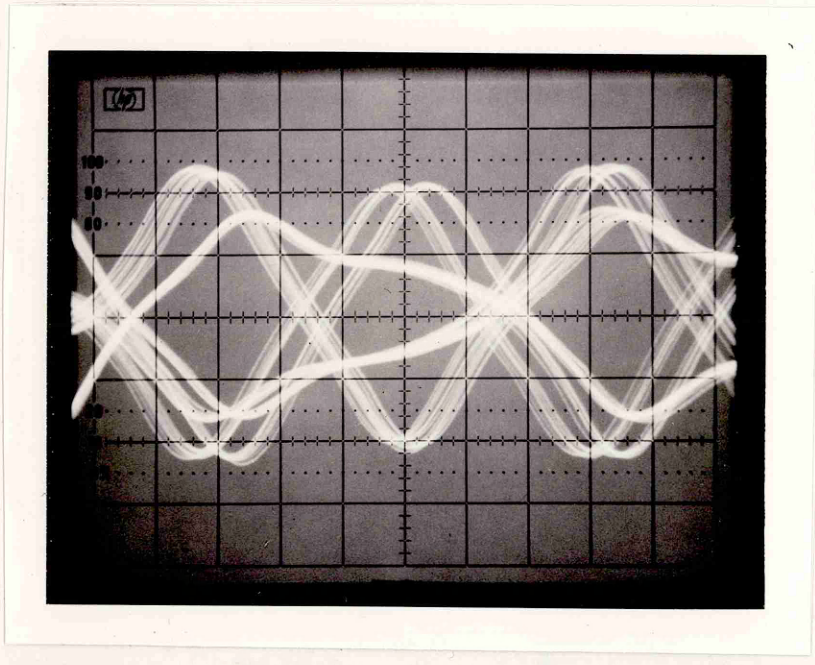

Timebase ≃ 50 µs/div

Photograph 5.6 The 'eye diagram' of the decoder playback signal with phase equalization provided by switched pre-filtering.

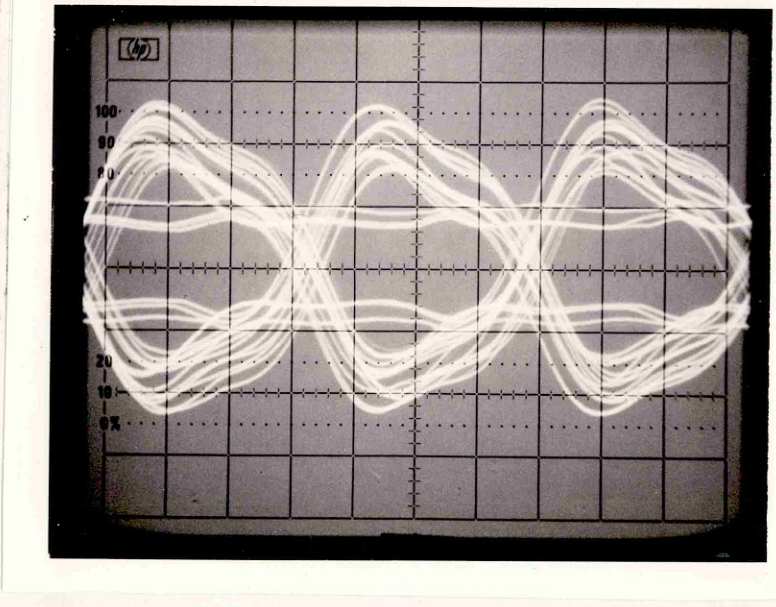

Timebase ≃ 50 µs/div

Photograph 5.7 The 'eye diagram' of the decoder playback signal with phase equalization provided by an all-pass filter.

Such a performance evaluation is valuable because, unlike the selection of a recorder, it is possible to make a recommendation on the choice of audio cassette tape to be used.

The tapes selected for test represented a cross section of the available range of ferric (gamma-phase ferric oxide), chrome (chromium dioxide) and ferrochrome formulations. Samples throughout the price range were included, although only ferric tapes were available in the lowest price range. Samples of tape specifically marketed for data storage in microcomputer applications were included.

The relevant results from the testing procedures are listed below. The available range of audio cassette tape is formidable and, therefore, these results should be taken only as indicative of the general case, rather than applicable in every instance. For the purposes of comparison, tapes were divided into three price ranges.

(1) There is little difference in performance between the formulations of tape within the same price range.

(2) The tapes in the high-price range consistently perform well and significantly better than other tapes.

(3) The performance of the medium-priced tapes varies widely. Some produce results no better than typical low-priced tapes. None of them give results to compare with any of the high-priced tapes.

(4) With some exceptions, low-priced tapes perform badly. Several tapes produce appreciable reduction in recording bandwidth. Many are poorly constructed and prone to tape jamming.

(5) With one exception, the performance of 'data storage' tapes is poor. The best of these tapes compares favourably with a typical medium-priced tape.

Although, in conventional audio applications with low-cost recorders, the advantages of high quality audio cassette tapes may not be so obvious, the test results show their superiority for this data storage application. While taking into account their relative high cost, the improved performance and reliability of these tapes is sufficiently significant to warrant recommendation of their use.

It is important when using audio cassette tape for data storage, that the tape surface should not be touched or damaged in any way. To avoid this damage, the tape should be rewound and placed in its protective container when not in use. The tape should never be exposed to strong magnetic fields or extremes of temperature [85].

6. ERROR CORRECTION

6.1 Introduction

It is highly desirable that students should have confidence in the accuracy of the study material presented to them. While they are likely to be tolerant to errors in material of an administrative nature, items such as names, formulae and numerical and graphical information, are rightly expected to be free of error.

The major causes of system errors are impulse noise on the broadcast channel and 'drop-out' due to tape damage during data storage. The occurrence of impulse noise on the broadcast channel was described in Section 3.4 . The properties of this noise cause the errors to occur in bursts. In between these bursts, the high signal to noise ratio of the channel ensures a negligible probability of data error.

The error profile during data storage is observed to be similar to that of the broadcast channel. Tape damage causes bursts of error but, otherwise, the storage channel is virtually error free.

Since both the broadcast channel and data storage exhibit the error characteristics of the classic bursty channel, it should be possible to use a common error protection regime throughout the system.

6.2 Error Correction Coding Methods

The two major classes of codes for error correction are block codes and convolutional or tree codes.

In block-coding the information bits are formed into blocks of fixed size. Check bits are added to each block independently, according to the rules of the particular code employed. Each block, including the check bits, is usually transmitted and checked separately.

Convolutional codes operate on the information sequence without breaking it up into independent blocks. In these codes, the information bits and check bits are interleaved in a continuous stream. Convolutional codes have similar error correcting capabilities and the same fundamental limitations as block codes [86].

In general, convolutional codes have a low code efficiency (code efficiency = k/n, where k is number of information bits and n is number of bits transmitted), typically 50%, with subsequent high redundancy for a given error correction capability. They have been found most useful in the additive white gaussian noise channel, such as the space channel, where long error bursts do not occur [87]. Decoding of convolutional codes, either by sequential or correlation (Viterbi) decoders, becomes extremely complex and prone to error when long bursts of errors are experienced [88].

In consequence, block-coding techniques were investigated for use in the Radiotext system. The requirement for blocking of data presents little problem because of the structured way in which 'pages' of information are prepared, as described in Chapter 2.

The simplest error-detecting code in common use is the parity-check code, in which an extra digit is added to each code word. In an even-parity system, the extra parity-check bit is added in such a way as to ensure an even number of data '1's in any correct code word. Alternatively, odd parity can be used. By examining the number of data '1's in a received pattern, these simple parity-check codes are able to detect single errors. To detect more than one error, it is necessary to add more digits to each code word. By adding still more check digits, it is possible to correct as well as detect errors. The Hamming code gives a simple method of performing some error correction in terms of these simple parity checks [89].

In the geometrical or block parity code, the parity-check principle has been extended to a two-dimensional array [90]. In this case, the information bits are arranged into a rectangular array, then horizontal parity-check bits (either odd or even) are added to each row and vertical parity-check bits added to each column. This code can detect all odd numbers of errors within each row or within each bit position of all rows in the block. Additionally, it may detect some even numbers of errors and limited error correction may also be possible with certain error configurations.

The most useful class of block codes, for use when long error bursts are experienced, is that of the cyclic codes [91]. Data is formed into blocks and check bits appended prior to transmission. The check bits are the remainder after binary division of the information bits by the characteristic generator polynomial of the cyclic code.

It is a property of cyclic codes that r check bits are capable of

detecting error bursts of length $b \leqslant r$ bits, in any block of n transmitted bits, and that this error detection capability is independent of n. Additionally, the fraction of bursts of length $b > r$ remaining undetected is small and given by 2^{-r}, and for $b = r$ by $2^{-(r-1)}$ [92].

The property of error detection has led to cyclic codes being used extensively for packet switched and computer networks, where retransmission is used in the event of an error being detected.

With the use of additional check bits, to produce in effect a more structured code, cyclic codes may be used for error correction. Many such codes have been proposed and several, notably BCH (Bose-Chaudhuri-Hocquenghem) and Fire codes, have been implemented in practical systems [93,94,95,96]. For single short error bursts these codes perform well, however, the number of check bits becomes excessive when correction of long error bursts is required (e.g. typically, a Fire code will require 35 check bits to correct a single error burst of up to 12 bits in length).

6.3 Radiotext Error Correction

In Section 3.4, Figure 3.19 showed that, with a data rate of 2400 baud, approximately 10% of all error bursts experienced in Radiotext will be longer than 20 bits. It is clear that simple parity-check codes will not suffice for this application. Cyclic codes provide a simple and reliable method of detecting such long error bursts but, because of the large number of check bits required, they are complex and relatively expensive to implement for error correction.

As a result, an error correction procedure was designed for use in Radiotext in which the error detecting capabilities of a cyclic code were incorporated within the structure of a block parity code, to provide the necessary error correction.

In this procedure, k information bits are arranged in a rectangular array of V rows of L bits per row. Both horizontal and vertical check bits are formed. The vertical check bits are generated as the modulo 2 sum for each of the L columns within the array, as shown in Figure 6.1 .

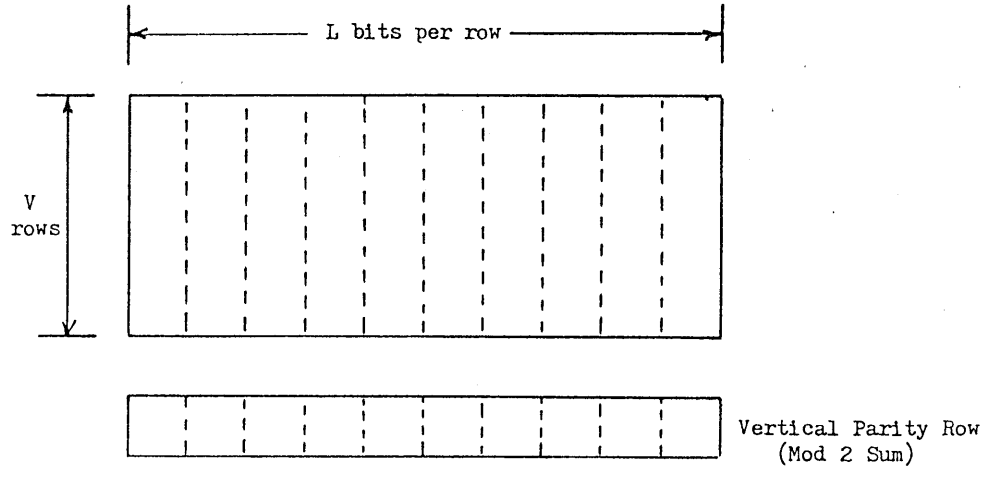

Figure 6.1 Generation of vertical check bits.

Horizontal check bits are formed by using the cyclic code on each of the V + 1 rows, as shown in Figure 6.2 .

The chosen cyclic code is that used in the U.K. packet switched data service, with a generator polynomial $X^{16} + X^{12} + X^{5} + 1$, (C.C.I.T.T. Recommendation V41) [97]. This generator polynomial produces 16 parity check bits. Therefore, a burst of 16 bits or less will be detected.

The fraction of bursts of length $b > 17$ remaining undetected is 2^{-16}. For $b = 17$, it is 2^{-15}.

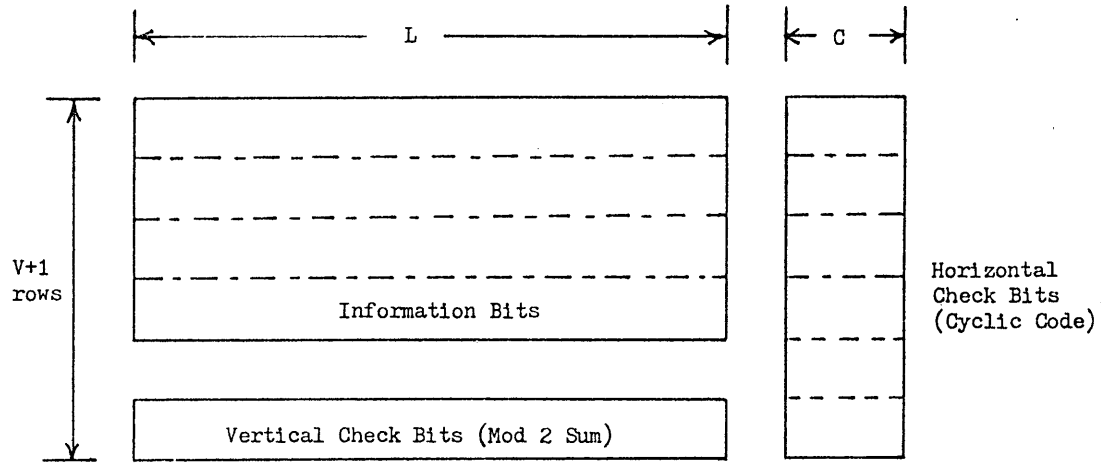

Figure 6.2 Generation of horizontal check bits.

The block is transmitted row by row, each row consisting of L information bits followed by C cyclic check bits.

The block size is $(V+1)(L+C)$ bits, of which VL bits are information bits.

Therefore,

$$\text{Code Efficiency} = \frac{VL}{(V+1)(L+C)},$$

and

$$\text{Redundancy} = \frac{C(V+1)+L}{(V+1)(L+C)}.$$

On reception, each row is checked for errors using the C cyclic row check bits. If an error in any one of the V information rows of the block is indicated, the block can be corrected by replacement of the row in error with the modulo 2 sum of the (V-1) remaining rows and the parity row.

Should two rows be in error in the same block, then correction cannot take place. Therefore, the possibility of a single error burst causing errors in two rows of the same block has to be avoided. This is achieved by interleaving rows of any single block with rows of other blocks during transmission. This will result in a long error burst, covering several rows, influencing only a single row of any one block and so being correctable.

The required degree of interleaving, measured by the separation between rows of the same block, will depend on the anticipated length and frequency of the error bursts.

Figure 6.3 shows the block row interleaving of the B information bits and $\frac{B}{V}$ parity bits during transmission. The rows of block 1 are indicated. Row 1 commences at bit 1, row 2 at bit $\frac{B}{V} + 1$, row 3 at bit $\frac{2B}{V} + 1$ and so on, until row V which commences at bit $\frac{(V-1)B}{V} + 1$. Each row is L bits long.

The rows of block 2 follow those of block 1, e.g. block 2 row 1 commences at bit $L + 1$, row 2 at bit $\frac{B}{V} + (L+1)$ and so on.

Hence, there is a separation between rows of the same block of $\frac{B}{V} - L$ bits. The vertical parity row of each block is appended to the B information bits, in order to maintain this separation between row V and the parity row of each block.

During transmission, C cyclic check bits are added to each row. This has the effect of increasing the separation between rows of the same block by $(\frac{B}{LV} - 1)C$. In most cases, C is significantly less than L and so this increase is of little consequence.

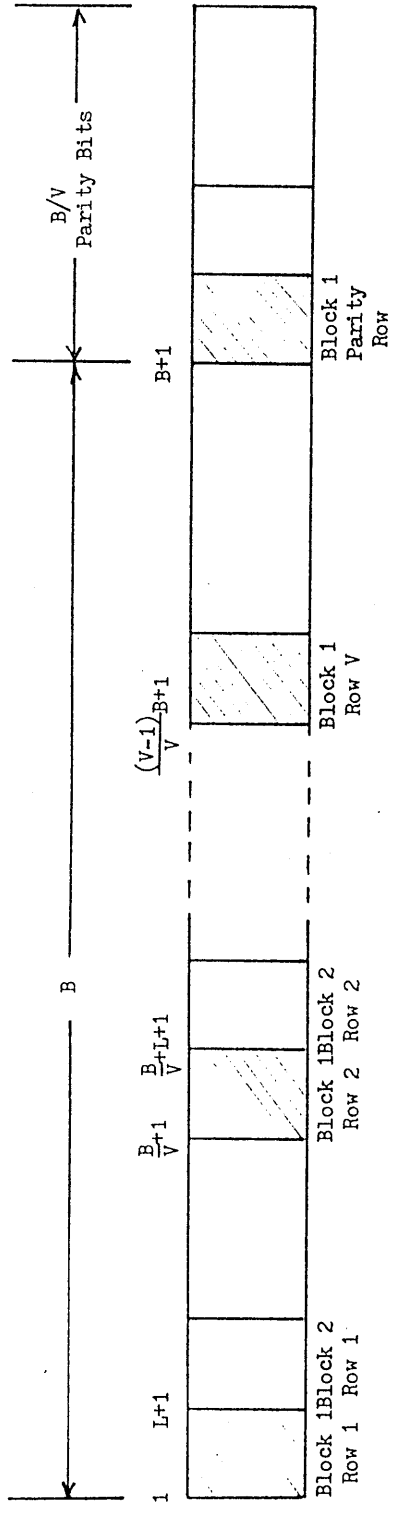

Figure 6.3 Block row interleaving during transmission.

The result of this interleaving is that any single burst of errors, of $\frac{B}{V}$ bits or less, is correctable during transmission of the total $\frac{B(V+1)}{V}$ bits.

To assess the effectiveness of this correction code, the channel was modelled in the manner described by Gilbert [98]. This model, shown in Figure 6.4, has two states, one when the transmission is error free, and the other when there is an error burst.

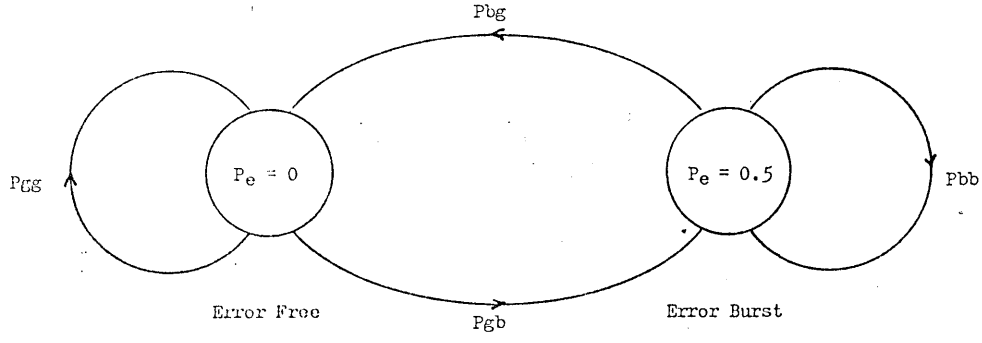

Figure 6.4 Transition diagram for the two state model.

In the error free state, the probability of error P_e is 0, the probability of remaining in this state is P_{gg} and the probability of transition to the error burst state is P_{gb}. In the error burst state, the probability of error $P_e = 0.5$, the probability of remaining in this state is P_{bb} and the probability of transition to the error free state is P_{bg} .

The results of the investigation into impulse noise on the broadcast path were used to calculate the transition probabilities shown in Figure 6.5 , for a data rate of 2400 baud.

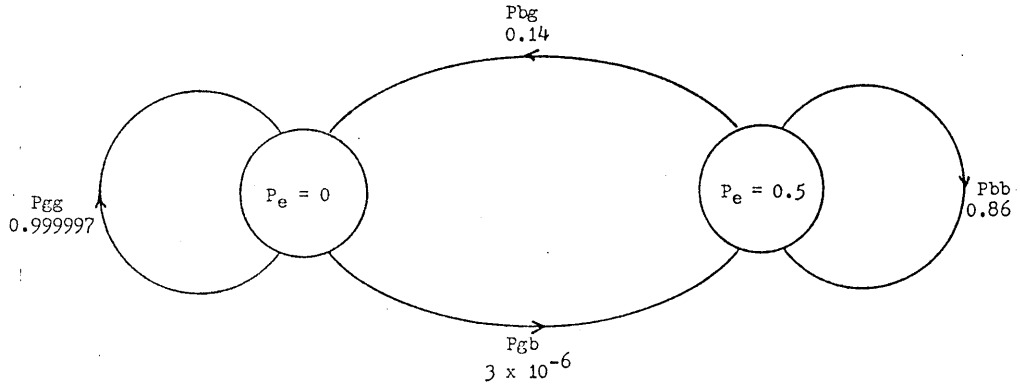

Figure 6.5 Calculated values of transition probabilities in the two state model at a data rate of 2400 baud.

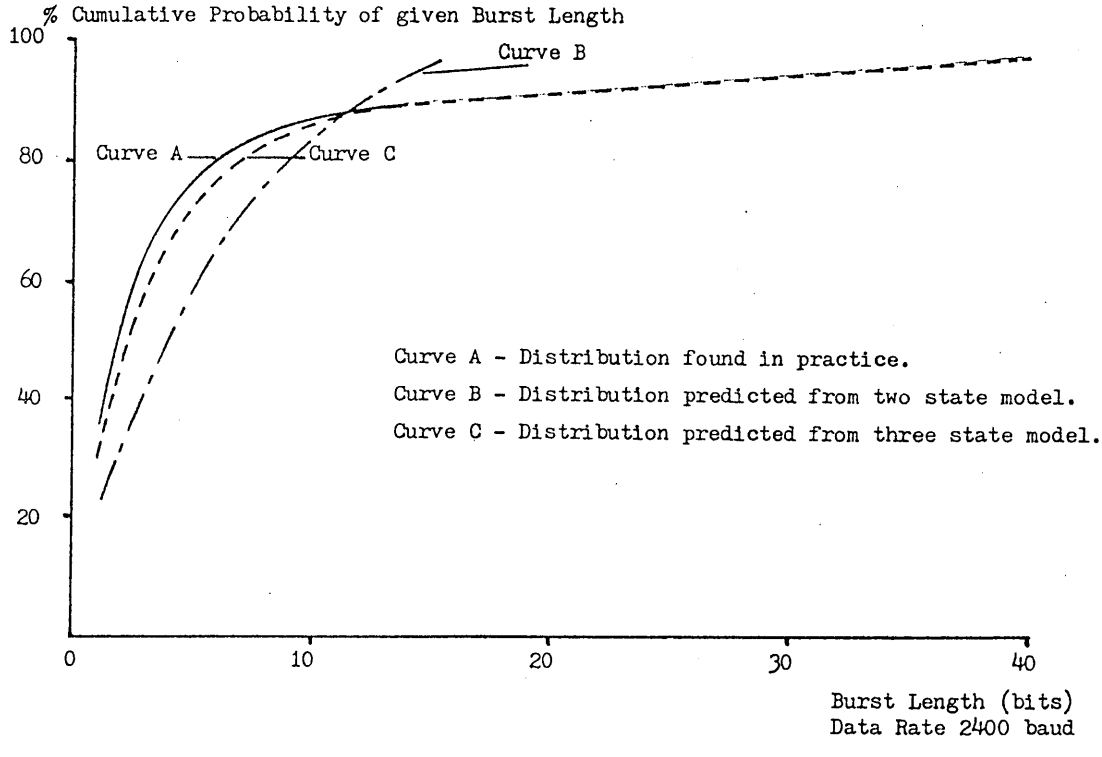

Figure 6.6 Error burst length distribution.

The accuracy of the model was examined by comparing the probability of a given burst length, calculated from the model (curve B of Figure 6.6), with that found in practice (curve A of Figure 6.6). The curves show that the model inadequately describes the error characteristics experienced in practice.

As a result, a three state model was developed by splitting the error state into a long error burst state (state 1), likely to produce an error burst duration in excess of 0.2 ms and a short error burst state (state 2), likely to produce an error burst duration of less than 0.2 ms.

With this model, shown in Figure 6.7 , the predicted probability of a given burst length is seen, in curve C of Figure 6.6, to be close to that found in practice.

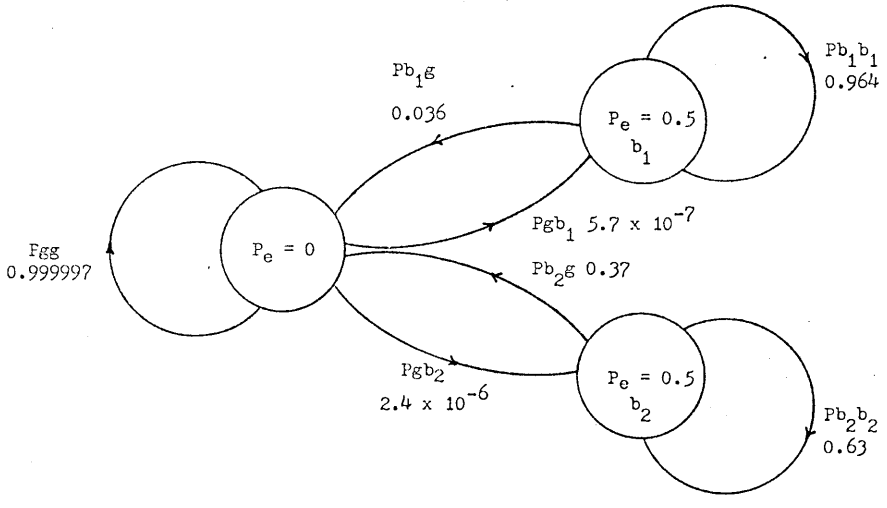

Figure 6.7 Calculated values of transition probabilities in the three state model at a data rate of 2400 baud.

With the error correction technique described, an uncorrectable error will occur if :

(1) the error burst exceeds $\frac{B}{V}$ bits,

(2) two or more bursts occur during the transmission of the total $\frac{B(V+1)}{V}$ bits and these bursts affect two or more rows of the same block.

With the aid of the three state model of Figure 6.7, it is possible to calculate the probability of these two occurences in terms of B, L, V and the transition probabilities of the model.

The probability P_{e1} of the error burst exceeding $\frac{B}{V}$ bits is given by

$$P_{e1} = P_{b1b1}^{(\frac{B}{V})} + P_{b2b2}^{(\frac{B}{V})} \qquad \ldots\ldots (1)$$

The probability P_{e2} that two or more error bursts are uncorrectable is found from the product of the probability P_{2+} that two or more error bursts occur and the conditional probability P_c that, given an error burst has occurred in a given block, a subsequent error burst will occur in another row of the same block. (The test results of Section 3.4 show that statistical independence can be assumed in the occurrence of the error bursts.)

P_{2+} is given by

$$P_{2+} = 1 - P_1 - P_0$$

where, P_1 is probability of one burst

P_0 is probability of no bursts

From Figure 6.7,

$$P_0 = P_{gg}^{BW},$$

$$P_1 = BW \times (P_{gb1} + P_{gb2}) \times P_{gg}^{(BW-1)}, \quad \text{where } W = \frac{V+1}{V}.$$

Therefore,

$$P_{2+} = 1 - \left[BW \times (P_{gb1} + P_{gb2}) \times P_{gg}^{(BW-1)}\right] - P_{gg}^{BW} \quad .....(2)$$

Given that one burst has occurred, the probability that the second or subsequent burst occurs in the same block is equal to $\frac{1}{G}$, where G is the total number of transmitted blocks, $G = \frac{B}{LV}$.

Therefore,

$$P_c = \frac{1}{G} \times \frac{V}{V+1}$$

$$\text{or } P_c = \frac{LV^2}{B(V+1)} \quad ..... (3)$$

From (2) and (3)

$$P_{e2} = \frac{LV^2}{B(V+1)} \left\{ 1 - P_{gg}^{BW} - \left[BW \times (P_{gb1} + P_{gb2}) \times P_{gg}^{(BW-1)}\right] \right\}$$

Table 6.1 shows some calculated values of the probability of uncorrected errors P_e, code efficiency and maximum correctable error burst length for example values of L and V. The influence of the total number of information bits transmitted and the data rate on P_e is shown by the examples of Table 6.2 .

B	V	L	E	R	MB	P_c	P_e
8192	2	64	53	47	4096	0.01	5.6×10^{-10}
		128	60	40	4096	0.02	1.1×10^{-9}
		256	62	38	4096	0.04	2.2×10^{-9}
		512	65	35	4096	0.08	4.5×10^{-9}
	4	64	64	36	2048	0.025	1.1×10^{-9}
		128	71	29	2048	0.05	2.2×10^{-9}
		256	75	25	2048	0.1	4.5×10^{-9}
		512	78	22	2048	0.15	9.0×10^{-9}
	8	64	71	29	1024	0.055	2.2×10^{-9}
		128	79	21	1024	0.11	4.5×10^{-9}
		256	84	16	1024	0.22	9.0×10^{-9}
		512	86	14	1024	0.44	1.8×10^{-8}

Table 6.1 Examples of the relationship of code parameters L and V to percentage code efficiency E, percentage redundancy R, maximum correctable error burst length MB and the probability of uncorrected error P_e. The Table refers to the transmission of a low resolution display 'page' at a data rate of 2400 baud.

V	L	Date Rate	B	MB	P_e
4	128	2400	2048	512	9.24×10^{-9}
			4096	1024	2.2×10^{-9}
			8192	2048	2.2×10^{-9}
			12288	4096	2.2×10^{-9}
		4800	8192	2048	5.7×10^{-10}
			12288	4096	5.7×10^{-10}

Table 6.2 Examples of the relationship of data rate and total number of transmitted information bits B to the probability of uncorrected error P_e .

6.4 Choice of Code Parameters

The examples of Tables 6.1 and 6.2 show that, using this error correction method, the probability of uncorrected error P_e is extremely small. Table 6.1 shows P_e to be proportional to block size K, where $K = LV$. In Table 6.2, P_e is shown to be essentially independent of the total number of transmitted bits B . However, at low values of maximum correctable error burst length MB , P_{e1} becomes significant and P_e increases accordingly (Table 6.2 with MB of 512).

In addition, these examples show that, for high code efficiency, the block size K should be high, with V having proportionally greater effect than L . The value of V is limited, however, due to its effect on MB for a given total number of transmitted information bits B .

At a data rate of 4800 baud, P_{e1} becomes a significant component of P_e at values of MB of 1024 and less. To avoid these values, with B = 8192 for a low resolution display 'page' , V must be no greater than 4. Given this value of V, the choice of L becomes a trade off between code efficiency and P_e.

A row length of 128 was chosen for use in Radiotext, giving a block size of 512 bits and a maximum correctable error burst length of 2048 bits from a total of 8192 transmitted bits. With V = 4 and L = 128, the probability of an uncorrected error is 2.2×10^{-9} per data bit, at a data rate of 2400 baud, achieved with a code redundancy of 29% .

Although the likelihood of an uncorrected error is small, it is important that, should two rows of the same block be in error, an indication of the uncorrected error is given on the display. In Radiotext, this is achieved by setting rows in error to black within a graphics 'page' and to the distinctive @ sign in a text 'page'.

This procedure will fail only if an error occurs in a row and remains undetected by the cyclic code. From the model of Figure 6.7, the probability of at least one error in any row is calculated to be 3.84×10^{-4} $(1 - 0.999997^{128})$. Figure 6.6 shows that 90% of all bursts (being less than 17 bits in length) will be detected by the cyclic code. Of the remainder, the fraction remaining undetected is 2^{-16} . Therefore, the probability of an undetected error is approximately 4.6×10^{-12} per transmitted data bit.

6.5 Implementation and Evaluation of the Error Correction Procedure

All the error correction within the Radiotext system is implemented in software. The coding procedure is described in the flow chart of Figure 6.8 and the correction procedure by the flow chart of Figure 6.9 . The error correction software occupies approximately 2 Kbytes of interface memory.

In Figure 6.3 , it was shown that, with every B transmitted information bits, $\frac{B}{V}$ parity bits are added. With the error correction parameters chosen for use, this means that every 1 Kbyte low resolution display 'page' initially requires 1.25 Kbytes of memory at the Radiotext interface, and similarly, every 8 Kbyte high resolution display 'page' initially requires 10 Kbytes of memory within the interface. The additional memory space occupied by the parity bits is only required until error correction has taken place. Consequently, to enable 2 low resolution and 2 high resolution 'pages' to be stored in the interface, it is necessary to provide an additional 2 Kbytes of memory, common to both low and high resolution 'pages', for temporary parity bit storage. Therefore, a total display memory size of 20 Kbytes is required.

The performance of the error correction procedure was evaluated in transmission tests, in which impulse noise was introduced to simulate the worst-case conditions likely to be experienced, in practice, during reception of Radiotext transmissions. In these tests, the correction procedure performed sufficiently well to indicate that the calculated residual error rate of, on average, one 'page' in error for every 10,000 transmitted low resolution 'pages' (or 1,200 high resolution 'pages') is likely to be achieved in practical operation.

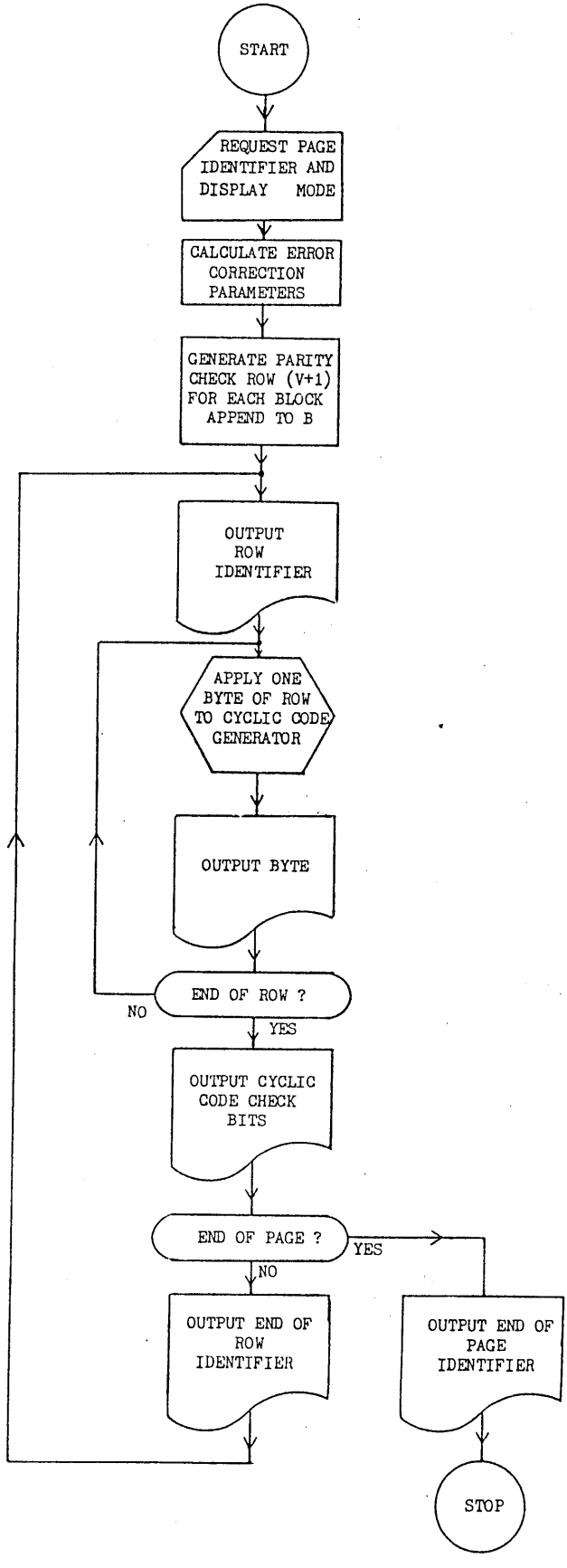

Figure 6.8 Error correction coding

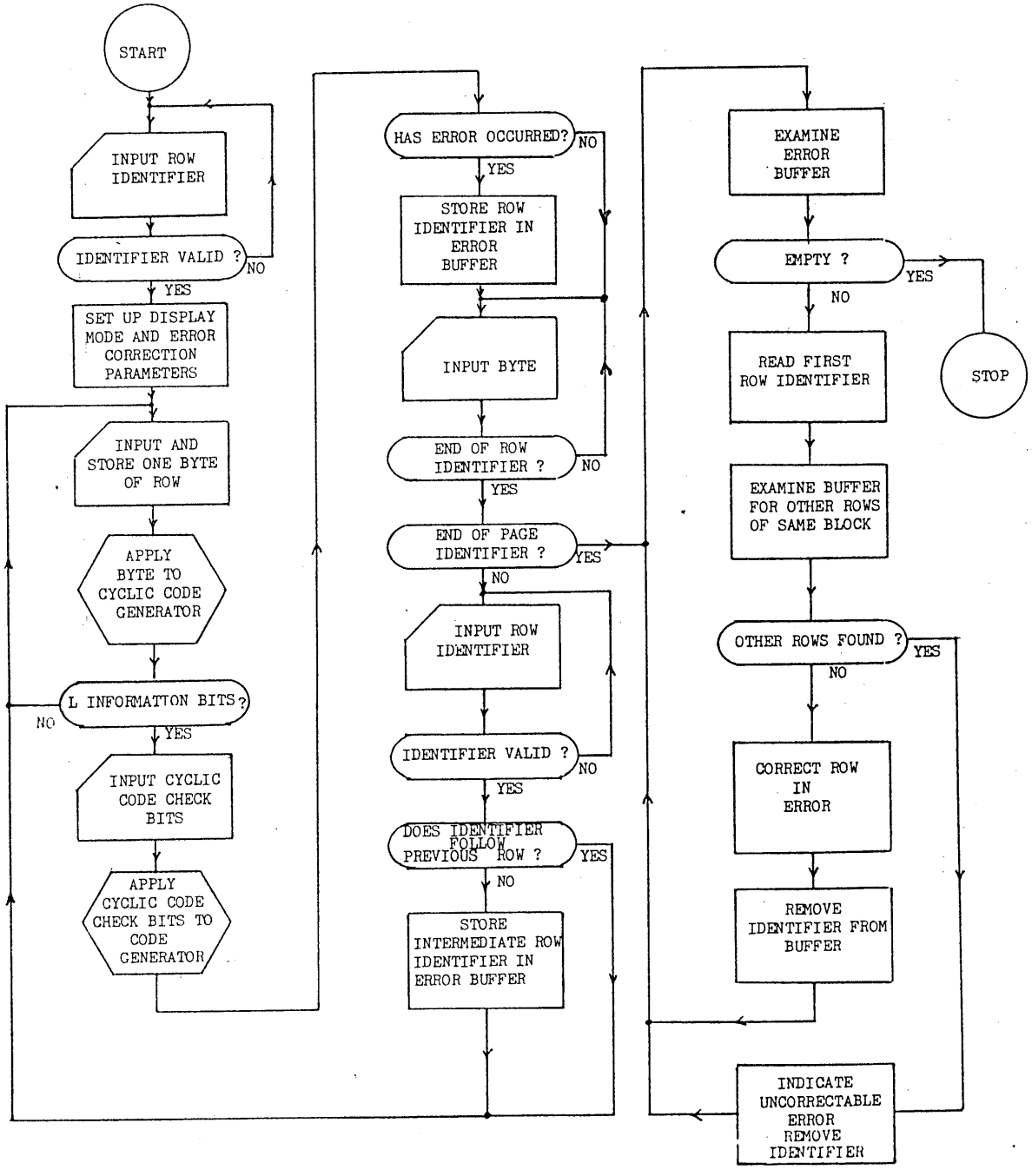

Figure 6.9 Error correction procedure

7. FUTURE DEVELOPMENTS

All the elements of Radiotext have been subject to extensive laboratory testing. These tests have shown that the existing system implementation should provide a sound base from which to conduct system trials under operational conditions. It is proposed that these trials are carried out in two stages.

In the first, a short broadcast of example data material, when received and recorded with the assistance of Open University Staff Tutors and student volunteers throughout the regions, will enable an assessment to be made of the practical levels of phase distortion (with the consequent intersymbol interference) and multipath propagation. In addition, this initial test will examine the way in which example Radiotext material will be handled for broadcasting within the University and by the broadcasting authority.

Following this test, it should be possible to finalise the choice of modulation method used for the broadcast component of the system, together with the design of the encoder and decoder.

It is then proposed that a full system trial will take place. In this case, it is hoped that the system will be used by a number of students over an extended period of time. This trial should indicate the likely levels of system operability and reliability. In particular, it will be

useful to examine,

(1) the extent of the practical difficulties of connecting the radio receiver, audio cassette recorder and television to the Radiotext interface,

(2) the general level of performance of the radio receivers used by students including their ability to maintain accurate tuning over long periods of time,

(3) the effectiveness of the system error correction technique.

Remedial action will then be taken, as required.

In addition to this system trial, two components of Radiotext require further investigation before full system implementation can occur. The first is the provision of a suitable low-cost printer to provide the student with a 'hard copy' of Radiotext material and the second is the design of a stereophonic radio receiver to be incorporated within the Radiotext interface.

Although not part of the original system concept, the incorporation of a stereophonic radio receiver within the interface is useful and, in many cases, may be necessary because existing Open University radio broadcasts are monophonic, with the result that many radio receivers, purchased by students specifically for Open University use, are not capable of receiving the stereophonic transmissions necessary for audio-visual Radiotext material.

Due to recent developments in digital synthesizer integrated circuits and to the availability of combined I.F. amplifier and stereo decoders

on a single integrated circuit, it is possible to provide a suitable stereophonic receiver at a cost of less than £20 (1982) [99,100,101]. Such a receiver will provide precise tuning, in 25 kHz steps, to any station within the V.H.F. radio broadcast band. Decoding of the S.C.A. channel may be provided at little extra cost. By incorporating the radio receiver within the interface in this way, the provision of time clock on/off switching is considerably simplified.

Conclusion

Radiotext promises to be a highly reliable method of transmission of text and graphic teaching material. Use of an unmodified broadcast system ensures that it will be cheap to implement and should not affect the conventional broadcast service in any significant way.

In the student's home, the cost of the interface is kept low by utilising the radio receiver, audio cassette recorder, television and, in some areas, microcomputer already used by students in their existing studies. The provision of a reliable method of data storage allows material received by radio to be studied at any desired rate, with repetition as often as required.

The cost to the Open University of the 'stand-alone' interface is estimated to be £65 (July 1982), or as a microcomputer 'add-on', in the region of £15. The operating cost of such a system is dependent to a large extent on the charges imposed by the broadcasting authority. On a 'per student' basis, these are expected to be small.

REFERENCES

(1) Makitalo O., Utilization of the FM-Broadcasting Network for Transmission of Supplementary Information, Swedish Telecommunications Administration, Report R1 001/77.

(2) Whythe D.J., and Ely S.R., Data and Identification Signalling For Future Radio Receivers, IBC 78, (I.E.E., London, 1978), 324-326.

(3) Audio-Frequency Parameters for the Stereophonic Transmission and Reproduction of Sound, Recommendations and Reports of the CCIRR, 1978, Vol. X, Broadcasting Service (Sound), (ITU, Geneva, 1978).

(4) Crosby M.G., Frequency-Modulation Propagation Characteristics, Proceedings I.R.E., Vol. 24, June 1936, 898-913.

(5) Corrington M.S., Frequency-Modulation Distortion caused by Multipath Transmission, Proceedings I.R.E., Vol. 33, December 1945, 878-891.

(6) Hawker P., How serious is multipath distortion?, Wireless World, Vol. 86, No. 1532, April 1980, 45-48.

(7) Hawker P., Multipath Distortion - does polarization matter?, Wireless World, Vol. 87, No. 1543, April 1981, 83-85.

(8) Ohara M., Distortion and Crosstalk caused by Multipath Propagation in Frequency-Modulated Sound Broadcasting, I.E.E.E. Transactions on Broadcasting, Vol. BC-26, No. 3, September 1980, 70-81.

(9) Crosby, loc. cit.

(10) Corrington, loc. cit.

(11) Ohara, loc. cit.

(12) Panter P.F., Modulation, Noise, and Spectral Analysis, (McGraw Hill, New York, 1965), 364-370.

(13) Crosby M.G., Observations of Frequency-Modulation Propagation on 26 Megacycles, Proceedings of I.R.E., Vol. 29, July 1941, 398-403.

(14) Susans D.E., A V.H.F. Multipath Simulator, British Broadcasting Corporation, Report RD 1976/13.

(15) BBC Handbook 1980, (British Broadcasting Corporation, London, 1980), 196-198.

(16) Hawker, How serious is multipath propagation?

(17) Ishigaki Y., Muraoka T. and Hagiwara M., Electronic Reduction of FM Distortion caused by Multipath Transmission, I.E.E.E. Transactions on Consumer Electronics, Vol. CE-26, February 1980, 28-34.

(18) Date H., et al., An Automatic Cancellation System for Multipath Echo Distortion in FM Broadcasting, Preprint of Spring Convention of the Acoustic Society of Japan, 1979, 249-250.

(19) Buehler W.E., and Lunden C.D., Signature of Man-Made High-Frequency Radio Noise, I.E.E.E. Transactions on Electromagnetic Compatibility, Vol. EMC-8, September 1966.

(20) Skomal E.N., Distribution and frequency dependence of unintentionally generated man-made VHF/UHF noise in metropolitan areas, I.E.E.E. Transactions on Electromagnetic Compatibility, Vol. EMC-11 (2), September 1965, 263-278.

(21) Skomal E.N., Man-Made Radio Noise, (Van Nostrand Reinhold, New York, 1978).

(22) Schwartz M., Information Transmission, Modulation, and Noise (Third Edition), (McGraw Hill, New York, 1980), 176-188.

(23) Bowyer L.R. and Highleyman W.H., An Analysis of Inherent Distortion in Asynchronous Frequency-Shift Modulators, Bell Systems Technical Journal, Vol. 41, No. 6, November 1962, 1695-1736.

(24) Mauch H., Digital Data on Cassette Recorders, Byte, Vol. 1, No. 7, March 1976, 40-45.

(25) Kinsner W., Seiler D., and Britt R., FSK Digital Data Converter for Cassette Tape Recorder, Proceedings of the International Symposium of Mini and Micro Computers, Toronto Canada, 8-11 November 1976, (I.E.E.E., New York, 1977).

(26) Koanantakool T., 4800 Baud Cassette Interface, New Electronics, Vol. 12, No. 21, 30 October 1979, 36.

(27) Moir J., Magnetic Recording Review, Wireless World, Vol. 87, No. 1542, March 1981, 54-58.

(28) McWilliams A.A., Tape Recording and Reproduction, (Focal Press, London, 1964), 112-129.

(29) Wallace R.L. Jr., The Reproduction of Magnetically Recorded Signals, Bell Systems Technical Journal, Vol. 30, No. 2, 1951, 1145.

(30) Pear C.B. Jr., ed. Magnetic Recording in Science and Industry, (Reinhold, New York, 1967), 37.

(31) Ibid., 49.

(32) Cook E., The Cassette Lives On, Byte, Vol. 5, No. 5, May 1980, 12-18.

(33) The Apple II Tapes, (Apple Computer Inc, Cupertino, California, 1979).

(34) Hellyer H.W., Tape Recorders, (Fountain Press, London, 1970), 59.

(35) Pastoriza J.J., Trade-offs Among Binary Codes in Magnetic Tape Cassettes, Computer Design, Vol. 15, No. 1, Jan 1976, 102-104.

(36) Cook, loc. cit.

(37) Severt R.H., Comparison of four classes of digital data encoding techniques, Computer Design, Vol. 19, No. 5, May 1980, 181-190.

(38) Loc. cit.

(39) Sallet H.W., Magnetic tape: a high performer, I.E.E.E. Spectrum, July 1977, 26-31.

(40) Loc. cit.

(41) Loc. cit.

(42) Johnson C.E. Jr., A miniature low cost magnetic tape system for programmable games, I.E.E.E. Transactions on Consumer Electronics, Vol. CE-23, No. 3, August 1977, 266-270.

(43) Severt, loc. cit.

(44) Sallet, loc. cit.

(45) Mallinson J.C., and Miller J.W., On Optimal Codes for Digital Magnetic Recording, Proceedings of the Conference on Video and Data Recording, Birmingham, England, 20-22 July 1976, (I.E.R.E., 1976), 161-169.

(46) Artwick B.A., Microcomputer Interfacing, (Prentice-Hall, Englewood Cliffs, New Jersey, 1980), 132-136.

(47) Severt, loc. cit.

(48) Sallet, loc. cit.

(49) Artwick, loc. cit.

(50) Severt, loc. cit.

(51) Sallet, loc. cit.

(52) Severt, loc. cit.

(53) Sallet, loc. cit.

(54) Mallinson, loc. cit.

(55) Artwick, loc. cit.

(56) Kinsner, loc. cit.

(57) Severt, loc. cit.

(58) Sallet, loc. cit.

(59) Artwick, loc. cit.

(60) Kinsner, loc. cit.

(61) Severt, loc. cit.

(62) Sallet, loc. cit.

(63) Mallinson, loc. cit.

(64) Severt, loc. cit.

(65) Sallet, loc. cit.

(66) Mallinson, loc. cit.

(67) Patel A.M., New Method for Magnetic Encoding Combines Advantages of Older Techniques, Computer Design, Vol. 15, No. 8, August 1976, 85-91.

(68) Severt, loc. cit.

(69) Mallinson, loc. cit.

(70) Artwick, loc. cit.

(71) Kinsner, loc. cit.

(72) Loc. cit.

(73) Artwick, loc. cit.

(74) Kinsner, loc. cit.

(75) Severt, loc. cit.

(76) Patel, loc. cit.

(77) Mallinson, loc. cit.

(78) Peschke, Byte's audio cassette standards symposium, Byte, Vol. 1., No. 6, February 1976, 72-73.

(79) Hopner E., High-Density Binary Recording Using Nonsaturation Techniques, I.E.E.E. Transactions on Electronic Computers, Vol. EC-13, No. 3., June 1964, 255-261.

(80) Cottis B., and Blandford M., A High Speed Cassette Interface, Personal Computer World, Vol. 1, No. 8, December 1978, 64-68.

(81) Smith R.A., A Low Cost Storage System For Use on Audio Cassettes, Electronic Technology, Vol. 13, No. 3, March 1979, 65-69.

(82) Koanantakool, loc. cit.

(83) Weinstein L., How to get your Tarbell going, Byte, Vol. 3, No. 7, July 1978, 162-171.

(84) Smith, loc. cit.

(85) Manildi A.B., Designer's Guide For Selecting Magnetic Mini-Media, Computer Design, Vol. 16, No. 9, September 1977, 120a-120f.

(86) Peterson W.W., and Weldon E.J., Error Correction Codes (2nd Edition) (M.I.T. Press, Cambridge, Massachusetts, 1972), 7.

(87) Forney G.D., Coding and its application to Space Communications, I.E.E.E. Spectrum, June 1970, 47-58.

(88) Berlekamp E.R., Long burst codes which use soft decisions and correct erasure bursts without interleaving, N.T.C. Conference Record, Los Angeles, 5-7 December 1977, 36:1.1.

(89) Hamming R.W. Error Detecting and Correcting Codes, Bell Systems Technical Journal, Vol. 26, April 1950, 147-160.

(90) Morris D.J., Introduction to Communication Command and Control Systems, (Pergamon, Oxford, 1977), 246.

(91) Schwartz, op. cit., 535-551.

(92) Peterson, op. cit., 228-230.

(93) Bose R.C., and Ray-Chaudhuri D.K., A class of error-correcting binary group codes, Information and Control, Vol. 3, March 1960, 68-79.

(94) Fire P., A Class of Multiple-Error-Correcting Binary Codes for Non-Independent Errors, Sylvania Electric Products Inc., Mountain View, California, Report no. RSL-E-2, March 1959.

(95) Chien R.T., Block-Coding Techniques for Reliable Data Transmission, I.E.E.E. Transactions on Communications Technology, Vol. COM-19, no. 5, October 1971, 743-751.

(96) Maniar M., and Rallapalli K., Fire codes on custom chip clean up hard disk data, Electronics, 5th May 1981, 122-125.

(97) The U.K. Post Office, Handbook of Data Communications, (NCC, Manchester, 1975), 200-201.

(98) Gilbert E.N., Capacity of a Burst-Noise Channel, Bell System Technical Journal, Vol. 39, September 1960, 1253-1265.

(99) Breeze E., A New Design Technique for Digital PLL Synthesizers, I.E.E.E. Transactions on Consumer Electronics, Vol. CE-24, No. 1, February 1978, 24-33.

(100) Mills T.B., An AM-FM Digital Tuning System, I.E.E.E. Transactions on Consumer Electronics, Vol. CE-24, No.4, November 1978, 507-512.

(101) Blaser L., and Taira T., An AM/FM Radio Subsystem IC, I.E.E.E. Transactions on Consumer Electronics, Vol. CE-23, No. 2, May 1977, 129-137.